Optimal Allocation of Multiple Distributed Generation Technologies in Distribution Systems

(配電系統における分散電源の最適配置)

by

Karar Mahmoud Badawy Mostafa

D141195

A Doctoral Thesis

Graduate School of Engineering

Hiroshima University

Hiroshima University, Japan

April 2016

Abstract

Recently, the penetration of renewable distributed generation (DG) technologies has dramatically increased in distribution systems. The most notable DG types are wind power, photovoltaic, and solar systems. These DG units are often distributed according to load centers in distribution systems. Renewable DG technologies are described as intermittent sources, for the reason that their output power varies depending on environmental conditions. Consequently, the performances distribution systems are greatly affected by these DG units. These resources may have positive or negative technical impacts on the grid, according to their selected sizes, locations, and types.

The main objective of this work is to perform comprehensive modeling, analysis of distribution systems and optimally install multiple DG technologies. The methodology of DG allocation must be generic, where different DG technologies are incorporates to the optimization process. In addition, the performance of the developed method must be efficient in terms of CPU time and accuracy. To represent the allocation problem from a practical view, distribution system constraints, such as voltage limits, line flow limits, and maximum DG penetration are required to be completely considered.

For this purpose, firstly, distribution system component models are developed using state of the art phase and sequence components frame of references. An efficient power flow method for analyzing distribution systems is presented. The proposed method utilizes efficient quadratic-based (QB) models for various components of distribution systems. The power flow problem is formulated and solved by a backward/forward sweep (BFS) algorithm. The proposed QBBFS method accommodates multi-phase laterals, different load types, capacitors, distribution transformers, and distributed generation (DG). The advantageous feature of the proposed method is robust convergence characteristics against ill conditions, guaranteeing lower iteration numbers than the existing BFS methods. The proposed method is tested and validated on several distribution test systems. The accuracy is verified using OpenDSS. Comparisons are made with other commonly used BFS methods. The results confirm the effectiveness and robustness of the proposed QBBFS with different loading conditions, high R/X ratio, and/or excessive DG penetration.

Secondly, an efficient analytical (EA) method is proposed for optimally installing multiple distributed generation (DG) technologies to minimize power loss in distribution systems. Different DG types are considered, and their power factors are optimally calculated. The proposed EA method is also applied to the problem of allocating an

optimal mix of different DG types with various generation capabilities. Furthermore, the EA method is integrated with the optimal power flow (OPF) algorithm to develop a new method, EA-OPF that effectively addresses overall system constraints. The proposed methods are tested using 33-bus and 69-bus distribution test systems. The calculated results are validated using the simulation results of the exact optimal solution obtained by an exhaustive OPF algorithm for both distribution test systems. The results show that the performances of the proposed methods are superior to existing methods in terms of computational speed and accuracy.

Acknowledgement

First of all, praise to Allah for his kindness to let me possible to complete this thesis. I would like to take this opportunity to extend my heartfelt appreciation to following persons whose have contributed directly or indirectly towards the completion of the study.

Primarily, I would like to express my deep thanks to my supervision Prof. Yorino Naoto for his professional support during my study in Hiroshima University. His guidance in performing research work and writing the thesis and the publications is extremely helpful. Besides his technical support, I have benefit from him positively in my personal live.

I owe my deepest gratitude to my Egyptian supervisors Prof. Abdella Ahmed and Prof. Loia Saad from Aswan University for the continuous support of my PhD study and research, for their patience, motivation, and enthusiasm. Also, I would like to thank the Egyptian Ministry of Higher Education for their fund of my study in Japan.

I would like to express my greatest gratitude to all members of EPESL laboratory, especially Prof. Yoshifumi Zoka and Prof. Yutaka Sasaki who aided me at all research steps as well as living in Japan.

Last but not the least, I would like to thank my family: my parents, my wife, my brothers, my sisters, and my friends for supporting me spiritually throughout my life.

Karar Mahmoud

2015

Table of Contents

List of Figures

Figure **PP**

List of Tables

Table **PP**

List of Abbreviations

PF	Power Flow
QB	Quadratic-Based
RPL	Real Power Loss
RPLR	Real Power Loss Reduction
DSO	Distribution System Operator
DSM	Distribution System Management
DERs	Distributed Energy Resources
DG	Distributed Generator
PV	Photo-Voltaic
WTGS	Wind Turbine Generation Systems
IEEE	Institute of Electrical Electronic Engineering
PCC	Point of Common Coupling
OPF	Optimal Power Flow
AMPL	Comprehensive & Powerful Algebraic Modeling Language
OOP	Object Oriented Programming
PCU	Power Conditioning Unit
MPP	Maximum Power Point
DNs	Distribution Networks
MWp	Megawatt Peak
Y, D	Star-Connection, Delta-Connection
CP,CI,CZ	Constant Power, Constant Current, Constant Impedance Loads
MV,LV	Medium-Voltage, Low-Voltage
AC	Alternate Current
DC	Direct Current
kV, kW	Kilo-Volt, Kilo-Watt
p.u.	Per Unit

Chapter 1

Introduction

Chapter 1: Introduction

1.1 Background

In recent years, the use of distributed generation (DG) technologies has remarkably increased worldwide due to their potential benefits. DG units generate power near load centers, avoiding the cost of transporting electric power through transmission lines. Another benefit of DG is cost savings in electricity production compared with large centralized generation stations [1]. Furthermore, renewable DG technologies, such as wind power, photovoltaic (PV), and solar thermal systems, are considered to be one of the fundamental strategies in the fight against climate change, as they can reduce dependence on fossil fuels [2]–[5]. Figure 1.1 describes the structures of traditional and modern (i.e., without and with DG integration) power systems.

With the rapid increase of DG penetration, distribution systems are being converted from passive to active networks. Normally, DG units are small in size and modular in structure. Therefore, their impacts on distribution system operation, control, and stability vary depending on their locations and sizes [6], [7]. One of the most common positive impacts of DG is the ability to reduce distribution system losses [8]. However, inappropriate DG allocation may lead to increased system losses and system operation costs [9], [10]. It is also a fact that most of the electrical power losses in electric power systems are dissipated in distribution systems due to heavy currents flowing in primary and secondary feeders. Therefore, there is a critical need to develop efficient tools that can optimally allocate different DG types in distribution systems, thereby reducing losses.

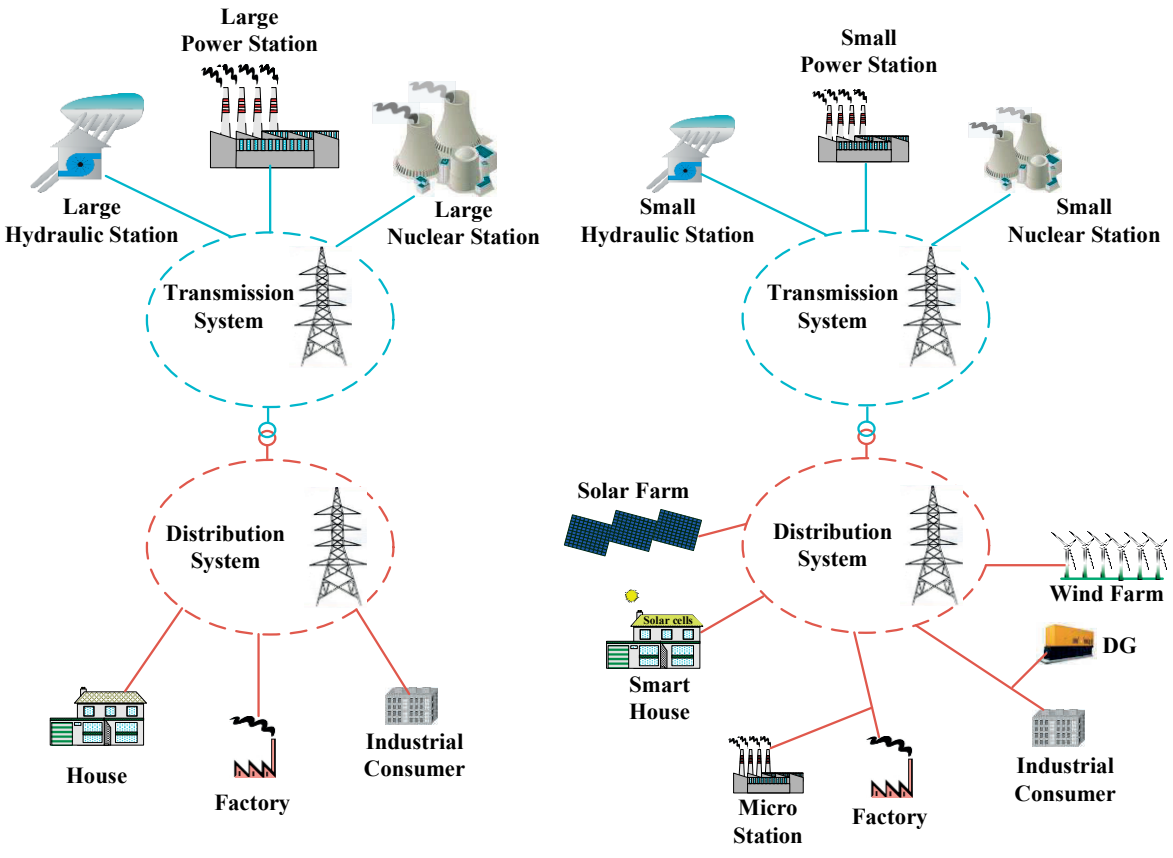

a) Traditional Power System b) Modern Power System

Figure 1.1 Traditional and modern power system structures.

Several methods have recently been proposed for the planning of distribution systems with DG to minimize losses. These methods can be classified as numerical-based (NB), heuristic-based (HB), and analytical-based (AB) methods [10]. The most common examples of NB methods are gradient search (GS)]11[, linear programming (LP) [12], optimal power flow (OPF) [13], and exhaustive search (ES) [14], [15]. The GS, LP, and OPF algorithms are considered efficient ways for obtaining the optimal DG sizes at certain locations. The ES algorithm is based on searching for the optimal DG location for a given DG size or under different load models. Therefore, these methods fail to represent the accurate behavior of a DG optimization problem that involves two continuous variables, both optimal DG size and optimal DG location. The HB methods are based on employing advanced artificial intelligence (AI) techniques, such as genetic algorithms (GAs) [16], [17], particle swarm optimization (PSO) [18], harmony search (HS) [19], and tabu search [20] The main feature of these methods is their computational robustness. They can provide near-optimal solutions but involve intensive computational efforts.

It is notable that great interest is directed to the AB methods, as they are easy to implement and fast. AB methods often follow various strategies to simplify the optimization problem, either by assuming uniformly distributed loads as in [21] or by allocating only a single DG unit in the entire system [21], [22]. Reference [23] has proposed a method for determining the optimal locations of multiple DG units, while the corresponding optimal DG sizes are obtained by the Kalman filter algorithm. A load centroid concept [24] is proposed in [25] for allocating multiple DG units. The authors of [26] have proposed an approach to allocate a single DG unit that operates at unity power factor, which has recently been extended to an improved analytical (IA) method [27]. The IA method involves allocating a single DG with various capabilities to generate both active and reactive power. More recently, the IA method has been upgraded to solve the multiple DG allocation problem [28] and validated by comparison with the exhaustive power flow solution. The main idea of the IA method for allocating multiple DG units is to update the load data after each time the DG is allocated to determine the next DG location. After each DG placement, the calculated DG size is corrected by using the exhaustive power flow method until the optimal point is reached. Although this method is relatively fast compared with the exhaustive solution, the obtained optimal DG locations are erroneous. This is mainly due to the cumulative procedure for selecting sequentially optimal locations for

multiple DG units, where the errors are accumulated. Furthermore, this method assumes that the multiple DG units have equal and specified power factors.

Based on the above review, it is clear that considerable research has been conducted to resolve the DG allocation problem; however, the AB methods and most of the other methods assume that DG power factors are not state variables but specified values. In addition, these methods cannot provide the optimal solution for allocating a mix of different DG types.

1.2 Objectives and Scopes of the Study

The main objective of this work is to optimally allocate different DG technologies in distribution systems. This objective is achieved through the following sub-objectives:

1.2.1 Efficient Power Flow Analysis Tool

To assess and analysis the impacts of DG on distribution systems, an efficient three-phase power-flow tool is firstly required. The developed power flow algorithm should be able to effectively solve distribution systems with different configurations and structures. Efficient load flow performance requires superior convergence rate, low memory allocation, and ability to solve large scale distribution systems. The developed power flow models are recommended to include following distribution system components:

- Asymmetric four-wires, three-phase, two-phase, and single-phase laterals.
- Different load types including CP, CC, and CI loads with different connections.
- Uniformly distributed loads.
- Capacitor banks.
- Three-phase transformers with various connection configurations.
- Voltage regulators.
- DG models including diesel engines, PV and wind generating systems.

1.2.2 Comprehensive Analyses of Distribution Systems with DG

Generic and efficient mathematical formulations for studying the impacts of different DG technologies on distribution systems are developed. By employing these formulations, a fast assessment of the contribution of renewable energy penetration can be handled. In addition, comprehensive analysis of large scales distributions systems with different DG technologies is performed. Moreover, internal modeling features of special DG types are included.

1.2.3 Generic and Effective DG Allocation

In this thesis, an allocation problem of multiple DG types is formulated and solved by an efficient analytical (EA) method. The proposed EA method is based on deriving a generalized formula that efficiently estimates the amount of reduction in real power loss due to the contributions of DG units. In addition, a combined EA-OPF method is proposed to minimize system losses. The main contributions of this paper can be summarized here.

- The proposed EA method is intended for the installation of DG technologies in distribution systems. A new advantageous feature of this method is the ability to accurately provide the optimal solution with fast computational speed. A direct solution can be obtained for installing any number of DG units without using the iterative process of power flow computations.
- Unlike conventional AB methods, the optimal DG power factors can be accurately computed mathematically using the EA method.
- The proposed EA-OPF method can handle highly constrained DG allocation problems.
- Both methods can be used for determining the optimal mix of different types of DG technologies to minimize losses. They are also useful for computing the optimal number of DG units for minimizing losses.

1.3 Thesis Organization

The thesis consists of seven chapters. The research topics are mainly distributing among the chapters as follows:

Chapter 1 presents the introduction to distribution systems, research objectives, scope of the research and organization of the thesis.

Chapter 2 provides comprehensive review about power flow analysis techniques, modeling and analysis of distribution systems.

Chapter 3 presents an improved Quadratic-based (QB) power flow method for solving the nonlinear iterative process in active distribution systems. The proposed method is validated via the OpenDSS software, and its performance is tested evaluated against existing methods.

Chapter 4 presents generic formulations for expressing the loss reduction with integrating multiple DG units in distribution systems. In addition, comprehensive analyses of several distribution systems are included, and the impacts of different DG units are deeply addressed.

Chapter 5 provides two new methods, namely EA and EA-OPF methods, for optimally allocating multiple DG units to minimize power loss in distribution systems. The proposed methods are tested on many test systems and compared with existing methods. The results demonstrate the effectiveness of the EA and EA-OPF methods.

Chapter 6 deals with allocating different DG types in distribution systems for reducing the losses. Different scenarios with different DG types to be allocated are studied and compared.

Chapter 7 provides a conclusion part, where contributions of the study are discussed. In addition, some recommendations for further research in the future are presented.

To facilitate understanding the contents and the distribution of contributions among the seven chapters, Figure 1.2 is provided, which describes the work flow in the thesis. According to the figure, the contents of the thesis are divided into three parts, namely, Part I, Part II, and Part III.

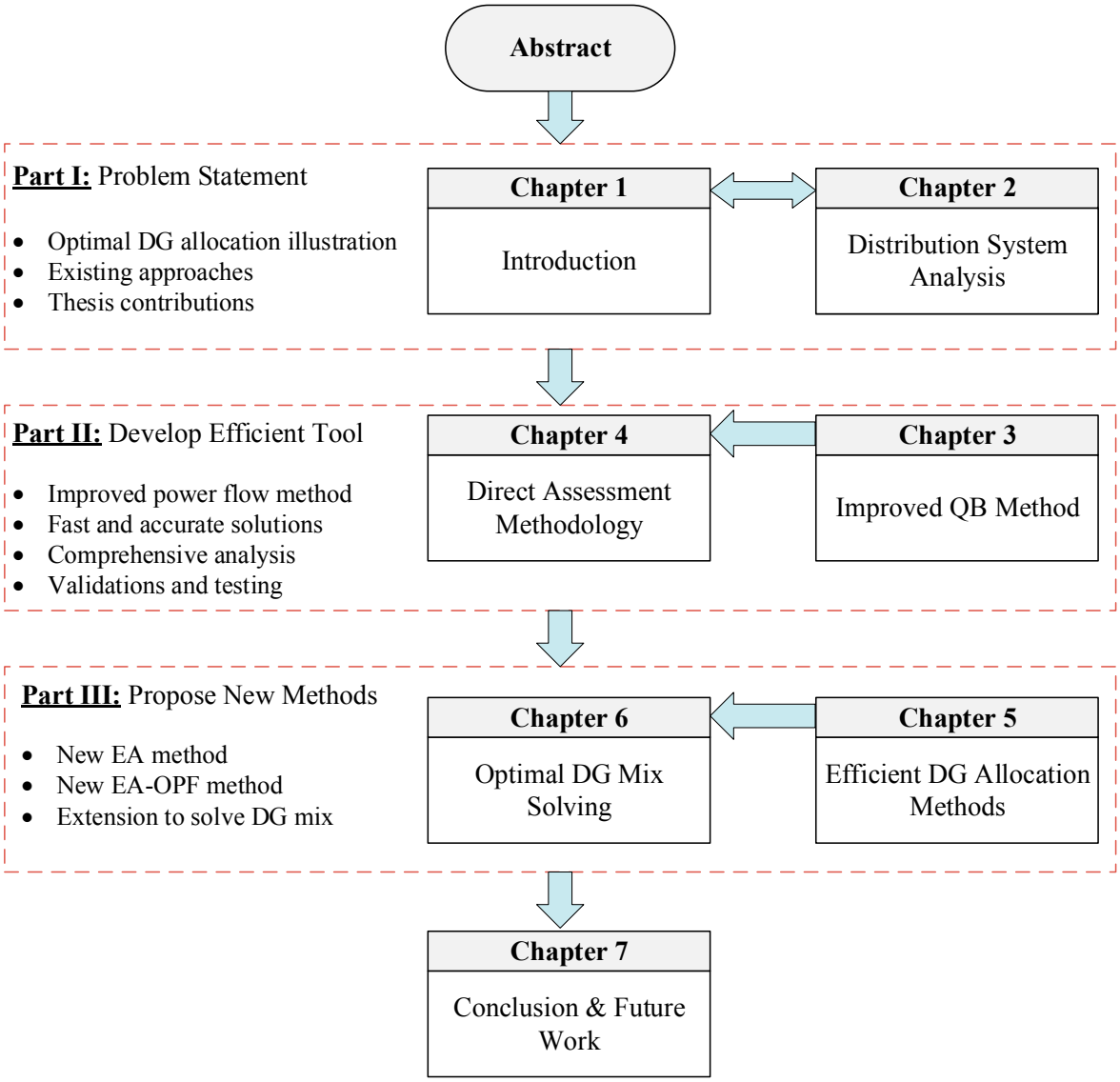

Figure 1.2 Structure of the thesis.

Chapter 2

Distribution System Analysis

Chapter 2: Distribution System Analysis

2.1 Introduction

Distribution system analysis plays a vital role in power system design, analysis, and operation. There are many methods in the literature that are used for solving power flow problem. Most of these classical methods may become inefficient in the analysis of distribution systems that are characterized by high R/X ratios or special network structures. So, there are some efficient methods which are developed specially to solve the nonlinear model of the distribution systems. These methods have the capability of solving the power flow analysis problem without convergence problems, especially for ill distribution systems, including high R/X ratios and different loading conditions. For exploring these systems, this chapter presents an overview about the main features of such electrical distribution systems and summarizes mathematical formulations of some distribution power flow methods.

The contribution of this chapter is directed to developing an efficient quadratic-based BFS power flow method for analyzing active DSs. The LV lines with neutral circuits, MV lines, and MV-LV transformers are represented explicitly. A generic decoupled quadratic-based model for both LV and MV lines are developed. For the interfaced MV-LV transformer, a sequence model is efficiently utilized, and hence a quadratic-based model is created. Furthermore, power flow models of PV and wind generation systems are developed. For wind units, quadratic equations are used to represent the nonlinearity of their models. By using the proposed method, a complete power flow solution can be handled to accurately study the behavior of active DSs. In addition, the developed power flow method has good performances in terms of accuracy, computational speed, and convergence characteristics.

2.2 Distribution System Characteristics

Generally, distributions systems have unique features, configurations, and characteristics. These systems are constructed in order to transmit electrical power from the terminals of transmission systems (i.e., load centers) to the low voltage consumers. Unlike transmission systems, distributions systems has normally neither radial structure or sometimes weakly meshed systems where the electrical power flows in one direction from the distribution stations towards loads through distribution lines. It is demonstrated that the computation processes in distribution systems are a challenge task due to their special characteristics, which requires comprehensive modeling of different components. The main characteristics of electrical distribution systems can be summarized as follows [39]:

- Their configurations are often radial or weakly meshed;
- High R/X ratios;
- Unsymmetrical phases (i.e., transposed lines);
- They contain a mix of four wire (three-phase and neutral wire), three-phase, two-phase and one-phase lines as well as under grounded cables;
- Isolated or multi-grounded configurations;
- Three-phase transformers and voltage regulators;
- High penetration of different types of DG technologies;

- Various combinations of different load types, where they are unbalanced and voltage dependent loads;
- Distribution systems are normally large-scale systems.

Driven by these features, the convergence of computation methods are negatively affected and the computational burdens are expected to be degraded. Therefore, the analysis of distribution systems requires detailed modeling of different components and efficient calculation methods. The increase of penetration of DG technologies in distribution systems also represents another challenge, where it is essential to accurately assess their impacts and contributions. These DG sources can improve or worsen system performance, and therefore, an efficient software tools are needed by DSO to effectively investigate their effects. It is important to notice that the DG units affect not only distribution systems but also transmission systems caused by the reverse power flow at the peak DG generation points which vary with environmental conditions (i.e., PV and wind units). The reverse power flow during the maximum generation powers of the distributed resources as well as high loading conditions.

2.3 Power Flow Analysis methods

Power flow computation is considered a vital numerical analysis for controlling and optimizing the operation of electrical power systems. A power flow program is a very helpful tool for distribution system operators (DSO) to study the steady state operation of modern distribution systems. Such distribution systems are characterized with unbalanced loads, unsymmetrical lines, and high distribution generation (DG) penetration [57], [58]. Fast power flow calculation is an important requirement for an effective distribution management system (DMS) [59]. The essential requirements for developing an efficient power-flow algorithm are shown in Figure 2.1 [60]. These requirements must be considered for selecting a proper power flow method for solving and analysing an electrical distribution system.

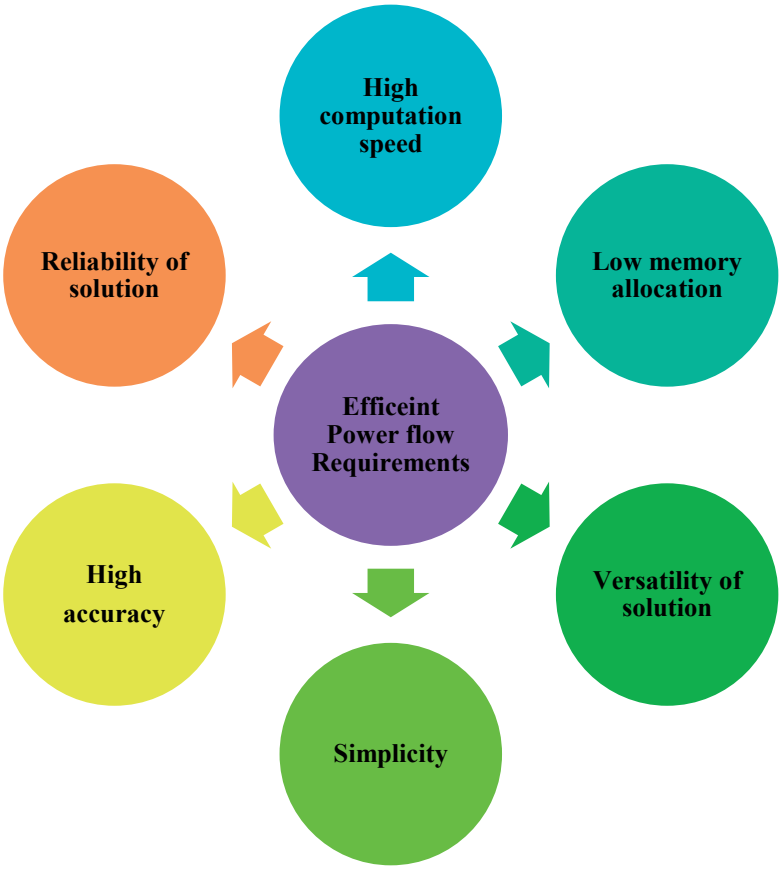

Figure 2.1 Requirements for power flow methods.

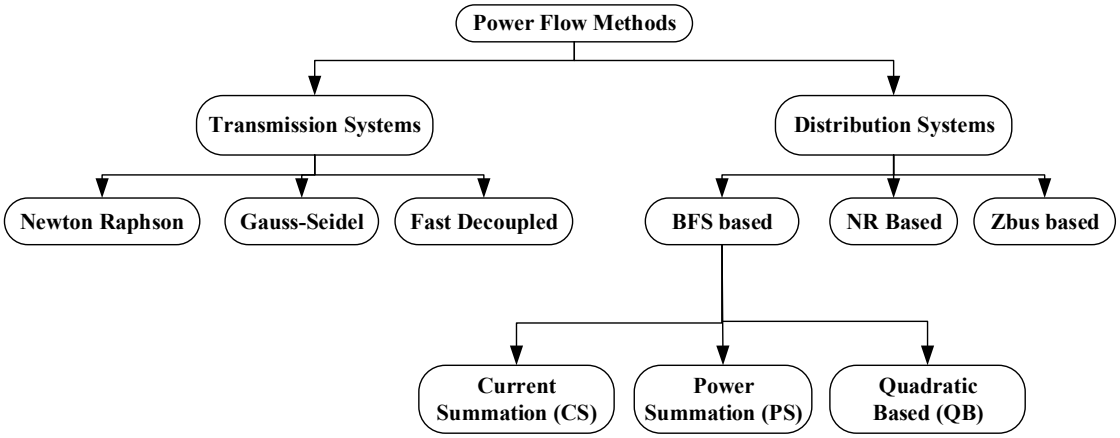

Figure 2.2 Classifications of power flow methods.

By considering these requirements in the figure, an efficient power flow can be attained. Low memory allocation is required especially for large scale systems, whereas high computation speed is important for on line control of distribution systems and DMS applications. The important of reliability of the power flow solution appears when dealing with ill-conditioned or highly stressed distribution systems. So, the key point for evaluating a power flow method is based on system's size and its condition in terms of loading level and complexity.

2.4 Power Flow for Distribution Systems

Recently, the integration of distributed generation (DG) technologies in distribution systems (DSs) has remarkably increased worldwide due to their environmental and technical benefits [1], [10]. Consequently, the characteristic of DSs has changed to be active systems that can deliver locally the electric power to load centres. The introduction of DG units in medium voltage (MV) and low voltage (LV) distribution networks has profound impacts on the system efficiency, operation, and reliability [33], [34]. To assess these impacts, an efficient power-flow method is required.

There are several methods in the literature that have been used for solving the power flow problem. Due to the special characteristics of distribution systems, many of these methods are inefficient [35], [36]. Popular methods are the backward/forward sweep (BFS) methods [37]-[39]. These methods are able to take full advantage of the radial structure of distribution systems, easy to implement, and can handle accurate results for large-scale distribution systems. In addition, they have been efficiently generalized to solve meshed distribution networks [40]. However, the convergence characteristic of these methods is very sensitive to load levels and R/X ratios [41]. For instance, the number of iterations in BFS algorithms increases considerably for systems with high R/X ratios or heavy loading conditions. It is also a fact that the excessive integration of DG units, such as wind generators with strong nonlinearity, has a massive impact on load flow results [42], and may degrade the performance of the power flow solution process [43]. Figure 2.2 shows a brief list of different power flow methods that are employing for both transmission and distribution systems.

2.5 BFS power Flow Methods

In general, the BFS methods can be classified as Kirchhoff-based (KB) [44]-[48] and quadratic-based (QB) methods [49]-[52]. These methods use a backward sweep step for calculating the branch power/current flow for each branch starting from the far ends, and a forward sweep step for computing the voltage at each receiving bus staring from slack bus to the end of the distribution system. The KB methods are further divided into current-summation (CS) [44]-[46] and power-summation (PS) methods [47]-[49]. In this work, we focus on the BFS methods due to their effectiveness and robustness for ill distribution systems under different conditions.

To facilitate understanding the BFS methods, they are applied to the IEEE 13-bus distribution system [63]. This IEEE standard test system, which are shown in Figure 2.3.a), has 13 buses, 12 distribution lines and a single power source (i.e., distribution substation) at the reference bus (bus 650). The steps of the BFS algorithms will be investigated using this presented system. With specifying of the voltage at the reference bus, an iterative solution process can be developed for power flow methods. The solution process of the three BFS methods includes the three main steps as in Figure 2.3.b). The details of the three BFS methods and their formulations can be founded in the literature. The solution steps of these methods are summarized as follows:

Step 1) ***Nodal injections:*** this solution step involves calculating the power/current injections at each bus caused by loads, DG, capacitor banks, and/or line capacitance.

Step 2) ***Backward Sweep:*** this step is started by calculating the branch currents/powers flow summations starting from the far ends until reaching the reference bus.

Step 3) ***Forward Sweep:*** with knowing the voltage of the reference bus, the voltage of the busses can be updated staring from the receiving bus of Bus-650 until the last bus.

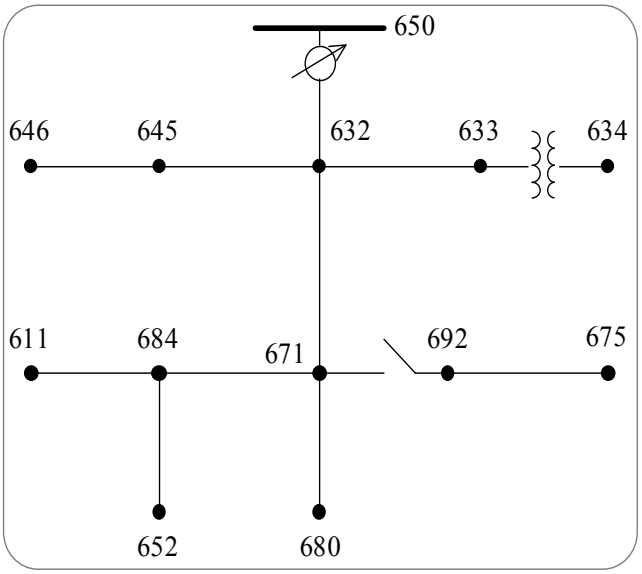

a) The IEEE 13-bus system

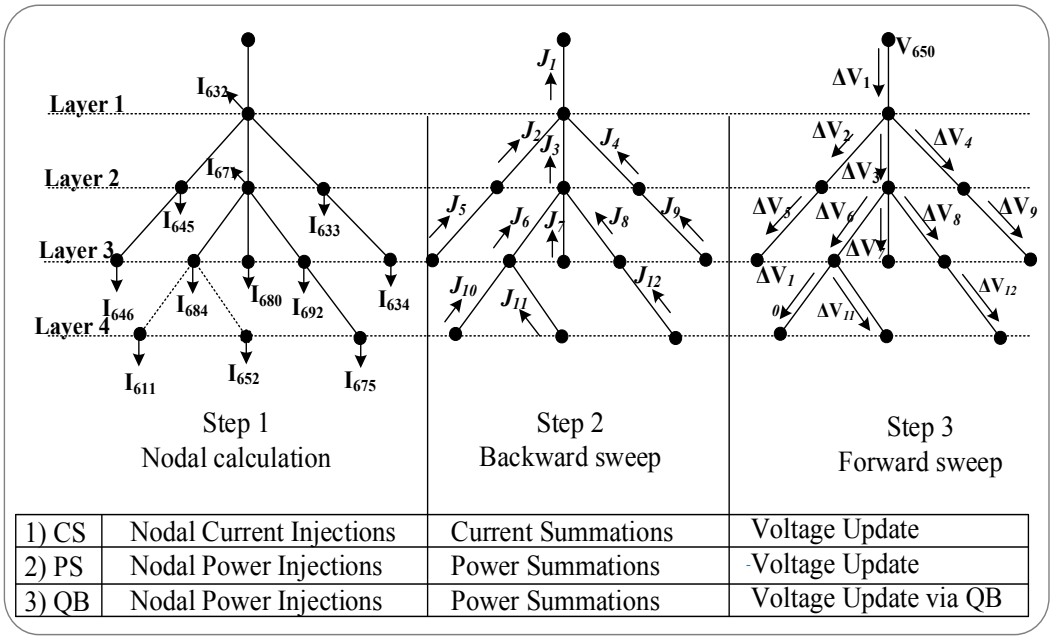

1) CS	Nodal Current Injections	Current Summations	Voltage Update
2) PS	Nodal Power Injections	Power Summations	Voltage Update
3) QB	Nodal Power Injections	Power Summations	Voltage Update via QB

b) Solution Steps

Figure 2.3 Solution steps of the BFS methods.

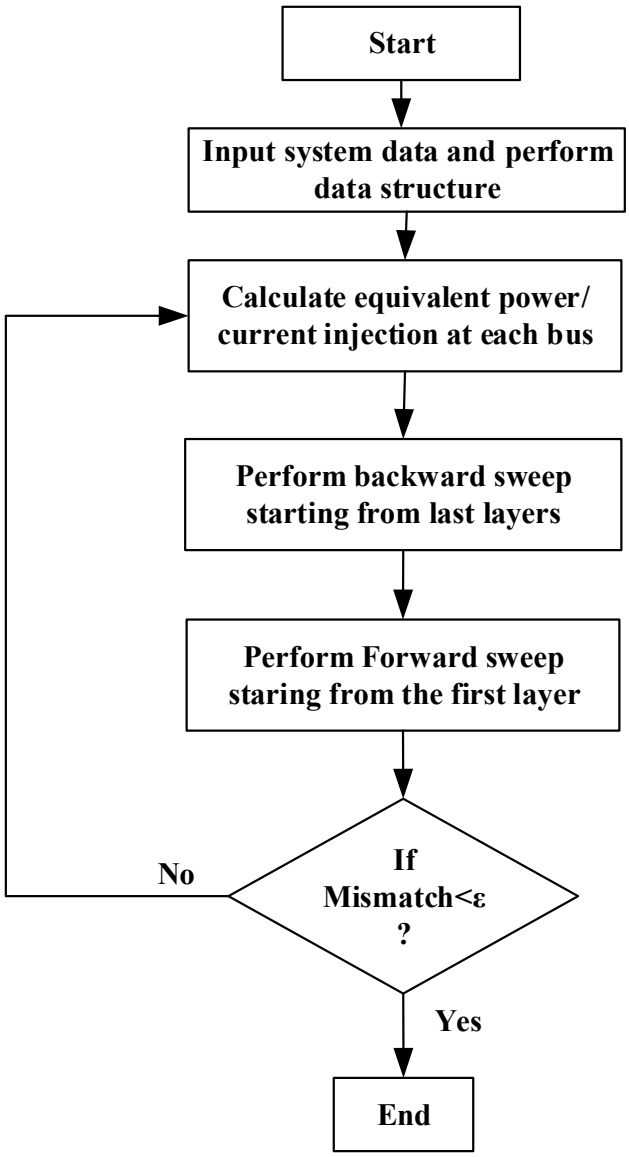

Figure 2.4 Solution steps of BFS.

After completing the above three steps, the power/voltage mismatches are computed at each bus. If the solution is converged, then terminate the solution process. Figure 2.4 shows the solution of the BFS methods. It is important to notice that for all BFS power flow methods, the branch power or current are calculated during the backward sweep step.

Great interest has been directed to the QB methods due to their robust convergence characteristics [37], [49]. Table 2.1 compares the convergence rate of the three BFS methods under different loading types. It is clear that the QB method has good features, especially for CP loading. However, most of these methods assume that the system is

balanced as in [49]-[52]. In reference [53], the authors have proposed a QB method that is applicable to unbalanced distribution systems. However, this method cannot be employed for computing voltage angles, and the treatment of the mutual coupling between the three phases is not presented. These methods cannot accurately deal with multiphase DSs. Such active DSs are characterized by integrated 3-wire MV and 4-wire LV lines that are interfaced by MV-LV distribution transformers. For the 4-wire LV sections, the neutral wire and grounding impedances must be taken into consideration to represent the neutral current due to voltage unbalance[29], [54].

Based on the above review, although considerable research has been performed to develop various QB formulations, these methods cannot effectively represent multiphase distribution systems. The key feature of the QB methods is that their QB power flow model is based active and reactive power representation of the load, where the ZIP load model is employed. Except for constant power (CP) loads, the active and reactive powers of loads are greatly affected by voltage variation, according to the ZIP model. Therefore, this load representation will degrade the convergence rate of the iterative power flow process when dealing with other load types, such as constant impedance (CI) and constant current (CC) loads. As illustrated in [53], the iterative power flow process requires much more iterations for CI loading than those for CP loading. Table 2.2 compares between the existing QB and the recommended QB approach. The existing QB formulation involves CP representation for all load types, while the recommended QB formulation suggests various models for each load types. Consequently, the load representation in the recommended formulation will solve the problem of voltage dependency and hence improve convergence rate. However, this recommendation needs a new formulation for such model and this formulation will be presented in the next chapter.

Table 2.1

Comparison of the power flow methods

Algorithms	CP Loading	CC Loading	CI Loading
CS	Good	Good	Good
PS			
QB	The best	Slow	Very Slow

Table 2.2

Summary of Different Algorithms

Load Types	Existing QB	Recommended QB
CP		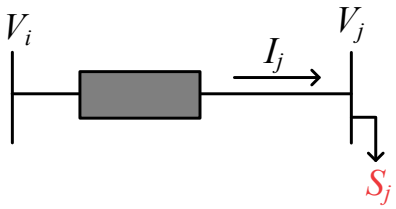
CC	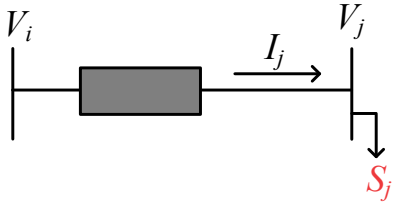	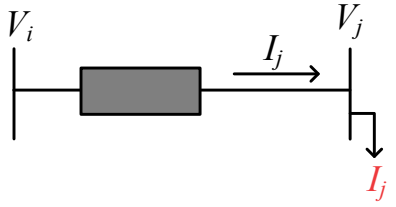
CI		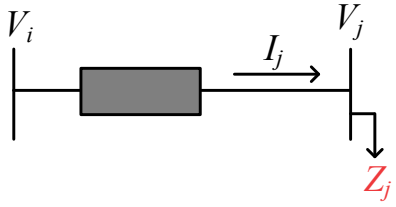

2.6 Summary

This chapter focused on providing some facts about the main features of distribution systems. These special features affect harmfully the computational process in distribution systems. Therefore, many algorithms are created to solve the ill conditioned power flow in such systems. A literature review on these methods has been performed and important conclusions have been listed. It is demonstrated that the performance of the BFS are supervisors to other methods for solving large scale multi-phase distribution systems. The QB FBS method has a good convergence for CP loading. However, as a result of voltage dependency in the case of CI and CC loading, the QB BFS method has convergence problem in such loading conditions. A review about the variant of BFS has also been given. For the power flow purpose, an improved QB power flow method will be presented in the next chapter (i.e., Chapter 3) based on the recommended treatment of the load recommended in this chapter.

Chapter 3

An Improved QB Power Flow Method For Distribution Systems

Chapter 3: An Improved QB Power Flow Method for Distribution Systems

3.1 Introduction

This chapter presents an efficient power flow method for analyzing active distribution systems (DSs). The proposed method suggests efficient quadratic-based models for various components of DSs. The power flow problem is formulated and solved by a backward/forward sweep (BFS) algorithm. Different distributed generation (DG) technologies, including photovoltaic (PV) and wind generators, are efficiently modeled and integrated to the power flow process. The proposed method is tested and validated on medium voltage (MV), low voltage (LV), and integrated MV-LV distribution test systems. Comparisons are made between the proposed BFS method and other commonly used BFS methods. The effectiveness of the proposed method is confirmed through comprehensive analyses of the IEEE distribution test systems.

3.2 Existing QB Formulation

In this section, the solution process of the BFS power flow methods is discussed. Figure 3.1 shows an example of a balanced two-bus distribution system. The power flow equation that relates the receiving bus variables to the sending bus variables is expressed as follows

$$V_j - V_i + I_j Z_{ij} = 0 \tag{3.1}$$

The loads can be modelled as constant power (CP), constant current (CC), and constant impedance (CI) [62]. For such system, the solution process of BFS is started with calculating the load current (I_j), and then updating the voltage using (3.1). This sequential procedure is repeated until the convergence is reached. Even for the simple two bus system, an iterative solution process is required, depending on the load level and the impedance of the line (i.e., the third term in (3.1)).

Regarding the QB power flow methods, they employ a direct formula to calculate the sending bus voltage as follows

$$|V_j| = f\left(|V_i|, R_{ij}, X_{ij}, P_j, Q_j\right) \tag{3.2}$$

in which

$$P_j = P_{j0}\left(|V_j|\right)^k,\ Q_j = Q_{j0}\left(|V_j|\right)^k \tag{3.3}$$

where k is equal to 0, 1, and 2 for CP, CC, and CI load types. A Direct power flow solution can be provided for CP loading where voltage dependency in (3.3) is not exist (i.e., $k=0$). On contrast, an iterative process is required in other loading types; as the voltage dependency is appear. The CI loading is considered the worst case in terms of convergence rate where the voltage dependency is the highest (i.e, $k=2$). So, the active and reactive power representation of the load, represented by (3.3), will greatly affect the robustness of the iterative process of the power flow computation for some load types.

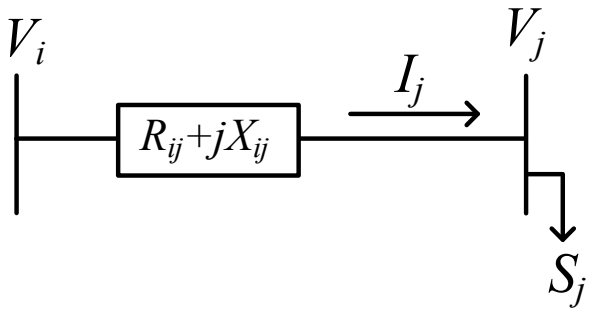

Figure 3.1 Distribution line model.

3.3 Proposed QB Formulation

In this section, a QB power flow model for distribution system branches is presented. For the system branch from bus *i* to bus *j*, the sending bus *i* variables are V_i^{Re} and V_i^{Im}, which stand for the real and imaginary parts of the voltage, respectively. The receiving bus variables include S_j, V_j^{Re} and V_j^{Im}, which refer to, respectively, the incoming power, the real and imaginary parts of the voltage at the ending bus *j*. The power flow equation that relates the receiving bus variables to the sending bus variables is expressed by (3.1). By decomposing it into real and imaginary parts, the following two equations are satisfied

$$V_j^{Re} - V_i^{Re} + \Re\left(I_j Z_{ij}\right) = 0 \tag{3.4}$$

$$V_j^{Im} - V_i^{Im} + \Im\left(I_j Z_{ij}\right) = 0 \tag{3.5}$$

The loads at each bus can be treated as CP, CC, and CI representation. Based on the load type at bus *j*, the load current (I_j) is expressed according to the second row of Table 3.1.

By solving the quadratic equation resulting from (3.4) and (3.5), a set of equations can be written in a general form as follows

$$\begin{bmatrix} V_j^{Re} \\ V_j^{Im} \end{bmatrix} = \begin{bmatrix} A_{ij} & B_{ij} \\ C_{ij} & D_{ij} \end{bmatrix} \begin{bmatrix} V_i^{Re} \\ V_i^{Im} \end{bmatrix} \tag{3.6}$$

The ABCD parameters for each load type are formulated in Table 3.1. Equation (3.6) shows that a direct power flow solution is possible in a particular loading condition for the corresponding branch. In contract, by employing (3.1), an iterative process is required to solve such power flow problem. For a multi-phase line, without considering mutual coupling, its QB line model can be expressed by

$$\begin{bmatrix} \begin{bmatrix} V_j^{Re} \\ V_j^{Im} \end{bmatrix}^a \\ \begin{bmatrix} V_j^{Re} \\ V_j^{Im} \end{bmatrix}^b \\ \begin{bmatrix} V_j^{Re} \\ V_j^{Im} \end{bmatrix}^c \end{bmatrix} = \begin{bmatrix} \left[ABCD_{ij} \right]^a & & \\ & \left[ABCD_{ij} \right]^b & \\ & & \left[ABCD_{ij} \right]^c \end{bmatrix} \begin{bmatrix} \begin{bmatrix} V_i^{Re} \\ V_i^{Im} \end{bmatrix}^a \\ \begin{bmatrix} V_i^{Re} \\ V_i^{Im} \end{bmatrix}^b \\ \begin{bmatrix} V_i^{Re} \\ V_i^{Im} \end{bmatrix}^c \end{bmatrix} \tag{3.7}$$

Equation (3.7) can be rewritten, in condensed form, as

$$\begin{bmatrix} \mathbf{V}_j^{Re} \\ \mathbf{V}_j^{Im} \end{bmatrix}^{abc} = \left[\mathbf{ABCD}_{ij} \right]^{abc} \begin{bmatrix} \mathbf{V}_i^{Re} \\ \mathbf{V}_i^{Im} \end{bmatrix}^{abc} \tag{3.8}$$

Table 3.1 Parameters of the proposed QB model for different load types

	CP Load	**CI Load**	**CC Load**
I_j	$S_j = P_j + jQ_j$	$Z_j = \lvert V_{j,rated} \rvert^2 \big/ \left(S_j \right)^*$	$I_{j,rated} = S_j^* \big/ \lvert V_{j,rated} \rvert$
	$I_j = \left(S_j / V_j \right)^*$	$I_j = \left(V_j / Z_j \right)$	$I_j = I_{j,rated} \left(V_j \big/ \lvert V_j \rvert \right)$
A_{ij}	$\frac{1}{2} + \sqrt{\frac{1}{4} - \left(\frac{P_j R_{ij} +}{Q_j X_{ij}} \right) \Big/ \lvert V_i \rvert^2 - B_{ij}^2}$	$\frac{R_j^2 + X_j^2 + R_j R_{ij} + X_j X_{ij}}{\left(R_j + R_{ij} \right)^2 + \left(X_j + X_{ij} \right)^2}$	$\frac{\lvert V_j \rvert + I_{j,rated}^{Re} R_{ij} - I_{j,rated}^{Im} X_{ij}}{\lvert V_j \rvert + 2\left(I_{j,rated}^{Re} R_{ij} - I_{j,rated}^{Im} X_{ij} \right) + \lvert I_{j,rated} \rvert^2 \lvert Z_{ij} \rvert^2 / \lvert V_j \rvert}$
B_{ij}	$\frac{P_j X_{ij} - Q_j R_{ij}}{\lvert V_i \rvert^2}$	$\frac{R_j X_{ij} - X_j R_{ij}}{\left(R_j + R_{ij} \right)^2 + \left(X_j + X_{ij} \right)^2}$	$\frac{I_{j,rated}^{Im} R_{ij} + I_{j,rated}^{Re} X_{ij}}{\lvert V_j \rvert + 2\left(I_{j,rated}^{Re} R_{ij} - I_{j,rated}^{Im} X_{ij} \right) + \lvert I_{j,rated} \rvert^2 \lvert Z_{ij} \rvert^2 / \lvert V_j \rvert}$
C_{ij}	$-B_{ij}$	$-B_{ij}$	B_{ij}
D_{ij}	A_{ij}	A_{ij}	$-A_{ij}$

3.4 QB Models of distribution system Components

Based on the proposed QB model, generic models of various system components are established. In general, the distribution system components are unbalanced; hence, unsymmetrical mutual coupling exists among the three phases. Therefore, modelling of such components requires special formulations. In this section, efficient models for the

three phase-coupled components are established. QB models are derived by fully utilizing uncoupled three phase characteristics without approximations.

3.4.1 Modelling of Three-phase Lines

The distribution lines are modelled with a 3×3 impedance matrix for multi-grounded systems [62], as shown in Figure3.2.a). The following basic equation represents the relationship between bus voltages and branch currents

$$\begin{bmatrix} \begin{bmatrix} V_j^{\mathrm{Re}} \\ V_j^{\mathrm{Im}} \end{bmatrix}^a \\ \begin{bmatrix} V_j^{\mathrm{Re}} \\ V_j^{\mathrm{Im}} \end{bmatrix}^b \\ \begin{bmatrix} V_j^{\mathrm{Re}} \\ V_j^{\mathrm{Im}} \end{bmatrix}^c \end{bmatrix} - \begin{bmatrix} \begin{bmatrix} V_i^{\mathrm{Re}} \\ V_i^{\mathrm{Im}} \end{bmatrix}^a \\ \begin{bmatrix} V_i^{\mathrm{Re}} \\ V_i^{\mathrm{Im}} \end{bmatrix}^b \\ \begin{bmatrix} V_i^{\mathrm{Re}} \\ V_i^{\mathrm{Im}} \end{bmatrix}^c \end{bmatrix} + \begin{bmatrix} \begin{bmatrix} R_{ij} & -X_{ij} \\ X_{ij} & R_{ij} \end{bmatrix}^{aa} & \begin{bmatrix} R_{ij} & -X_{ij} \\ X_{ij} & R_{ij} \end{bmatrix}^{ab} & \begin{bmatrix} R_{ij} & -X_{ij} \\ X_{ij} & R_{ij} \end{bmatrix}^{ac} \\ \begin{bmatrix} R_{ij} & -X_{ij} \\ X_{ij} & R_{ij} \end{bmatrix}^{ba} & \begin{bmatrix} R_{ij} & -X_{ij} \\ X_{ij} & R_{ij} \end{bmatrix}^{bb} & \begin{bmatrix} R_{ij} & -X_{ij} \\ X_{ij} & R_{ij} \end{bmatrix}^{bc} \\ \begin{bmatrix} R_{ij} & -X_{ij} \\ X_{ij} & R_{ij} \end{bmatrix}^{ca} & \begin{bmatrix} R_{ij} & -X_{ij} \\ X_{ij} & R_{ij} \end{bmatrix}^{cb} & \begin{bmatrix} R_{ij} & -X_{ij} \\ X_{ij} & R_{ij} \end{bmatrix}^{cc} \end{bmatrix} \begin{bmatrix} \begin{bmatrix} I_j^{\mathrm{Re}} \\ I_j^{\mathrm{Im}} \end{bmatrix}^a \\ \begin{bmatrix} I_j^{\mathrm{Re}} \\ I_j^{\mathrm{Im}} \end{bmatrix}^b \\ \begin{bmatrix} I_j^{\mathrm{Re}} \\ I_j^{\mathrm{Im}} \end{bmatrix}^c \end{bmatrix} = 0 \tag{3.9}$$

For the phase k

$$\begin{bmatrix} V_j^{\mathrm{Re}} \\ V_j^{\mathrm{Im}} \end{bmatrix}^k - \begin{bmatrix} V_i^{\mathrm{Re}} \\ V_i^{\mathrm{Im}} \end{bmatrix}^k + \begin{bmatrix} R_{ij} & -X_{ij} \\ X_{ij} & R_{ij} \end{bmatrix}^{kk} \begin{bmatrix} I_j^{\mathrm{Re}} \\ I_j^{\mathrm{Im}} \end{bmatrix}^k + \begin{bmatrix} \Delta V_{ij-mutual}^{\mathrm{Re}} \\ \Delta V_{ij-mutual}^{\mathrm{Im}} \end{bmatrix}^k = 0 \quad , \quad k \in (a,b,c) \tag{3.10}$$

in which $$\begin{bmatrix} \Delta V_{ij-mutual}^{\mathrm{Re}} \\ \Delta V_{ij-mutual}^{\mathrm{Im}} \end{bmatrix}^k = \sum_{\substack{m\in(a,b,c) \\ m\neq k}} \begin{bmatrix} R_{ij} & -X_{ij} \\ X_{ij} & R_{ij} \end{bmatrix}^{km} \begin{bmatrix} I_j^{\mathrm{Re}} \\ I_j^{\mathrm{Im}} \end{bmatrix}^m \tag{3.11}$$

where $\Delta V_{ij-mutual}^{k}$ represents the voltage drop at each phase k caused by the mutual coupling between the distribution lines. This voltage drop can be modelled as voltage sources in system phases, as shown in Figure 3.2.b). It is clear from the figure that a dummy bus can be created between buses i and j, and the following equation is satisfied

$$\begin{bmatrix} V_{j-dummy}^{\mathrm{Re}} \\ V_{j-dummy}^{\mathrm{Im}} \end{bmatrix}^k = \begin{bmatrix} V_i^{\mathrm{Re}} \\ V_i^{\mathrm{Im}} \end{bmatrix}^k - \begin{bmatrix} \Delta V_{ij-mutual}^{\mathrm{Re}} \\ \Delta V_{ij-mutual}^{\mathrm{Im}} \end{bmatrix}^k \tag{3.12}$$

For the line section between the dummy bus and bus j, the following equation holds.

$$\begin{bmatrix} V_j^{\mathrm{Re}} \\ V_j^{\mathrm{Im}} \end{bmatrix}^k - \begin{bmatrix} V_{j-dummy}^{\mathrm{Re}} \\ V_{j-dummy}^{\mathrm{Im}} \end{bmatrix}^k + \begin{bmatrix} R_{ij} & -X_{ij} \\ X_{ij} & R_{ij} \end{bmatrix}^{kk} \begin{bmatrix} I_j^{\mathrm{Re}} \\ I_j^{\mathrm{Im}} \end{bmatrix}^k = 0 \tag{3.13}$$

The resulting decoupled line segment, from the dummy bus to bus j, which is represented by (3.6), can be expressed by the proposed QB model as follows

$$\begin{bmatrix} V_j^{Re} \\ V_j^{Im} \end{bmatrix}^k = \left[ABCD_{ij} \right]^k \begin{bmatrix} V_{j-dummy}^{Re} \\ V_{j-dummy}^{Im} \end{bmatrix}^k \quad , \qquad k \in (a,b,c) \tag{3.14}$$

In the same manner in (3.8), by substituting (3.12) in (3.14), the complete QB model for the three-phase line is expressed by

$$\begin{bmatrix} \mathbf{V}_j^{Re} \\ \mathbf{V}_j^{Im} \end{bmatrix}^{abc} = \left[\mathbf{ABCD}_{ij} \right]^{abc} \begin{bmatrix} \mathbf{V}_i^{Re} - \mathbf{\Delta V}_{ij-mutual}^{Re} \\ \mathbf{V}_i^{Im} - \mathbf{\Delta V}_{ij-mutual}^{Im} \end{bmatrix}^{abc} \tag{3.15}$$

Regarding the shunt capacitances of the distribution lines and capacitors banks, they are considered as a CI loads and integrated to the power flow process.

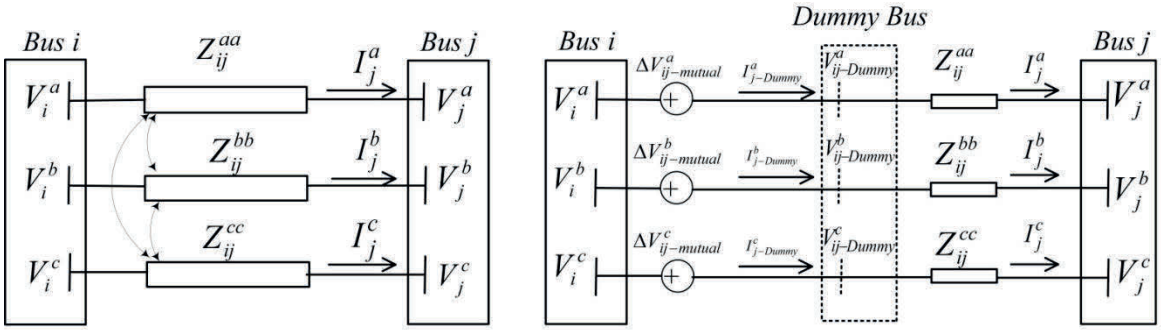

a) Coupled Model *b) Decoupled Model*

Figure 3.2 Model of distribution lines.

3.4.2 Modelling of Transformers

Transformers are used in distribution systems for interfacing between MV and LV distribution lines, where D-GY transformers are normally employed. Another usage is to interface different DG types to distribution systems. It is demonstrated that the power flow models of distribution transformers have many challenges [48]. A distribution transformer can be represented by three decoupled sequence networks, as shown in Table 3.2. The sequence voltages at the primary side of the transformer can be computed from the phase voltages as follows

$$\begin{bmatrix} \begin{bmatrix} V_p^{Re} \\ V_p^{Im} \end{bmatrix}^0 \\ \begin{bmatrix} V_p^{Re} \\ V_p^{Im} \end{bmatrix}^1 \\ \begin{bmatrix} V_p^{Re} \\ V_p^{Im} \end{bmatrix}^2 \end{bmatrix} = \frac{1}{3} \begin{bmatrix} \begin{bmatrix} 1 & 0 \\ 0 & 1 \end{bmatrix} & \begin{bmatrix} 1 & 0 \\ 0 & 1 \end{bmatrix} & \begin{bmatrix} 1 & 0 \\ 0 & 1 \end{bmatrix} \\ \begin{bmatrix} 1 & 0 \\ 0 & 1 \end{bmatrix} & \begin{bmatrix} \beta & -\alpha \\ \alpha & \beta \end{bmatrix} & \begin{bmatrix} \beta & \alpha \\ -\alpha & \beta \end{bmatrix} \\ \begin{bmatrix} 1 & 0 \\ 0 & 1 \end{bmatrix} & \begin{bmatrix} \beta & \alpha \\ -\alpha & \beta \end{bmatrix} & \begin{bmatrix} \beta & -\alpha \\ \alpha & \beta \end{bmatrix} \end{bmatrix} \begin{bmatrix} \begin{bmatrix} V_p^{Re} \\ V_p^{Im} \end{bmatrix}^a \\ \begin{bmatrix} V_p^{Re} \\ V_p^{Im} \end{bmatrix}^b \\ \begin{bmatrix} V_p^{Re} \\ V_p^{Im} \end{bmatrix}^c \end{bmatrix} \quad , \quad \alpha = sin(120), \beta = cos(120) \tag{3.16}$$

where 0,1, and 2 refer to zero, positive, and negative sequence component of the transformer. V_p and V_s are the voltages of the primary and secondary sides of the transformer, respectively. Expressing (3.16) in condensed form

$$\begin{bmatrix} \mathbf{V}_p^{Re} \\ \mathbf{V}_p^{Im} \end{bmatrix}^{012} = [\mathbf{W}] \begin{bmatrix} \mathbf{V}_p^{Re} \\ \mathbf{V}_p^{Im} \end{bmatrix}^{abc} \tag{3.17}$$

Since the sequence networks are completely decoupled, a QB model for sequence equivalent circuits of the transformer can be expressed by

$$\begin{bmatrix} \begin{bmatrix} V_s^{Re} \\ V_s^{Im} \end{bmatrix}^0 \\ \begin{bmatrix} V_s^{Re} \\ V_s^{Im} \end{bmatrix}^1 \\ \begin{bmatrix} V_p^{Re} \\ V_s^{Im} \end{bmatrix}^2 \end{bmatrix} = \begin{bmatrix} [ABCD_{ps}]^0 & [ABCDT_{ps}]^1 & [ABCDT_{ps}]^2 \end{bmatrix} \begin{bmatrix} \begin{bmatrix} V_p^{Re} \\ V_p^{Im} \end{bmatrix}^0 \\ \begin{bmatrix} V_p^{Re} \\ V_p^{Im} \end{bmatrix}^1 \\ \begin{bmatrix} V_p^{Re} \\ V_p^{Im} \end{bmatrix}^2 \end{bmatrix} \tag{3.18}$$

in which

$$[ABCDT_{ps}] = [ABCD_{ps}] \begin{bmatrix} T^{Re} & -T^{Im} \\ T^{Im} & T^{Re} \end{bmatrix}$$

where **T** represents the phase shifts in the positive and negative equivalent circuits and expressed in (3.18) to incorporate the phase shifts in the transformer model. Rewriting (3.18) in condensed form

$$\begin{bmatrix} \mathbf{V}_s^{Re} \\ \mathbf{V}_s^{Im} \end{bmatrix}^{012} = [\mathbf{ABCD}_{ps}] \begin{bmatrix} \mathbf{V}_p^{Re} \\ \mathbf{V}_p^{Im} \end{bmatrix}^{012} \tag{3.19}$$

Similar to (3.17), the phase voltages at the secondary side of the transformer can be computed from the sequence voltages by

$$\begin{bmatrix} \mathbf{V}_s^{Re} \\ \mathbf{V}_s^{Im} \end{bmatrix}^{abc} = [\mathbf{W}]^{-1} \begin{bmatrix} \mathbf{V}_s^{Re} \\ \mathbf{V}_s^{Im} \end{bmatrix}^{012} \tag{3.20}$$

If (3.17) and (3.19) are substituted in (3.20),

$$\begin{bmatrix} \mathbf{V}_s^{Re} \\ \mathbf{V}_s^{Im} \end{bmatrix}^{abc} = [\mathbf{Y}] \begin{bmatrix} \mathbf{V}_p^{Re} \\ \mathbf{V}_p^{Im} \end{bmatrix}^{abc} \tag{3.21}$$

where

$$[\mathbf{Y}] = [\mathbf{W}]^{-1} [\mathbf{ABCD}_{ps}] [\mathbf{W}]$$

Regarding to the shunt elements in the zero sequence circuit, they are represented by their current injection equivalents in phase domain. The phase shifts and parameters of the zero sequence circuit for different transformer connections are given in Table 3.3.

Table 3.2 Generalized transformer models

Positive Sequence	Negative Sequence	Zero Sequence
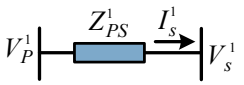	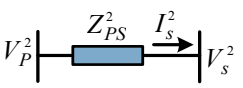	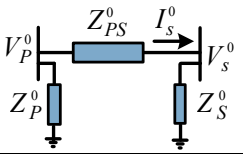

Table 3.3 Parameters of different transformer connections

Transformer Connections	Transformer Parameters				
	T^1	T^2	Z_{ps}^0	Z_p^0	Z_s^0
GY-GY	1.0	1.0	Z_t	∞	∞
GY-D	$1\angle 30$	$1\angle -30$	∞	Z_t	∞
D-GY	$1\angle -30$	$1\angle 30$	∞	∞	Z_t
D-Y	$1\angle -30$	$1\angle 30$	∞	∞	∞

3.4.3 Modelling of DGs

Generally, DG units can be treated as PQ or PV buses, based on their type and size. References [39] and [60][62] have presented comprehensive models of different DG types. These models can be integrated to the proposed QB power flow model. Here, the methodology of developing their QB model is generally illustrated. A typical DG unit often consist of two major parts: 1) a DG technology (e.g. gas turbine, wind turbine, photovoltaic arrays, etc.) and 2) an interfaced device (e.g. synchronous generator, induction generator, power conditioning unit (PCU), etc.). Sequence models for induction synchronous and generators are illustrated in [39], [60]. In the same manner with the transformer, the QB models for these generators can be constructed in sequence domain, where the equivalent circuits are decoupled. It is important to notice that the calculated DG power injections ($P_{DGi}^{abc}, Q_{DGi}^{abc}$) must be updated for each power flow iteration until the convergence is reached. For the photovoltaic systems, the power injections can be calculated with considering the environmental conditions and the controller scheme of PCU.

3.4.3.1 Wind Generators

The wind generators consist of three components: wind turbines, induction generators (IG), and interface transformers to DSs. To model IGs that are connected to unbalanced systems with transformers, sequence equivalent circuits are usually employed, as given in Figure 3. The positive and negative equivalent circuits are completely decoupled. The terminal voltages at the terminal of the IG unit are specified, whereas the terminal currents are to be computed, thereby calculating the equivalent power injection at the point of common connection (PCC). The modeling procedures of IG are based on the available data about the machine as follows:

1) ***Specified Slip IG Model:*** this IG model is considered a linear model which can be solved directly using the equivalent circuits of the sequence components. With specifying the IG slip, the terminal current injections are given by

$$I_p^m = \frac{V_p^m}{Z_{eq}^m} \ , \ Z_{eq}^m = Z_t + Z_s + Z_M \,||\, Z_r^m \tag{3.22}$$

2) Specified Mechanical Power IG Model: In this case, the IG model is nonlinear. Therefore, an iterative process is required to calculate the equivalent current injections. The mechanical power (P_M) of the IG has a specified value, and the machine slip is unknown. The relationship between the shaft power and P_M can be expressed as follows

$$3\sum_{m=1}^{2}\left(I_r^m\right)^2\frac{\left(1-slip^m\right)}{slip^m}R_r-P_M=0 \tag{3.23}$$

To solve the IG model, an iterative solution process is developed as follows:

Step 1: Set an initial value for the machine slip.

Step 2: Calculate rotor currents for the two sequence circuits.

Step 3: Update the slip by solving the following quadratic equation, which is driven from (3.23):

$$\left(3I_r^{1^2}+3I_r^{l^2}+P_M\right)slip^{1^2}-\left(9I_r^{1^2}+3I_r^{l^2}+2P_M\right)slip^1+6I_r^{l^2}=0 \tag{3.24}$$

Step 4: Continue if the calculated slip is converged to a specified tolerance, otherwise go to step 2.

Step 5: Calculate the current injections at machine terminals using (3.24).

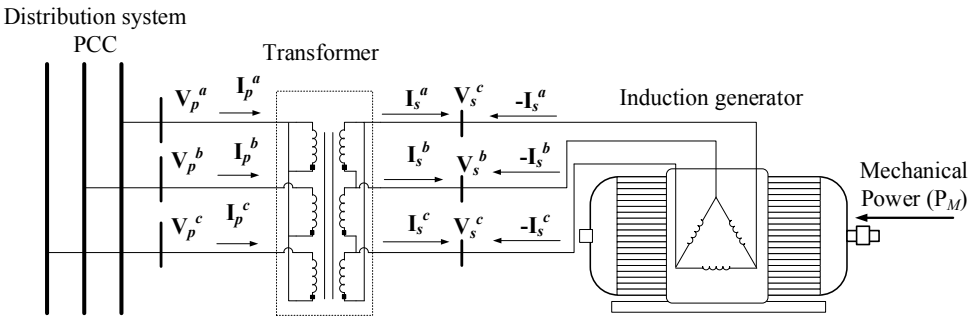

(a) Schematic diagram of the wind system

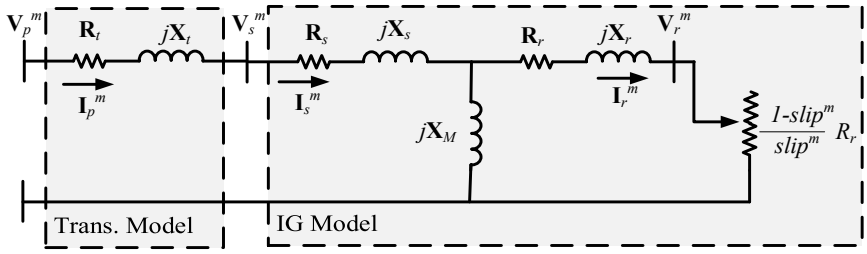

(b) Sequence components model of the wind system

Figure 3.3 The schematic diagram and the model of the wind unit.

It is worth noting that the generated power injections from the IG, in phase coordinates, are needed in the power flow iterative process. This can be computed by converting the calculated injected currents form the sequence domain to the phase domain. Consequently, the terminal power injections can be calculated.

3.4.3.2 PV Modeling

PV units are normally composed of two parts: PV arrays and a power conditioning unit (PCU). The main aim of this section is to develop a component model for the grid connected PV units which can be integrated with an unbalanced power flow solver as follows:

1) ***PV Array Model:*** the PV arrays convert the sunlight power to DC power under given environmental conditions. The DC power, P_{unit}^{DC} , can be calculated as follows:

$$P_{unit}^{DC}=N_{array}\,P_{array} \tag{3.25}$$

$$P_{array}=N_{cell}\,P_{cell} \tag{3.26}$$

where N_{cell} is the total number of the PV cells connected in series and parallel connections in the PV array, and N_{array} is the total number of arrays in the PV unit. Here, the maximum power point (MPP) of the PV unit at specific temperature and irradiation values is obtained by using an iterative process [34].

2) ***PCU Model:*** the PCU converts P_{unit}^{DC} to a specific AC power injection, P_{unit}^{AC} . Based on its efficiency (μ_{PCU}), the P_{unit}^{AC} value is calculated under given environmental conditions and the PV power factor (PF) as follows:

$$P_{unit}^{AC}=\mu_{PCU}\, P_{unit}^{DC} \tag{3.27}$$

$$Q_{unit}^{AC}= sin\left(cos^{-1}(PF_{unit})\right)\; P_{unit}^{AC} \tag{3.28}$$

3.5 Solution Process of QB

The solution process of the proposed power flow method is exemplified in Figure 3.4, where a 10-bus test system is used. The data structure algorithm in [44] is used here to arrange system data. Similar to BFS methods, the solution process of the proposed method involves three main steps: step1) calculate current injections, step2) backward sweep and step3) forward sweep. The first step involves calculating the current injections at all nodes. The main target of the second step is to calculate the power flow passing through the series elements, and bus voltages are updated using step 3. The QB models are employed in step 3 for all series components. These steps are repeated sequentially until precise absolute power mismatches are satisfied. The flow chart of the power flow solution process is described in Figure 3.5.

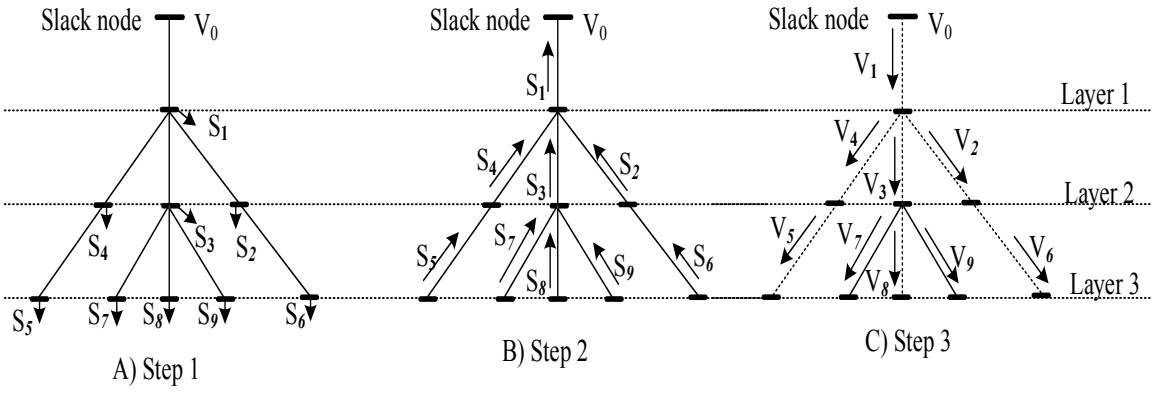

Figure 3.4 Steps of the proposed method.

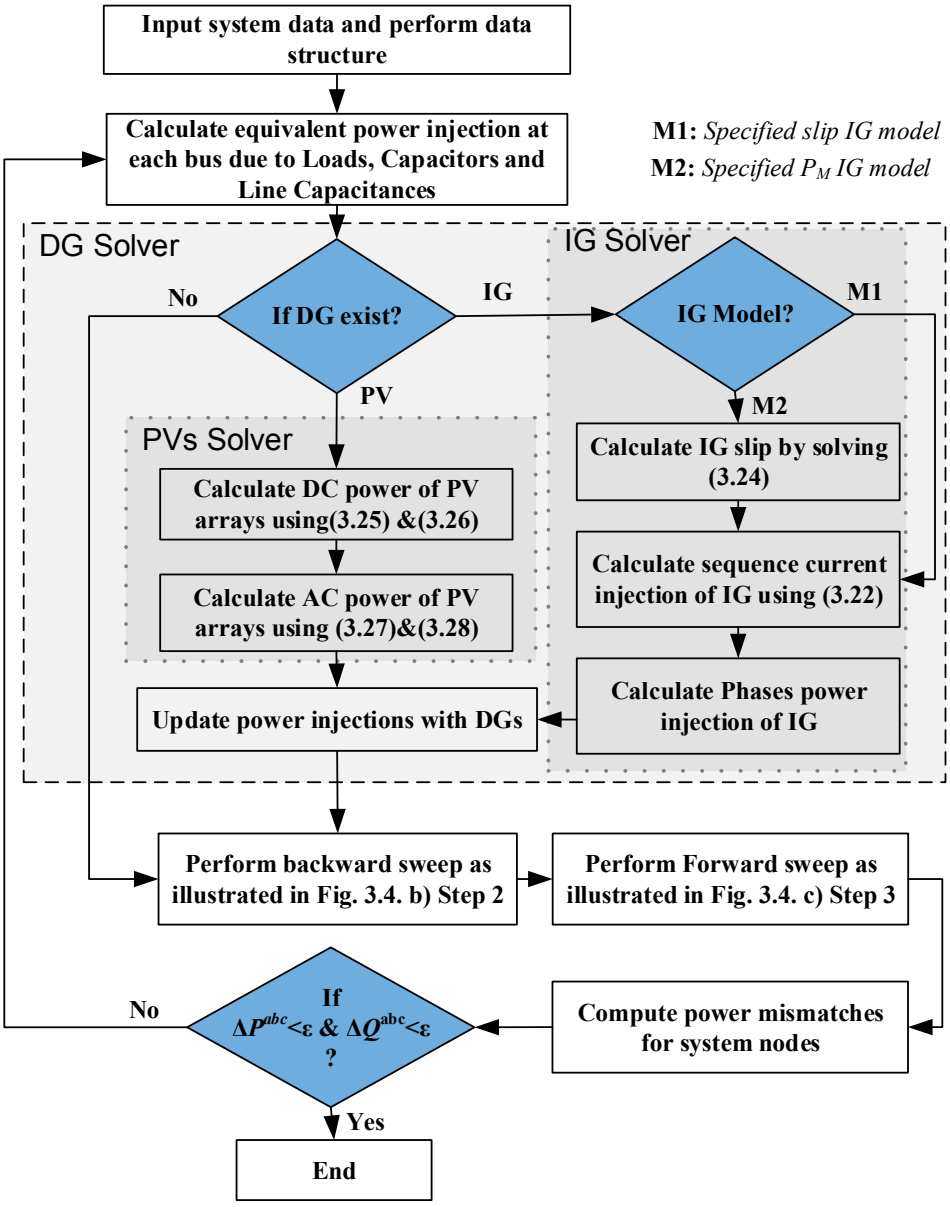

Figure 3.5 Flow chart of the proposed method.

3.6 Results and discussions

Several test systems were used to test the proposed method. Comprehensive comparisons were made among two existing methods, reported in [39] and [48], which represent the current-summation and the power-summation BFS methods, respectively. For convenience, these methods are labelled M1 and M2 in the figures, respectively. Regarding

the proposed QBBFS method, it is labelled QB. The methods are implemented in C++ and tested on a PC, with Intel Core i5 at 2.67 GHz and 4.00-GB RAM. Many tests were performed on different test systems to show the effectiveness of the proposed method as follows.

3.6.1 Validation and Performance Test

The methods were tested on many distribution systems with different sizes and configurations as follows:

- ***Balanced distribution systems***: 33-bus and 69-bus systems [31], [32].
- ***Unbalanced distribution systems***: 10-bus and 25-bus systems [55].
- ***Modified IEEE 123-bus distribution system:*** In this test [63], the regulators are ignored, and all loads are considered as CP loads.

A strong agreement is noticed in power flow results obtained by the three methods for both balanced and unbalanced distribution systems. The accuracy of the methods is also validated with employing OpenDSS software [64]. For instance, Table 3.4 compares the voltage magnitudes of the unbalanced 10-bus system for different methods, whereas the power flow results are almost identical. The matching in voltage angles are also observed for the test systems.

It is demonstrated that power flow methods often provide poor performances under critical conditions, such as heavy loading conditions and high R/X ratios. Therefore, the performances of the power flow methods are examined under the following ill conditions:

Table 3.4 Voltage magnitudes for 10-bus system

Bus	Phase	OpenDSS	QB	M1	M2
1	**A**	1.00000	1.00000	1.00000	1.00000
	B	1.00000	1.00000	1.00000	1.00000
	C	1.00000	1.00000	1.00000	1.00000
2	**A**	0.95564	0.95564	0.95564	0.95564
	B	0.99303	0.99303	0.99303	0.99303
	C	0.98639	0.98638	0.98638	0.98638
3	**A**	0.94459	0.94458	0.94458	0.94458
	B	0.99296	0.99295	0.99295	0.99295
4	**A**	0.93060	0.93059	0.93059	0.93059
	B	0.99166	0.99165	0.99165	0.99165
	C	0.97845	0.97844	0.97844	0.97844
5	**B**	0.99063	0.99063	0.99063	0.99063
	C	0.98424	0.98423	0.98423	0.98423
6	**A**	0.91901	0.91901	0.91901	0.91901
7	**A**	0.92359	0.92359	0.92359	0.92359
	C	0.97487	0.97486	0.97486	0.97486
8	**A**	0.92269	0.92268	0.92269	0.92268
	B	0.98996	0.98995	0.98995	0.98995
9	**C**	0.96712	0.96710	0.96710	0.96710
10	**B**	0.98155	0.98154	0.98154	0.98154

A) Different Load Levels: Concerning the effects of different load levels on the power flow process, Table 3.5 compares the number of iteration for the three methods under different load factors (LFs), and the corresponding execution times are compared in Figure 3.6. As seen in the table and the figure, the proposed method is fastest at all load levels. As the load level increases, the number of iterations and the execution time also increase, but the proposed method seems to be less sensitive to the load level than M1 and M2. The main reason for this improvement is that the proposed power flow method utilized efficient

QB models. These models affected in a positive manner on the convergence rate of the proposed method.

B) High R/X Ratios: Table 3.6 and Figure 3.7 compare the performance of the methods under different R/X ratios. It is interesting to note that, with increasing the R/X ratios, M1 and M2 exhibit poor convergences. On contrast, the proposed method is less sensitive to increasing R/X ratios.

To sum up this subsection, the proposed method has better convergence characteristics when compared with M1 and M2 at different load levels and R/X ratios. The proposed method shows robust performances, especially in the case of ill conditions (i.e, high LFs and R/X ratios).

Table 3.5 Number of iterations with different LF values

LF	33-Bus			69-Bus			10-Bus			25-Bus			123-Bus		
	QB	M2	M1	QB	M2	M1	QB	M2	M1	QB	M2	M1	QB	M2	M1
1.0	3	4	5	4	5	6	3	4	5	3	4	5	5	5	6
1.6	4	5	7	5	6	8	4	5	7	4	4	6	5	6	8
2.2	5	7	9	6	8	11	4	6	9	4	5	7	6	7	11
2.8	7	9	14	9	12	18	6	8	13	5	6	9	9	14	23

Table 3.6 Number of iterations with different R/X values

R/X	33-Bus			69-Bus			10-Bus			25-Bus			123-Bus		
	QB	M2	M2	QB	M2	M1	QB	M2	M1	QB	M2	M1	QB	M2	M1
2.0	4	5	7	5	6	9	3	4	6	3	4	6	5	5	7
2.6	5	6	9	6	8	12	4	5	7	4	5	6	5	5	7
3.2	6	8	11	9	12	17	4	5	7	4	5	7	5	6	8
3.8	8	11	16	-	-	-	4	6	9	4	5	8	5	6	9

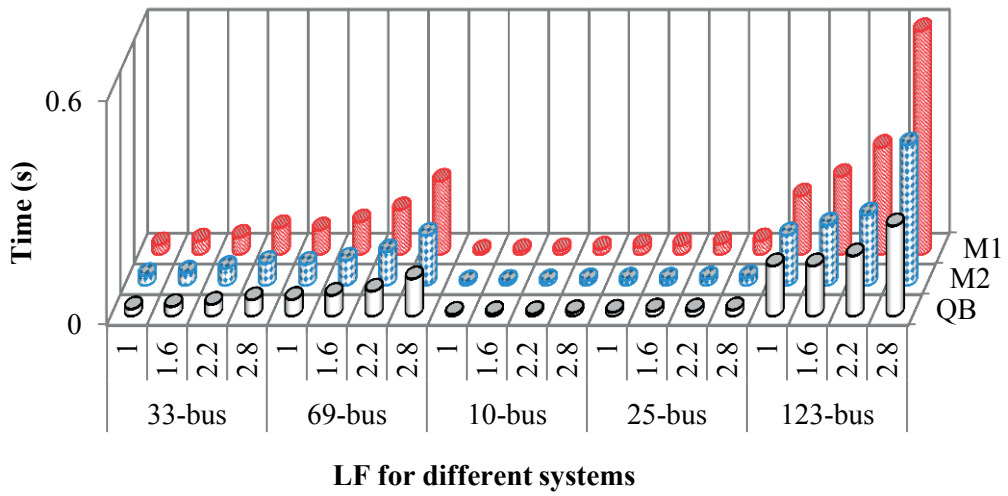

Figure 3.6 Execution time with different LF values.

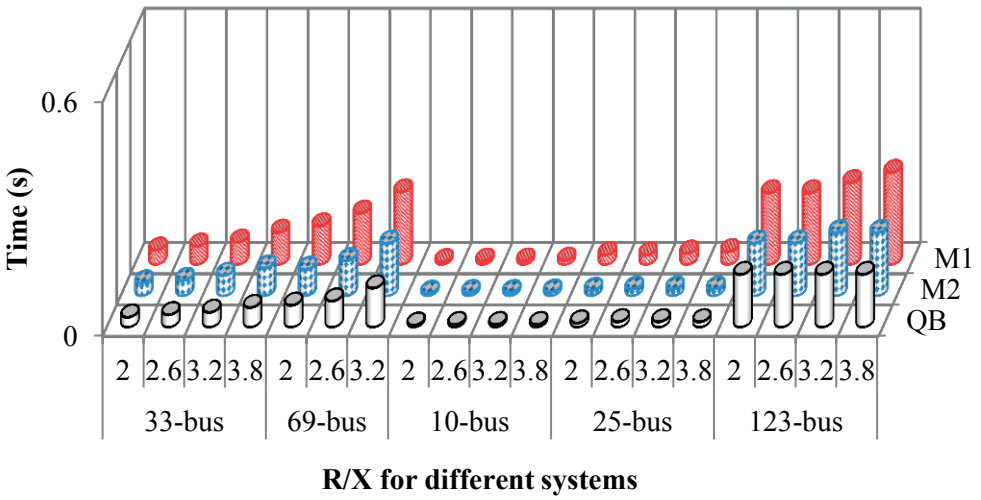

Figure 3.7 Execution time with different R/X values.

3.6.2 Analysis of a MV/LV System

The IEEE 4-bus DS is studied as an example of a MV/LV system. The connection of the step down interfaced transformer is D/GY, as shown in Figure 3.8. The rated line voltages at the MV and the LV line segments are 12.47 kV and 4.16 KV, respectively. The solution

of this system by using the proposed method is compared with the four-wire solution [54] and the classical three-phase solution under the following conditions:

1) *Different Grounding Resistances:* the grounding resistances at the LV side (bus 4) are changed from zero to 0.3 ohm, and the corresponding neutral current calculated by the methods is shown in Figure 3.9 (a).

2) *Different DG Sizes:* Figure 3.9 (b) compares the neutral current for different DG sizes at bus 4 (phase A).

It is obvious that the proposed method can provide accurate solutions at different conditions when comparing with the exact solution of the four-wire solution. In contrast, the classical three-phase power flow fails to describe the accurate behavior of the system under these conditions.

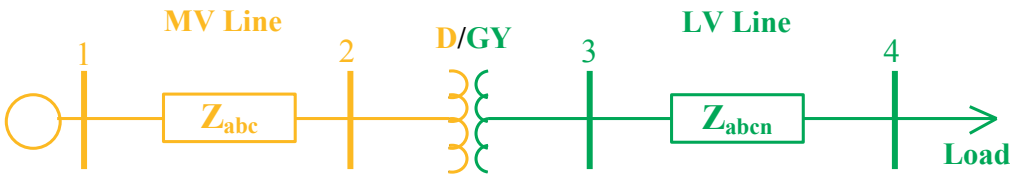

Figure 3.8 The IEEE 4-bus DS.

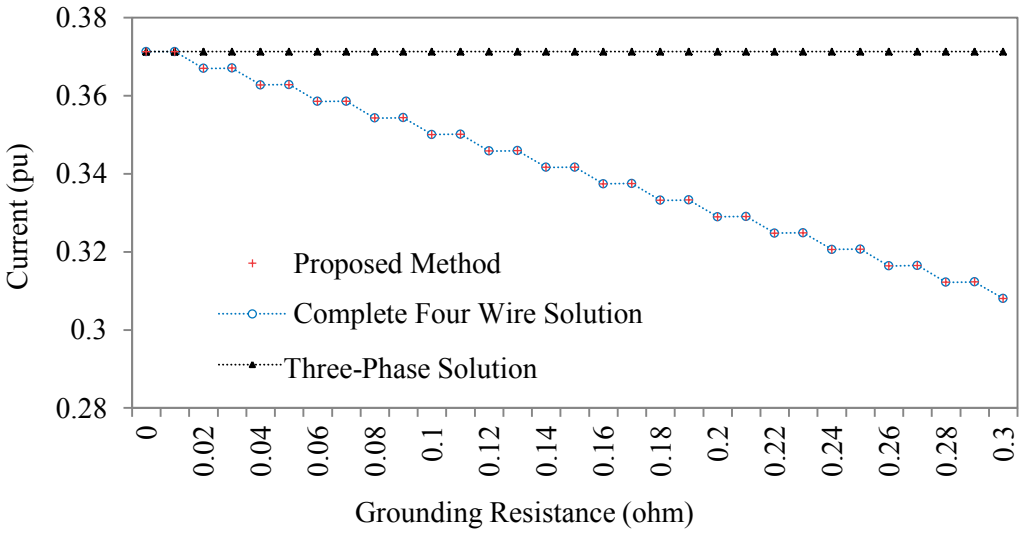

(a) Results for different grounding resistances

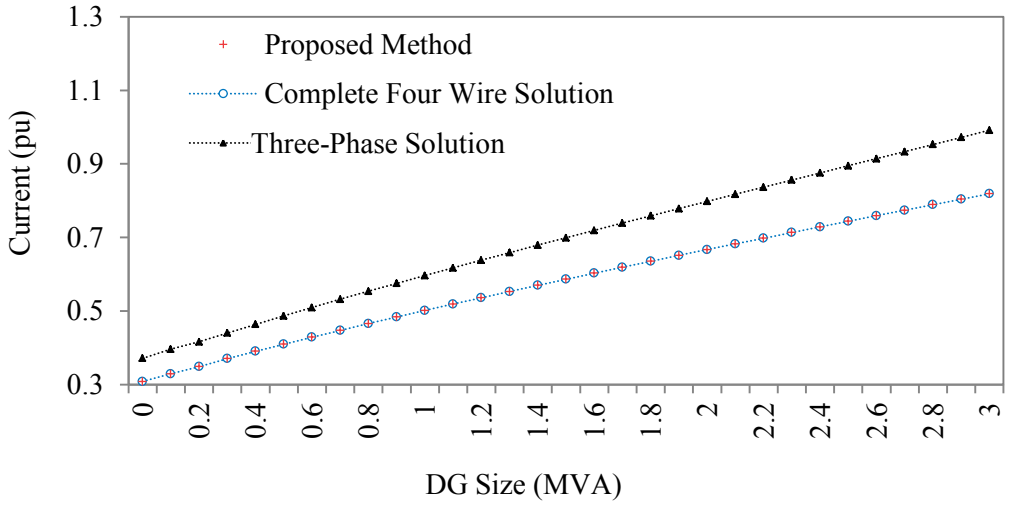

(b) Results for different DG sizes

Figure 3.9 Neutral current entering bus 4.

3.6.3 Impact of Load Models

In this subsection, the performance of the proposed method is examined on the modified 123-bus system, where all loads are assumed to be CI, and the LF is set to 280%. To prove the efficiency of the proposed method, its convergence characteristics is compared with the existing QB model in the literature (i.e, M3) [53]. In M3, a ZIP load model is employed, and a QB model for the distribution lines is utilized. For both cases, the power flow results are accurate, but the convergence speed is different. The convergence characteristics for the methods are presented by comparing the absolute power mismatch against the number of power flow iterations are shown in Figure 3.10. It can be observed that proposed method is converged much faster than M3 for CI loading. For instance, to converged to the pre-set mismatch, M3 needs 22 iterations, while only 8 iterations is required by QB. The slower convergence of M3 is caused by strong variation of the load powers with the calculated voltage at each iteration [53]. This variation is appeared as a result of utilizing a single QB line model for different load types. Unlike M3, the proposed method utilized different QB line models for different load types, as illustrated in table 3.1. Regarding to M1 and M2, they show relatively intermediate convergence performance, and they need 11, 12 iterations, respectively.

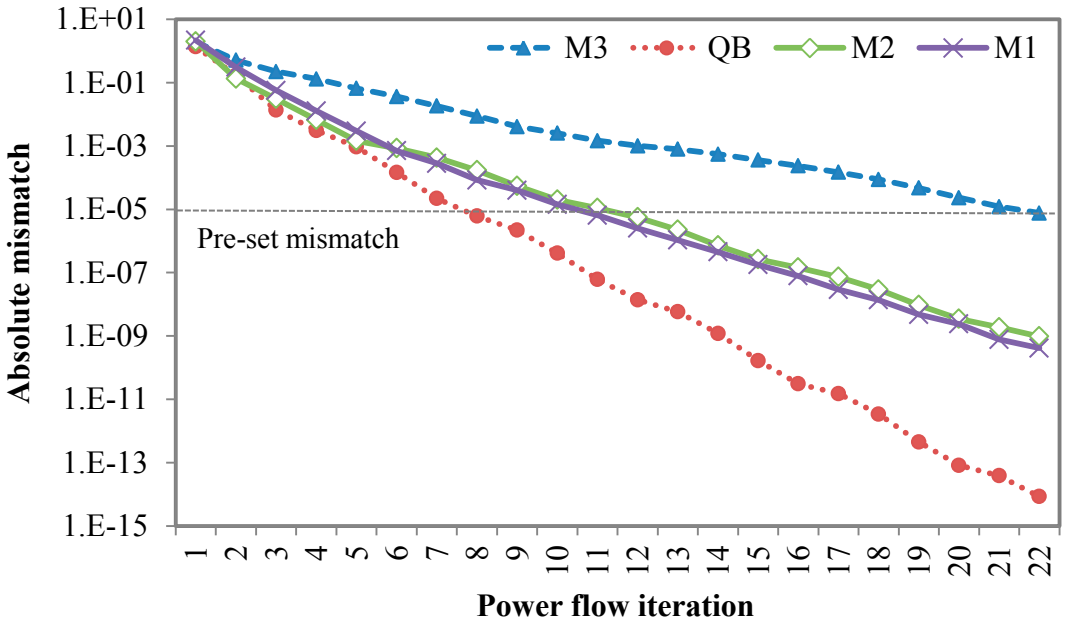

Figure 3.10 Convergence characteristics of 123-bus system with CI loading.

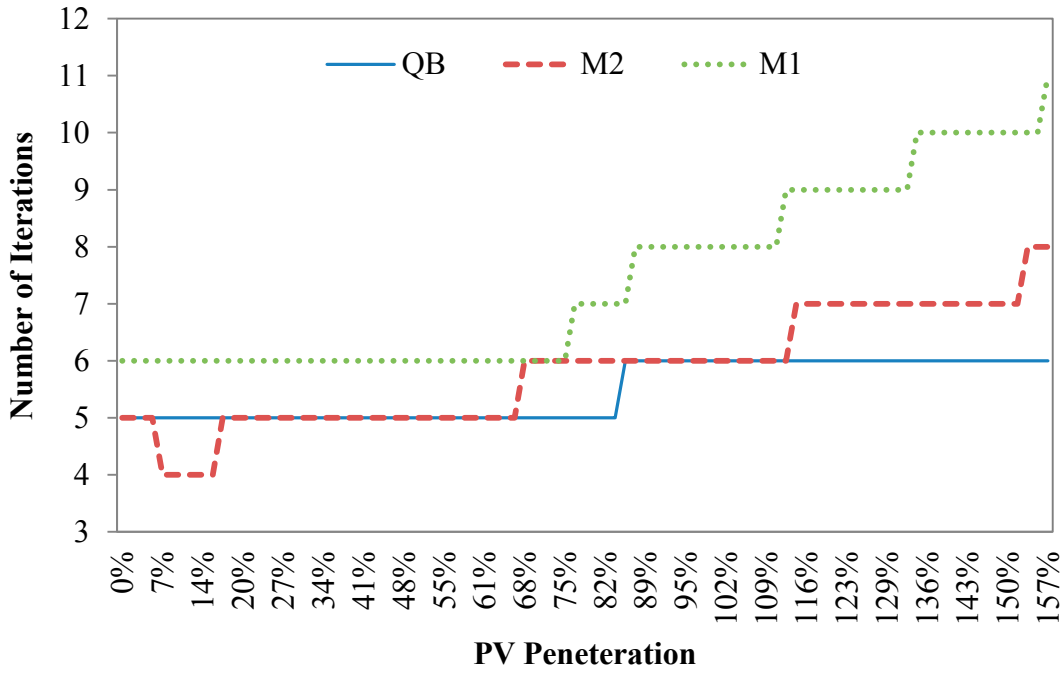

Figure 3.11 Comparison of the methods with increasing PV penetration.

3.6.4 Impact of DG Units

The modified IEEE 123-bus test system is used to test out the performances of the methods with DG penetration. In this distribution system, three PV units (the Kyocera KC200GT solar array [56]) are assumed to be connected to 63, 50, and 107 buses. It is worth to note that increasing the penetration of single-phase PV units will increase system unbalance, thereby worsening the iterative process of the power flow computation. Figure 3.11 compares the number of power flow iterations for M1, M3, and QB with increasing PV penetration. As expected, all methods show good performances in the case of low PV penetration, and the iteration numbers increase with rising PV penetration. As the number of PV penetration is increased, QB has robust performance compared with M1 and M2. Therefore, the proposed method can be very helpful for analysing active systems that involve excessive DG penetration.

3.7 Summary

The paper has proposed an efficient BFS power flow method for analyzing active DSs. The proposed method has been compared with two commonly used BFS methods using several balanced and unbalanced DSs. The results have shown that:

- The proposed method provides accurate solutions when compared with the exact solutions.
- A fast solution is provided by the proposed method that utilizes efficient quadratic models of various DS components.
- The convergence characteristics of the proposed method are better than those of the existing methods during the critical conditions, such as heavy loading conditions and high R/X ratios.

Furthermore, the proposed method can efficiently solve the power flow problem of MV, LV, and integrated MV/LV DSs. Comprehensive analyses of the impacts of DG units on the IEEE 123-bus DS have also been performed. The proposed method is a helpful tool to study the steady state condition of active DSs.

Chapter 4

Direct Assessment and Analysis of DG Impacts

Chapter 4: DIRECT ASSESSMENT AND ANALYSIS OF DG IMPACTS

4.1 Introduction

As presented in the previous Chapter (i.e., Chapter 3), an improved BFS power flow method are proposed form analysing balanced/unbalanced distribution systems. In this chapter, this improved power flow method will be employed for assess the DG impacts on distribution systems in terms of loss reduction, voltage profile, and voltage unbalance. Furthermore, a new fast index for estimating the amount of loss reduction after adding multiple DG technologies is presented. The proposed loss reduction formulation and the methodology of study the effects of DG impacts are deeply investigated using different systems. The presented formulations will be very helpful for solving the optimization problem of DG allocation in the next chapters.

4.2 General Formulation of Loss Reduction with DG

In this section, we propose direct formulae for expressing the amount of real power loss (RPL) and RPL reduction (RPLR) with multiple DG units in a distribution system.

4.2.1 RPL Formula

For a distribution system with N branches, a basic RPL formula can be expressed as follows:

$$P_{Loss} = \sum_{j=1}^{N} A_j \left(P_j^2 + Q_j^2 \right) \tag{4.1}$$

where

$A_j = \frac{r_j}{V_j^2}$

j	Subscript standing for the receiving side bus on each branch;
V_j	Voltage magnitude of bus j;
$r_j + jx_j = Z_j$	Branch impedance;
$P_j + jQ_j = S_j$	Incoming complex power to bus j.

An advantage of (4.1) is that the exact RPL can be computed directly from the corresponding branch resistances without using the nodal admittance or impedance matrices.

4.2.2 RPL Formula with a Single DG

The RPL formula is reformulated here as a function of the DG injected power. The total RPL of the six-bus distribution test system shown in Figure 4.1.a) can be computed directly using (4.1). However, the total RPL will be greatly changed when a DG unit is installed. As the load powers are constant, all additional generated power afforded by DG installation must flow to the reference bus. For instance, when a DG unit is installed at bus

3 as in Figure 4.1.b), its generated power will flow through branch 3 and branch 1 to the reference bus. Let the list of branches that the DG generated power passes through be denoted by BDG. Then, a formula to estimate RPL with the DG can be written as follows:

$$P_{Loss,DGi} = \sum_{j \in BDG} A_j \left(P_j^2 + Q_j^2\right) + \sum_{j \in BDG} A_j \left(\left(P_j - P_{DGi}\right)^2 + \left(Q_j - Q_{DGi}\right)^2\right) \tag{4.2}$$

By installing DG, only branches in the BDG list, corresponding to the second term of (4.2), will be affected. This restriction implies that the initial power flow, the base loading, is constant in (4.2); therefore, the losses are efficiently estimated from the additional flow by the DG unit. The validity of this formulation is verified and discussed in the results section.

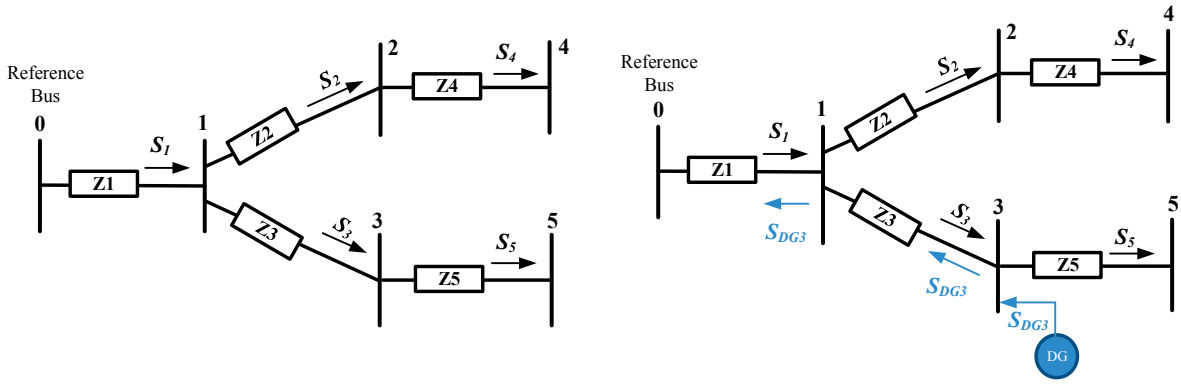

a) Without DG (base case) b) With a DG unit at bus 3

Figure 4.1 Single line diagram of the six-bus test system.

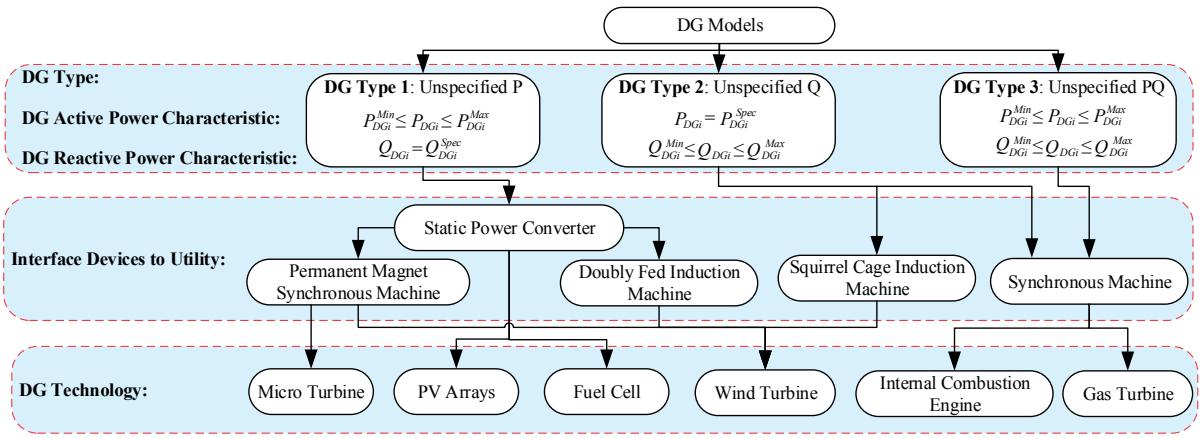

Figure 4.2 Classification of steady state models of different DG technologies.

4.2.3 Generalized RPL Formula with Multiple DG

For handling multiple DG allocation, let the list of nodes that are connected to DG units be denoted by *NDG*. A general RPL formula can be written as follows:

$$P_{Loss,DG} = \sum_{j \notin BDG} A_j \left(P_j^2 + Q_j^2\right) + \sum_{j \in BDG} A_j \left(\left(P_j - \sum_{i \in NDG} S_{ij} P_{DGi} \right)^2 + \left(Q_j - \sum_{i \in NDG} S_{ij} Q_{DGi} \right)^2 \right) \tag{4.3}$$

where *S* represents a binary matrix (*NDG* × *BDG*) whose elements are defined as follows:

$$S_{ij} = \begin{cases} 1 & if\ S_{DGi}\ passes\ through\ branch\ j \\ 0 & otherwise \end{cases} \tag{4.4}$$

Matrix *S* is employed here to define the list of branches that each DG generated power passes through. By using the proposed mathematical formulations, we can directly evaluate the losses after installing DG.

4.2.4 Proposed RPLR Formula

The basic formulation of RPLR can be expressed as follows:

$$RPLR_{DG} = P_{Loss} - P_{Loss,DG} \tag{4.5}$$

Substituting (1) and (3) into (5) leads to the following:

$$RPLR_{DG} = \sum_{j \in BDG} A_j \left(\sum_{i \in NDG} S_{ij} P_{DGi} \left(2P_j - \sum_{i \in NDG} S_{ij} P_{DGi} \right) + \sum_{i \in NDG} S_{ij} Q_{DGi} \left(2Q_j - \sum_{i \in NDG} S_{ij} Q_{DGi} \right) \right) \tag{4.6}$$

Equation (4.6) is useful for computing the total RPLR by the DG by evaluating only the branch losses in the BDG list. There is no need to calculate total power loss before and after installing DG to evaluate the benefits in terms of loss reduction. Substituting the DG power factor (PF_{DGi}) into the RPLR formula yields the following:

$$RPLR_{DG} = \sum_{j \in BDG} A_j \left(\begin{array}{l} 2\sum_{i \in NDG} S_{ij} P_{DGi} \left(P_j + Q_j \sum_{i \in NDG} S_{ij} R_{DGi} \right) \\ -\sum_{i \in NDG} S_{ij} P_{DGi}^2 \left(1 + \sum_{i \in NDG} S_{ij} R_{DGi}^2 \right) \end{array} \right) \tag{4.7}$$

where

$$R_{DGi} = Q_{DGi} / P_{DGi} \tag{4.7.a}$$

$$R_{DGi} = \sqrt{\frac{1 - PF_{DGi}^2}{PF_{DGi}^2}} \tag{4.7.b}$$

4.3 Generalized Models for Different DG Types

Different DG technologies can generally be classified into three main types based on their active and reactive power generation characteristics, as illustrated in Figure 2. The figure describes the possible energy sources and conversion devices for each DG type. Combining different energy sources with different energy converters represents special DG generation characteristics for each configuration. The bounds of the decision variables, the active and reactive DG powers, are specified for each DG type. For DG type 1, if $\left(Q_{DGi}^{Spec}\right)$ is equal to zero, its power factor is unity. DG type 2 represents those that can support reactive powers. The power factor of DG type 3 may not be specified. By these constraints, optimal values of decision variables will be determined. Note that the DG power factor will also be determined in the optimization problem. For a specific DG unit type, if its optimal active and reactive generated powers are defined, the interfaced device and the DG technology structure can be optimally selected and designed [29], [30].

4.4 Proposed Scheme

Figure 4.3 shows the solution process of the proposed methodology for analyzing distribution systems and assess the impact of different DG technologies.

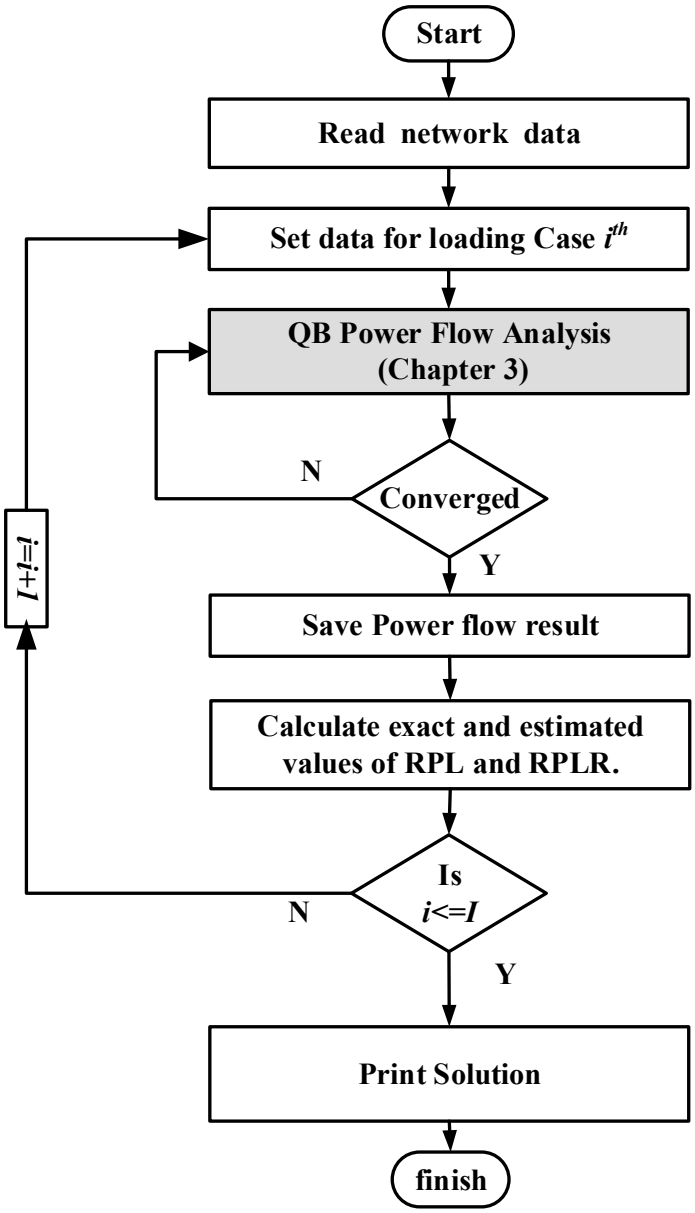

Figure 4.3 Flow chart of the proposed scheme.

4.5 Results

Two distribution systems are used for the analysis in this chapter, namely 33-bus system [31] and 123-bus [63] distribution systems. The 33-bus distribution system are used for validation of the proposed RPLR formulation for estimating the losses with DG integration, while the 123-bus systems are employed for simulating unbalanced systems and investigating their impacts.

4.5.1 Validation of RPLR Formula

The 33-bus distribution system (see system details in the appendix) is used as a test system for this analysis. Figure 4.4 shows the power losses, estimated RPLR and exact RPLR values at the individual possible DG locations, where a single DG installation is assumed in the 33-bus test system. To clarify the figure, the results are plotted by re-arranging the exact RPLR values in ascending order (from lowest to highest). We see that the estimated RPLR and the exact RPLR have their maximum values at the same DG location (Bus 6), which is the optimal bus where the calculated losses are the lowest. Thus, the optimal DG location can be obtained by the estimated RPLR without calculating exact RPLR.

Figure 4.5 illustrates the results for the cases of installing two and three DG units in the 33-bus test system. The results confirm the validity of the EA method even when allocating multiple DG units.

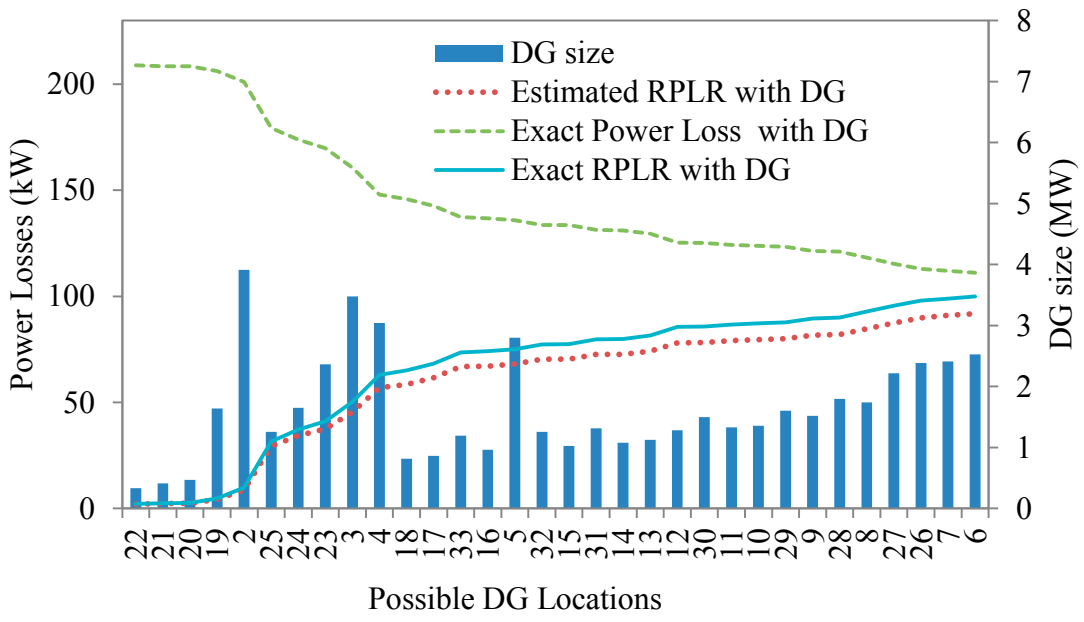

Figure 4.4 The calculated optimal DG size at all possible DG locations, the corresponding exact loss and the estimated RPLR for the 33-bus system.

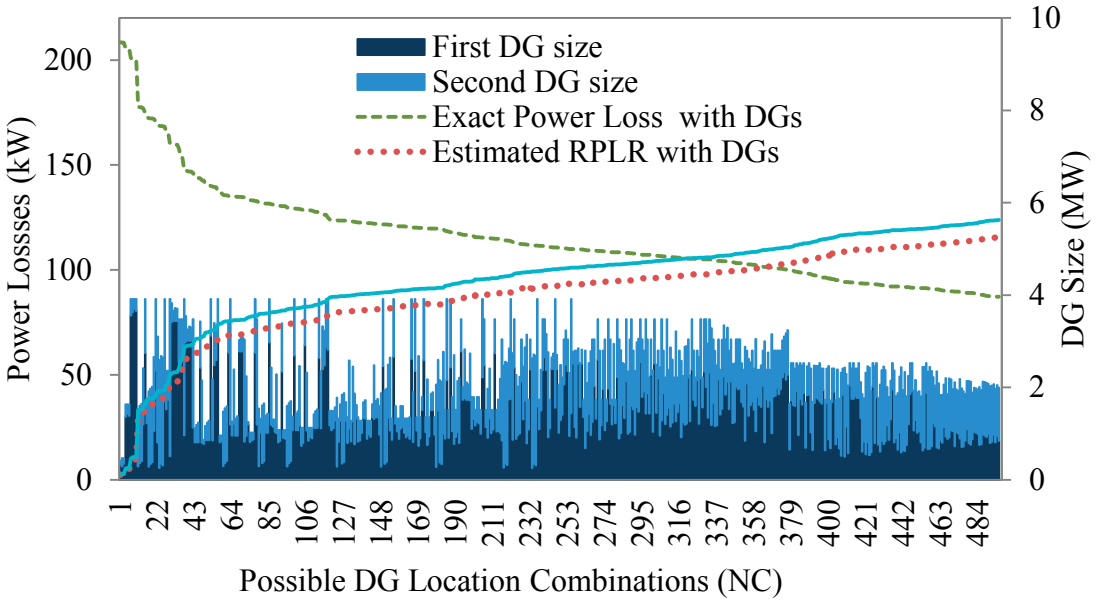

a) Two DG allocation

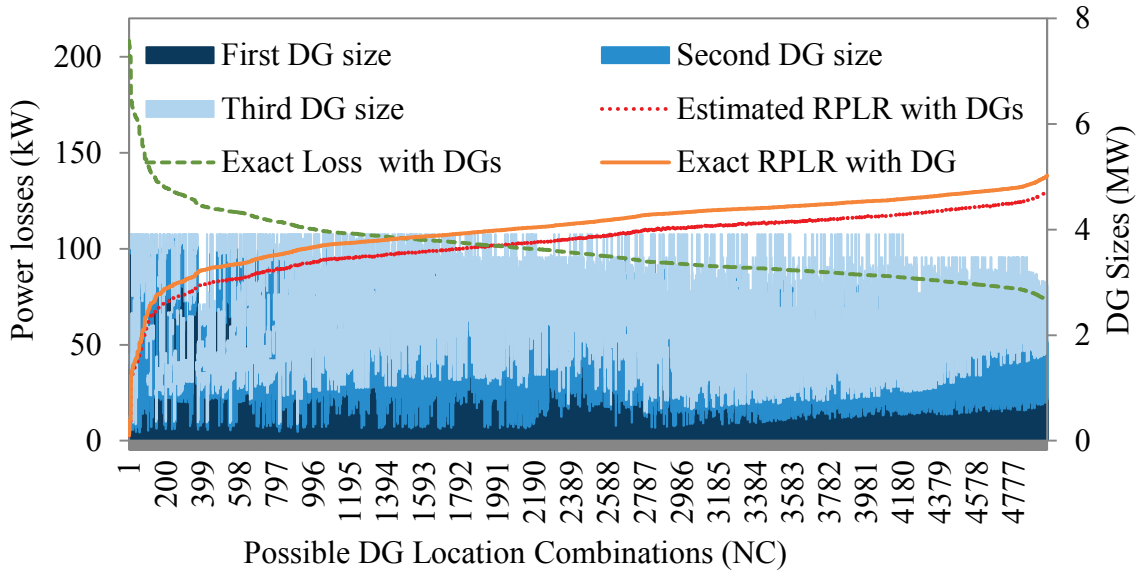

b) Three DG allocation

Figure 4.5 The calculated optimal DG sizes at all possible DG location combinations, the corresponding exact loss and the estimated RPLR for the 33-bus system.

4.5.2 Analysis of a Distribution system with DG

The proposed power flow method is applied on the IEEE 123-bus DS, Figure 4.6, with DG (PV and IG units). This test system is a multi-phase DS that consists of a main three-phase feeder, two-phase laterals, and single-phase laterals. The PV units (the

Kyocera KC200GT solar array) are assumed to be connected to all single-phase nodes, and two IG units are connected to buses 67 and 105. Regarding to the IG units, they consist of 150 HP induction machines interfaced to the DS using Delta-Delta transformers.

As a validation test for the IG model, Figure 4.7 shows the calculated IG slips at each iteration of the power flow process when they are worked with a specific PM mode. The slip values are finally converged to final values at iteration 6, as shown in the figure.

It is demonstrated that several operational problems in DSs occur normally at peak generation of DG [29], [34]. Therefore, the focus of this study is to clarify the impact of DG units on the DS during the peak generation point. In the following paragraphs, the effect of increasing PV penetration on the DSs is addressed. The penetration level of the PV units is changed by increasing the number of arrays of the PV units. Based on the assumed scenarios, the following aspects are investigated:

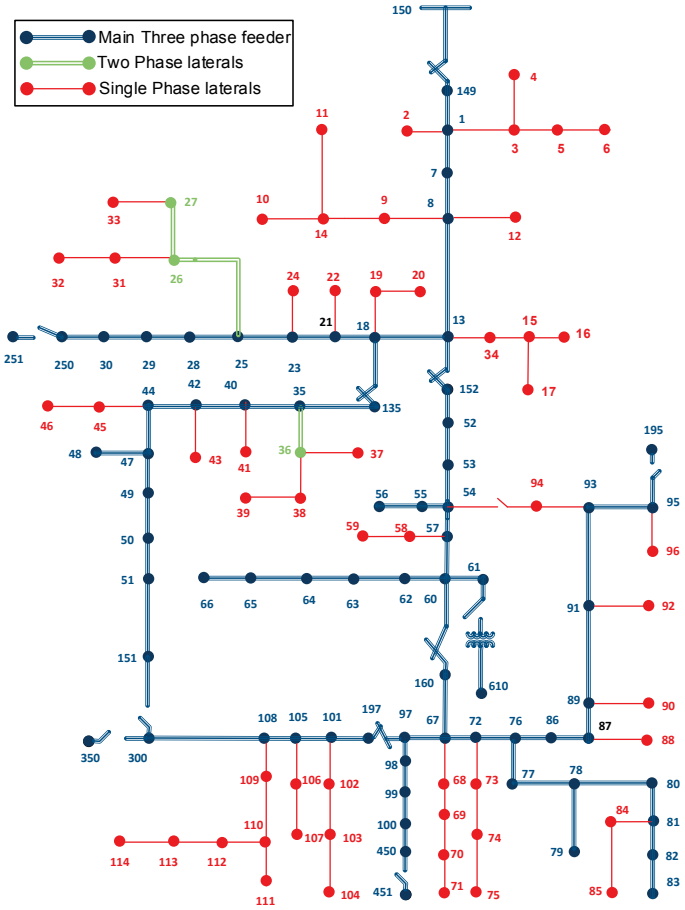

Figure 4.6 The 123-bus IEEE DS (without regulators).

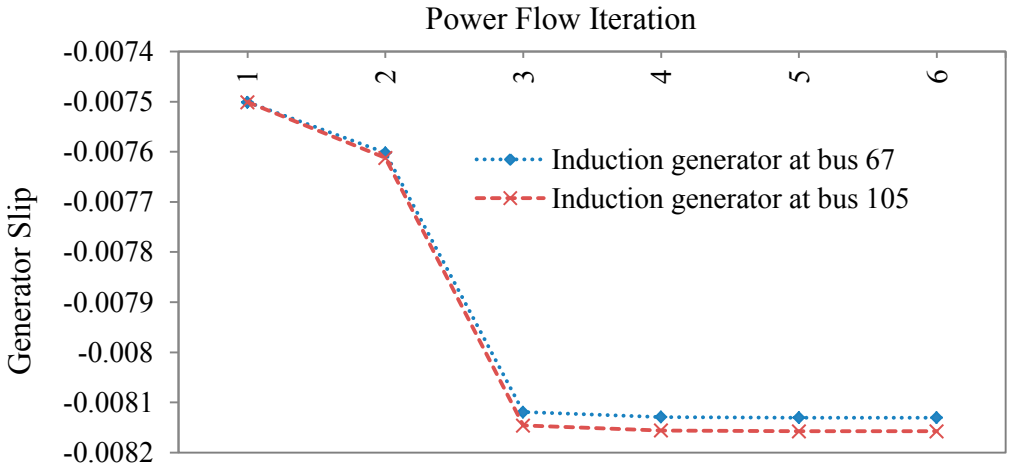

Figure 4.7 The calculated values of the slip for the IG units at each power flow iteration.

1) ***Generated Powers and System Losses:*** Figure 4.8 shows the impact of PV penetration levels on the sharing of the generated power among the distribution station, the wind units, and the PV units. It is clear that, by increasing the share of the PV generated power, the generated power from the substation is decreased. The wind power generation is almost constant. Regarding to the total active power loss, as the number of PV arrays are increased, the losses are reduced to a minimum value (21.5 kW) and increased again after exceeding a specific PV penetration level (298 arrays).

2) ***Voltage Profile****:* the common problem with increasing PV penetration is voltage rise, as shown in Figure 4.9, where the maximum voltage at each phase is given. Voltage rise may be harmful for many sensitive domestic/commercial loads that are normally widespread in active DSs.

3) ***Voltage Unbalance (VU):*** VU is the ratio of the negative sequence voltage divided to the positive sequence voltage at a specific bus. Here, as an indicator for voltage unbalance, the maximum VU for the DS buses with different penetration levels of the PV units is shown in Figure 4.10. It is clear that the voltage unbalance decreases until the number of PV arrays equals to 203 and then returns to increase again. Therefore, the optimal number of PV arrays to improve the voltage unbalance is 203.

The results show that increasing DG penetration will greatly improve electric energy systems performance in terms of loss reduction, voltage profile, and voltage unbalance until a specific optimal penetration level. It is also obvious that the proposed power flow method is considered a useful tool for accurately analyzing and examining the active DSs.

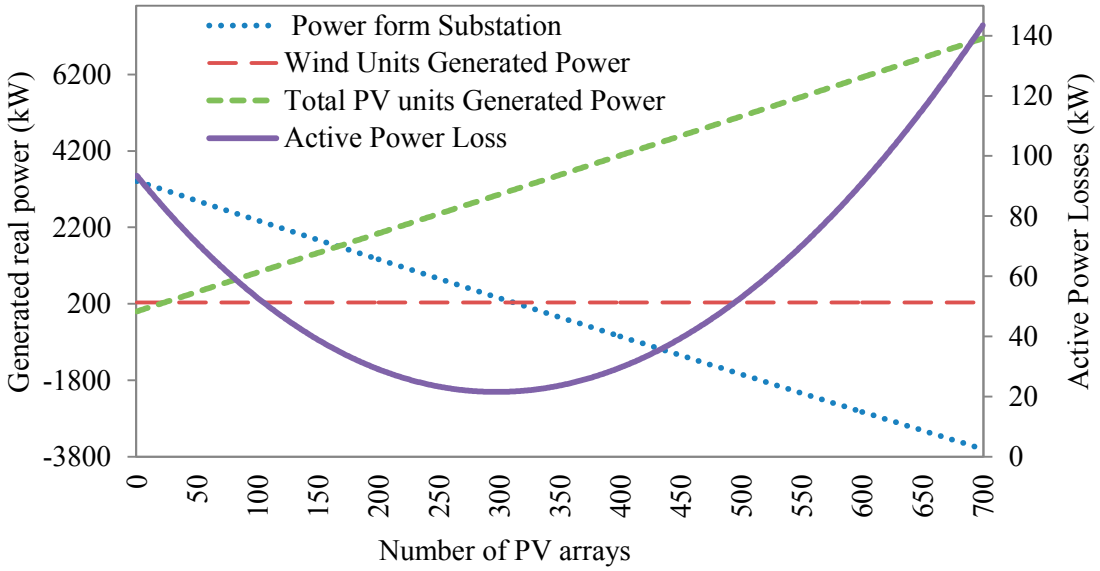

Figure 4.8. The effect of PV penetration on the generated power and losses.

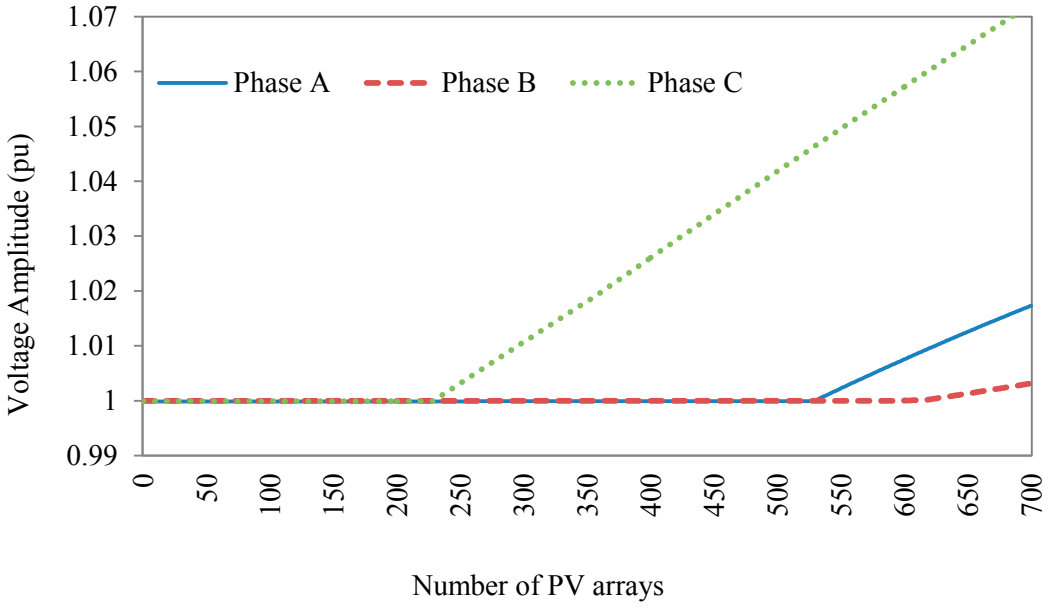

Figure 4.9 The effect of increasing of PV penetration on the maximum phase voltages.

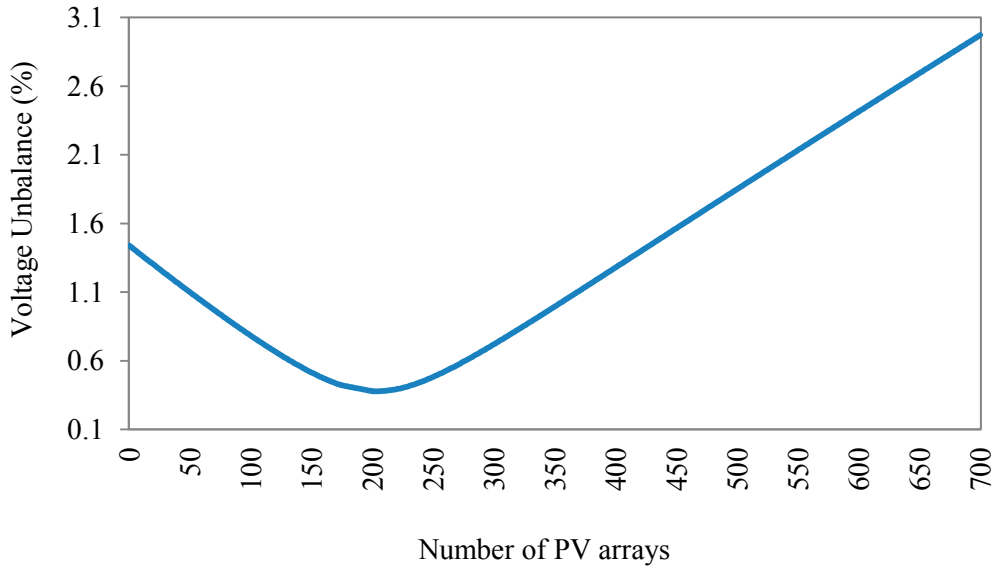

Figure 4.10 The effect of PV penetration on VU.

4.6 Summary

This chapter has presented comprehensive analysis of distribution systems where the impact of different DG types is investigated. Firstly, the benefits of introducing fast index, RPLR, for estimating the losses with DG technologies are outlined, where the 33-bus distribution system are employed. With employing the proposed RPLR formulation, the impact of DG units can be tested, with low computational burden. Secondly, the unbalanced IEEE 123-bus radial test system is analyzed with different DG integration cases. The work presented I this chapter will be helpful for developing efficient methods for DG allocation, as shown in the nest chapters.

Chapter 5

Efficient DG Allocation Methods for Power Loss Minimization

Chapter 5: Efficient DG Allocation Methods for Power Loss Minimization

5.1 Introduction

In this chapter, an efficient analytical method is proposed for optimally allocating DG units in electrical distribution systems to minimize power losses. The proposed analytical method can be employed for obtaining the optimal combination of different DG types in a distribution system for loss minimization. The validity of the proposed method is demonstrated using two test systems with different configurations by comparing with exact optimal solution obtained from exhaustive OPF algorithm. The calculated results and the comprehensive comparisons with existing methods prove the supervisory of the proposed method in terms of accuracy and calculation speed. The proposed loss minimization method can be a useful tool for a general DG allocation problem since it provides effective and fast loss evaluation taking into account other benefits.

5.2 DG Allocation Problem

Recently, many countries have followed a strategy to increase the integration rate of renewable energy resources in distribution systems. These distributed generation (DG) units contribute in an efficient way to tackle the environmental pollution problems caused by conventional power stations [1]. In addition, they can improve the reliability and the efficiency of not only the distribution systems, but also the entire power system.

Typically, the most notable types of the renewable DG technologies are solar power, photovoltaic systems, wind power, and small hydro stations. These resources have normally small capacities, and they are located close to critical loads and load centers. Consequently, the characteristics of distribution systems are greatly affected by installing the DG units. An appropriate combination between these different resources can positively maximize their benefits to the grid. On the other hand, improper DG allocation may lead to many technical problems to distribution systems, such as voltage rise, reverse power flow, increase system losses.

Many research studies have been directed to develop efficient techniques for allocating DG units in distribution systems. The DG allocation problem aims to determine the optimal DG locations and sizes to be installed in distribution systems with considering system constraints. The allocation methods of DG can be classified based on their objective function. The objective function could be, but not limited, to: 1) active power loss minimization ; 2) energy power loss minimization; 3) voltage profile improvement; or 4) cost minimization. The common feature between most of these methods is the assumption of allocating only a single DG type; therefore, they do not deal with the DG allocation problem for different DG types. A comprehensive review about various methods for solving the DG allocation problem is given in [10].

5.3 Proposed EA Method

The main idea of the EA method is based on employing the proposed RPLR formula as an indicator for the amount of loss reduction as a result of installing the DG units. The details of the EA method are listed as follows:

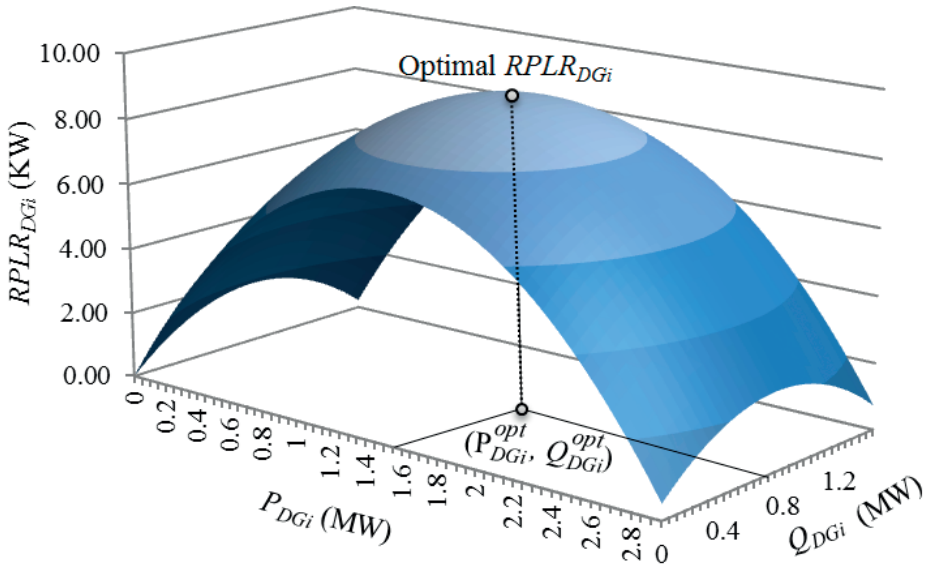

Figure 5.1 Characteristic of the RPLR with varying DG generated power.

5.3.1 Optimal DG Sizing

The first step to solve the problem of DG allocation is by introducing an efficient way to calculate the optimal DG size at a given bus *i* in a distribution system. Figure 5.1 shows the influence of changing both the active and reactive DG generated power on the $RPLR_{DGi}$ value. The main goal of the optimization problem is to calculate the optimal DG size (P^{opt}_{DGi}, Q^{opt}_{DGi}) to maximize the value of $RPLR_{DGi}$, i.e., minimize system losses. The methodology for calculating optimal DG sizes mainly depends on the DG power factor operating conditions as follows:

1) ***DG with Specified Power Factors:*** The specified generation values of DG type 1 (Q^{Spec}_{DGi}) and DG type 2 (P^{Spec}_{DGi}) are treated as negative loads. Therefore, the power factors for DG types 1 and 2 can be dealt with as unity and zero, respectively, during the optimization process.

The first derivative of the RPLR formula with respect to the real generated power of the DG at bus *m* can be expressed as follows:

$$\frac{\partial RPLR_{DG}}{\partial P_{DGm}} = 2\sum_{j\in BDG} S_{mj} A_j \begin{pmatrix} \left(P_j - \sum_{i\in NDG} S_{ij} P_{DGi}\right) + R_{DGm} \\ \left(Q_j - \sum_{i\in NDG} S_{ij} R_{DGi} P_{DGi}\right) \end{pmatrix}, \; m \in NDG \tag{5.1}$$

It is notable that A_j is assumed to be constant. At the maximum value of the RPLR, the first derivative is equal to zero.

$$\left.\frac{\partial RPLR_{DGs}}{\partial P_{DGm}}\right|_{P_{DGi}=P_{DGi}^{opt}} = 0 \tag{5.2}$$

Then, the equation to find the optimal size can be obtained as follows:

$$\sum_{j\in BDG} S_{mj} A_j \sum_{i\in NDG} S_{ij} P_{DGi}^{opt}\left(1+R_{DGm}R_{DGi}\right) = \sum_{j\in BDG} S_{mj} A_j \left(P_j + R_{DGm} Q_j\right) \tag{5.3}$$

The above equation is available for each DG at a typical bus *m*, so that the set of equations can be organized in matrix notation as follows:

$$\begin{bmatrix} P_{DG1}^{opt} \\ P_{DG2}^{opt} \\ \vdots \\ P_{DG\,N_{DG}}^{opt} \end{bmatrix} = \begin{bmatrix} X_{1,1} & X_{1,2} & \cdots & X_{1,N_{DG}} \\ X_{2,1} & X_{2,2} & \cdots & X_{2,N_{DG}} \\ \vdots & \vdots & \vdots & \vdots \\ X_{N_{DG},1} & X_{N_{DG},1} & \cdots & X_{N_{DG},N_{DG}} \end{bmatrix}^{-1} \begin{bmatrix} Y_1 \\ Y_2 \\ \vdots \\ Y_{N_{DG}} \end{bmatrix} \tag{5.4}$$

where

$$X_{n,m} = \sum_{j\in BDG} S_{nj} A_j S_{mj}\left(1+R_{DGm}R_{DGn}\right) \tag{5.4.a}$$

$$Y_m = \sum_{j\in BDG} S_{mj} A_j \left(P_j + R_{DGm} Q_j\right) \tag{5.4.b}$$

$$Q_{DGi}^{opt} = R_{DGi}\, P_{DGi}^{opt} \tag{5.5}$$

The final equations (5.4) and (5.5) can be employed to calculate the optimal DG sizes. These equations can be applied to all three DG types with specified power factors. Note that the equations are very simple, facilitating the calculation of the optimal DG sizes for the specified locations.

2) ***DG with Unspecified Power Factors:*** For installing DG technologies of type 3 that are capable of supplying both active and reactive power, their power factors may be viewed as decision variables to be calculated. Therefore, a special treatment is required for this DG type to obtain accurate results for calculating the optimal DG power factor. The main idea of this algorithm is to utilize the condition to maximize RPLR. An example of an

RPLR surface as a function of P_{DGi} and Q_{DGi} is given in Figure 5.1. At the maximum point of this surface, the following equation must be satisfied:

$$\left.\frac{\partial RPLR_{DG}}{\partial P_{DGm}}\right|_{\substack{P_{DGi}=P_{DGi}^{opt}\\ Q_{DGi}=Q_{DGi}^{opt}}} = \left.\frac{\partial RPLR_{DG}}{\partial Q_{DGm}}\right|_{\substack{P_{DGi}=P_{DGi}^{opt}\\ Q_{DGi}=Q_{DGi}^{opt}}} \tag{5.6}$$

Solving (5.6) for the DG reactive powers gives:

$$\begin{bmatrix} Q_{DG1}^{opt} \\ Q_{DG2}^{opt} \\ \vdots \\ Q_{DG\,N_{DG}}^{opt} \end{bmatrix} = \begin{bmatrix} P_{DG1}^{opt} \\ P_{DG2}^{opt} \\ \vdots \\ P_{DG\,N_{DG}}^{opt} \end{bmatrix} - \begin{bmatrix} U_{1,1} & U_{1,2} & \cdots & U_{1,N_{DG}} \\ X_{2,1} & X_{2,2} & \cdots & U_{2,N_{DG}} \\ \vdots & \vdots & \vdots & \vdots \\ U_{N_{DG},1} & U_{N_{DG},1} & \cdots & U_{N_{DG},N_{DG}} \end{bmatrix}^{-1} \begin{bmatrix} W_1 \\ W_2 \\ \vdots \\ W_{N_{DG}} \end{bmatrix} \tag{5.7}$$

where

$$U_{n,m} = \sum_{j \in BDG} S_{nj} A_j S_{mj} \tag{5.7.a}$$

$$W_m = \sum_{j \in BDG} S_{mj} A_j \left(P_j - Q_j\right) \tag{5.7.b}$$

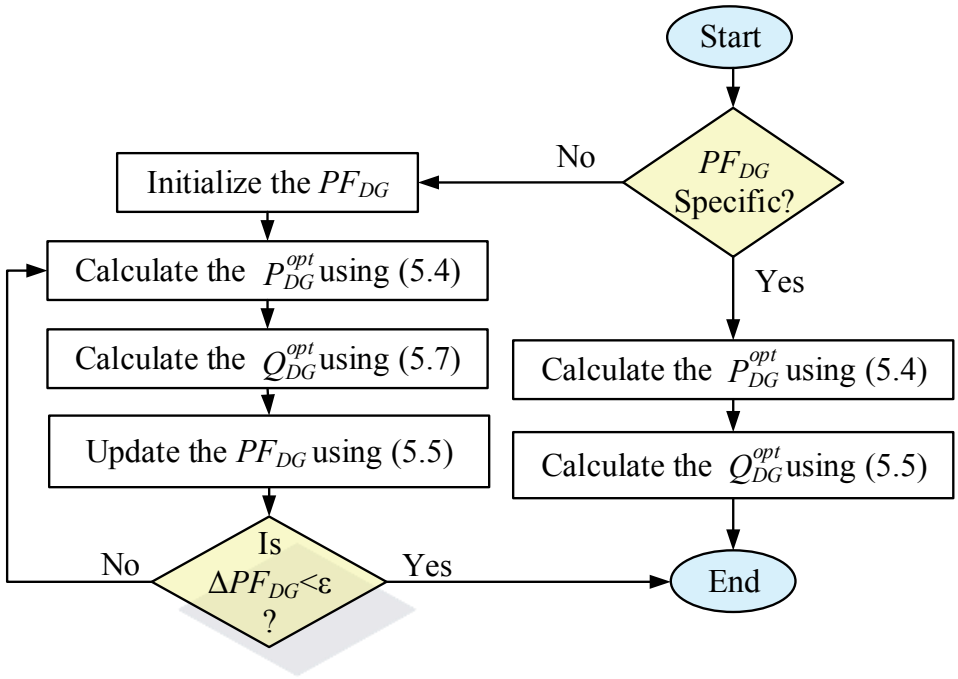

Figure 5.2 Flowchart depicting the optimal DG sizing algorithm.

Equations (5.4) and (5.7) are solved in a sequential manner to obtain the optimal DG power factors. The solution process will be repeated until convergence is obtained. The DG power factor mismatch is used as convergence criteria. The proposed DG sizing algorithm is illustrated in Figure 5.2.

5.3.2 Optimal DG Sizing in Meshed Distribution Systems

The mathematical formulation of the proposed method has been developed based on the radial structure of distribution systems. Therefore, a special treatment for meshed distribution systems is explained in this section. Figure 5.3 a) shows an example of a weakly meshed distribution system where the optimal DG size at bus 3 (S_{DG3}) must be calculated. Based on basic loop analysis techniques, it is clear from the figure that there are two possible paths for transmitting the DG generated power from bus 3 to the reference bus. Figure 5.3 b) shows the equivalent radial structure of the original meshed system where a new dummy bus is added and the DG is split into two equivalent DG units so that the following holds:

$$S_{DG3} = S^{1}_{DG3} + S^{2}_{DG3} \tag{5.8}$$

By employing (5.4)–(5.7), the optimal size of the two equivalent DG units (S^{1}_{DG3} , S^{2}_{DG3}) can be calculated, and hence the optimal DG size at bus 3 can be computed using (5.8). Therefore, the proposed formulation is applicable to the resulting radial system, which is exactly equivalent to the original meshed system.

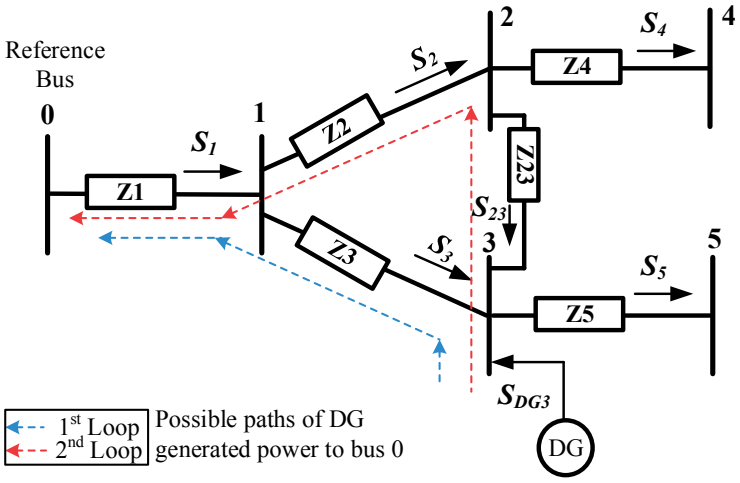

a) Meshed distribution system

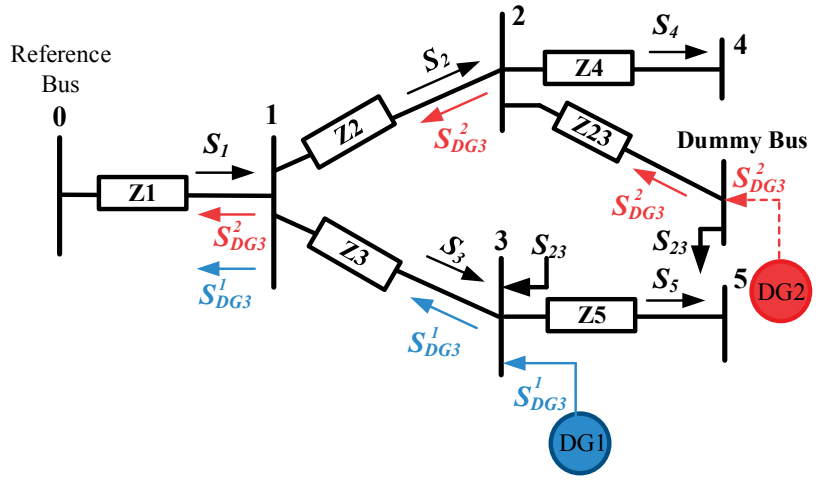

b) Equivalent radial distribution system

Figure 5.3 A simple distribution system with one loop.

5.3.3 Estimated RPLR with DG

To evaluate the positive impact of installing DG units on loss reduction, an estimated RPLR value ($RPLR_{DG}^{Est}$) is employed. By substituting the optimal DG sizes calculated with (5.4)–(5.7) and the specified DG generated powers into (4.6), and by using the power flow results of the base case, we obtain an estimated value for the RPLR by the following formula

$$RPLR_{DG}^{Est} = RPLR_{DG}\left(P_{DGi}^{opt}, Q_{DGi}^{opt}\right) \tag{5.9}$$

5.3.4 Solution Process

Note that, when allocating N_{DG} DG units in a distribution system with N_B buses that are eligible for DG allocation, the number of different possible combinations, N_C, of DG locations is calculated by

$$N_C = \frac{N_B!}{N_{DG}! \times (N_B - N_{DG})!} \tag{5.10}$$

Here, the main goal is to define the best combination of the DG sites in terms of loss reduction. The steps are as follows:

1) Read Data: Read the distribution system data, the required number of DG units to be installed and their types.

2) Data Structure: Build the distribution system data structure and the *S* matrix.

3) Power Flow: Perform the power flow computation for the base case loading (without DG).

4) Optimal DG Sizing: Calculate the optimal DG sizes for all the combinations of sites using the proposed sizing algorithm shown in Figure 5.2.

5) *Optimal DG Siting:* Calculate the estimated RPLR values for all the combinations using (5.9). Then, find the optimal combination of DG locations for which the estimated RPLR is the largest.

6) Print Results: Print the optimal DG locations and sizes as well as the RPLR value, etc.

It should be noted that the power flow is carried out only once to obtain the base case loading so that a direct optimal solution of the DG allocation problem can be efficiently solved. The complete computational procedure of the proposed EA method is shown in Figure 5.4.

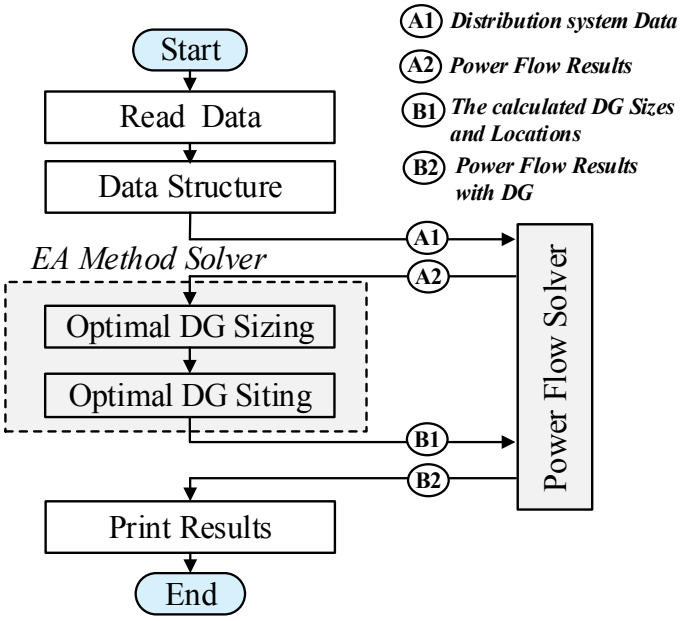

Figure 5.4 Solution process of the proposed EA method.

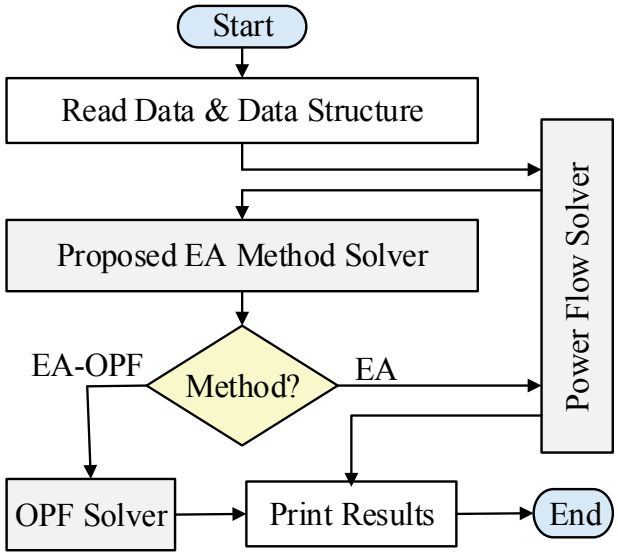

Figure 5.5 Solution processes of the proposed methods.

5.4 Proposed EA-OPF Method

The EA-OPF method is based on the combination of the EA method and an OPF to solve the DG allocation problem. Firstly, optimal DG locations are obtained using the EA

method. Secondly, the optimal DG sizes for the defined locations are computed by the OPF. The OPF algorithm takes into account the distribution system constraint conditions, including voltage limits, the DG penetration limit, maximum line flows, and DG size limits. The DG penetration is defined as the ratio of the total size of DG units to the total load. This combined method needs only one power flow solution for DG sizing and one OPF solution for DG sizing. The OPF is formulated as follows:

$$\text{Minimize: } P_{Loss,DG}(\mathbf{x},\mathbf{u}) \tag{5.11}$$

$$\text{Subject To} \quad \mathbf{H}(\mathbf{x},\mathbf{u}) = 0 \tag{5.11.a}$$

$$\mathbf{G}(\mathbf{x},\mathbf{u}) \leq 0 \tag{5.11.b}$$

where **x** represents a vector that includes node voltages and **u** is a vector that contains active and reactive DG generated powers. **H** and **G** are, respectively, the equality constraints representing the complex power-balance equation at each bus and the inequality constraints. Figure 5.5 shows the complete computational procedure of the proposed EA and EA-OPF methods.

5.5 Case Studies

The proposed methods for DG allocation have been implemented in C++. Intensive tests have been carried out on a 3.0 GHz PC with 4096 MB of RAM. The 33-bus and 69-bus distribution test systems are used to test the proposed methods. The detailed data of the systems appear in [31] and [32]. The first 33-bus system is a radial system with a total real power loss of 0.211 MW. The second 69-bus system is a widely used distribution system in the literature, and its total real power loss is 0.225 MW. For the two systems, bus 1 represents the main substation. The maximum DG penetration limit of 100% is set for both systems.

5.5.1 DG Type 1

The proposed EA method is applied first to install DG Type 1, where the DG reactive powers Q_{DGi}^{spec} are assumed to be zero and thus the power factors are unity. To evaluate the computational performance of the proposed methods, comprehensive comparisons have been performed. For this purpose, the methods in [26]-[28], and [25] are labeled as Method 1, Method 2, and Method 3, respectively. The solutions obtained by

those methods have been compared with the exact solution obtained by the exhaustive OPF algorithm. The algorithm involves running OPF for all possible DG site combinations, which required excessive calculation efforts.

Table 5.1 compares the results of the various methods for the two test systems for the allocation of a single DG unit, two DG units and three DG units. The comparison is carried out with respect to the DG locations, DG sizes, and RPL.

As seen from the table, the EA method can provide proper DG locations and accurate DG sizes compared with the exact solutions for the two test systems. More accurate solutions are obtained by the EA-OPF method, which are identical to the exact exhaustive OPF solutions. This is due to the effective combination of EA and OPF. From the results, it is also observed that Method 1 and Method 2 can lead to an acceptable optimal solution for allocating a single DG. However, in the cases where multiple DG units are allocated, Method 2 cannot provide the optimal DG locations and sizes. In the same manner, Methods 3 fails to provide the optimal solution for most cases.

The computational time required for each method is also given in Table 5.1. As expected, the EA method is the fastest for all cases. The main reason is that this method requires running the power flow only once for any number of DG units to be installed. Second, there is no need to construct special matrices, such as the node admittance matrix. Third, the method requires only the power flow through branches in the BDG list for optimal DG sizing. The EA-OPF method is slightly slower than the EA method as it requires one additional OPF. Method 2 consumes much more computational time to run the multiple power flows until reaching the optimal point. Method 1 is slower than the proposed EA and EA-OPF methods because it requires the impedance matrix. Finally, we observe that Method 3 is the slowest method, as it requires a number of power flow solutions.

TABLE 5.1 COMPARISON OF DIFFERENT ALGORITHMS FOR THE 33-BUS AND 69-BUS SYSTEMS WITH DG TYPE 1

DG No.	Applied Method	33-bus Test System				69-bus Test System			
		Optimal Bus	DG size (kW)	RPL (kW)	Time (S)	Optimal Bus	DG size (kW)	RPL (kW)	Time (S)
1	Method 1	Bus 6	2490	111.24	0.09	Bus 61	1810	83.4	0.54
	Method 2	Bus 6	2600	111.02	0.46	Bus 61	1900	83.25	1.27
	Method 3	Bus 30	1500	125.21	0.97	Bus 61	1900	83.25	6.09
	EA	Bus 6	2530	111.07	0.05	Bus 61	1878	83.23	0.16
	EA-OPF	Bus 6	2590	111.02	0.09	Bus 61	1870	83.23	0.20
	Exhaustive OPF	Bus 6	2590	111.02	1.30	Bus 61	1870	83.23	3.01
2	Method 2	Bus 6	720	91.63	1.08	Bus 61	1700	71.95	2.97
		Bus 14	1800			Bus 17	510		
	Method 3	Bus 30	1500	107.95	2.23	Bus 61	1900	83.23	12.3
		Bus 25	1000			Bus 64	20		
	EA	Bus 13	844	87.172	0.11	Bus 61	1795	71.68	0.45
		Bus 30	1149			Bus 17	534		
	EA-OPF	Bus 13	852	87.17	0.15	Bus 61	1781	71.68	0.50
		Bus 30	1158			Bus 17	531		
	Exhaustive OPF	Bus 13	852	87.17	20.2	Bus 61	1781	71.68	101
		Bus 30	1158			Bus 17	531		
3	Method 2	Bus 6	900	81.05	2.04	Bus 61	1700	69.97	5.61
		Bus 14	900			Bus 17	510		
		Bus 31	720			Bus 11	340		
	Method 3	Bus 30	1500	107.35	3.26	Bus 61	1900	72.65	17.3
		Bus 25	1000			Bus 64	20		
		Bus 24	220			Bus 21	470		
	EA	Bus 13	798	72.787	0.37	Bus 61	1795	69.62	1.62
		Bus 24	1099			Bus 18	380		
		Bus 30	1050			Bus 11	467		
	EA-OPF	Bus 13	802	72.79	0.41	Bus 61	1719	69.43	1.66
		Bus 24	1091			Bus 18	380		
		Bus 30	1054			Bus 11	527		
	Exhaustive OPF	Bus 13	802	72.79	202	Bus 61	1719	69.43	6655
		Bus 24	1091			Bus 18	380		
		Bus 30	1054			Bus 11	527		

5.5.2 DG Type 3 with Specified Power Factors

Examinations are performed to validate the proposed sizing methodology for allocating DG technologies of type 3. The results of installing three DG units with 0.82 lagging power factors in the 33-bus system are shown in Figure 5.6. The figure compares the estimated RPLR, the exact RPLR and the exact losses for each possible DG combination. As illustrated, the use of the estimated RPLR is an efficient way to select the proper locations of DG units of type 3.

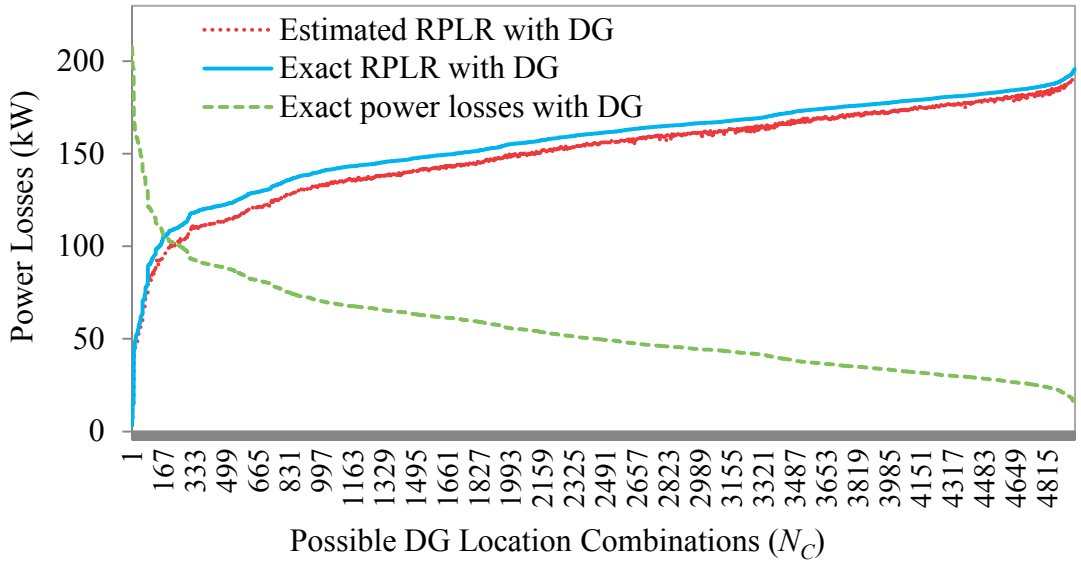

Figure 5.6 The calculated estimated RPLR, exact RPLR, and exact losses when allocating three DG units of type 3 in the 33-bus system.

TABLE 5.2 POWER LOSS ATTAINED BY EACH METHOD WITH DIFFERENT DG POWER FACTORS FOR THE 33-BUS SYSTEM

DG PF (lagging)	DG No.	Method 2		Method 3		EA Method		EA-OPF Method	
		RPL (KW)	RPLR (%)	RPL (kW)	RPLR (%)	RPL (kW)	RPLR (%)	RPL (KW)	RPLR (%)
0.82	1	67.90	67.8	72.10	65.8	67.87	67.8	67.86	67.8
	2	44.39	79.0	52.58	75.1	30.41	85.6	30.40	85.6
	3	22.29	89.4	51.87	75.4	15.14	92.8	14.04	93.4
0.85	1	68.20	67.7	73.57	65.1	68.17	67.7	68.16	67.7
	2	44.84	78.8	54.70	74.1	31.19	85.2	31.18	85.2
	3	23.05	89.1	53.72	74.5	15.52	92.6	14.58	93.1

To compare the amounts of loss reduction attained by methods with different DG power factors, we provide Table 5.2, which compares the RPL by different methods for the 33-bus system. The results show that the lowest RPL values are obtained with the proposed

methods compared with Method 2 and Method 3. For instance, for the case of installing three DG units with 0.82 lagging power factors, the RPL values are reduced to 15.52 kW and 14.58 kW when using the proposed EA and EA-OPF methods, respectively. In contrast, Methods 2 and 3 provide losses of 23.05 kW and 53.72 kW, respectively. This is because Methods 2 and 3 often fail to determine optimal locations, especially for multiple DG installations.

5.5.3 DG Type 3 with Unspecified Power Factors

This section addresses the results of installing DG technologies with unspecified power factors. Table 5.3 summarizes the results in terms of optimal DG locations, DG sizes, DG power factors and RPL with DG. The results show that the RPL is reduced to the lowest value by the proposed methods. This is reasonable since, unlike the existing methods, the proposed methods compute the optimal power factors to minimize RPL.

Figure 5.7 shows the convergence characteristics of the EA method in the 33-bus system for installing three DG units of type 3 at buses 13, 24 and 30. The DG power factors and the corresponding RPL computed in each iteration are illustrated in the figure. At the initial point, iteration 0, the DG power factors are set to 0.82 lagging, which are improved by using (5.4) and (5.7) in the following iterations to provide the optimal values. Thus, the RPL minimization is effectively obtained.

TABLE 5.3 RESULTS OF INSTALLING DG TECHNOLOGIES OF TYPE 3 IN THE TEST SYSTEMS

Test Sys.	DG No.	EA Method				EA-OPF Method		
		Bus	Size (kW)	PF (lagging)	RPL (kW)	Size (kW)	PF (lagging)	RPL (kW)
33-bus	1	6	2528	0.82	67.87	2558	0.82	67.86
	2	13	844	0.90	28.52	846	0.90	28.50
		30	1149	0.73		1138	0.73	
	3	13	798	0.90	11.80	794	0.90	11.74
		24	1099	0.90		1070	0.90	
		30	1050	0.71		1030	0.71	
69-bus	1	61	1878	0.82	23.26	1828	0.82	23.17
	2	61	1795	0.82	7.35	1735	0.81	7.20
		17	534	0.83		522	0.83	
	3	11	548	0.82	4.48	495	0.81	4.27
		18	380	0.83		379	0.83	
		61	1733	0.82		1674	0.81	

Figure 5.8 illustrates the effects of increasing the number of DG units on their total size and the amount of resulting loss reduction. For the two systems, the RPLR value and the corresponding total DG size increase dramatically when increasing the DG number from one to four units. However, the figures rise only slightly for five and six DG installations. This implies that the proposed method is also useful for determining the optimal number of DG units to be installed to obtain a desired loss reduction and maximize DG penetration.

To demonstrate the real contribution of calculating the optimal DG power factors for loss reduction, the following two cases are studied. The first case (case 1) is allocating DG with specified power factors (equal to the total load power factor), while the second case (case 2) involves implementing the proposed EA method to calculate the optimal DG power factors. It is interesting to note that the relative loss reduction between the two cases, calculated by $(RPL_{case1}–RPL_{case2})/(RPL_{case1})$, increases with respect to the number of DG units, as shown in Figure 5.9. This indicates that calculating the optimal DG power factors can play a vital role in reducing losses, especially in allocating multiple DG units.

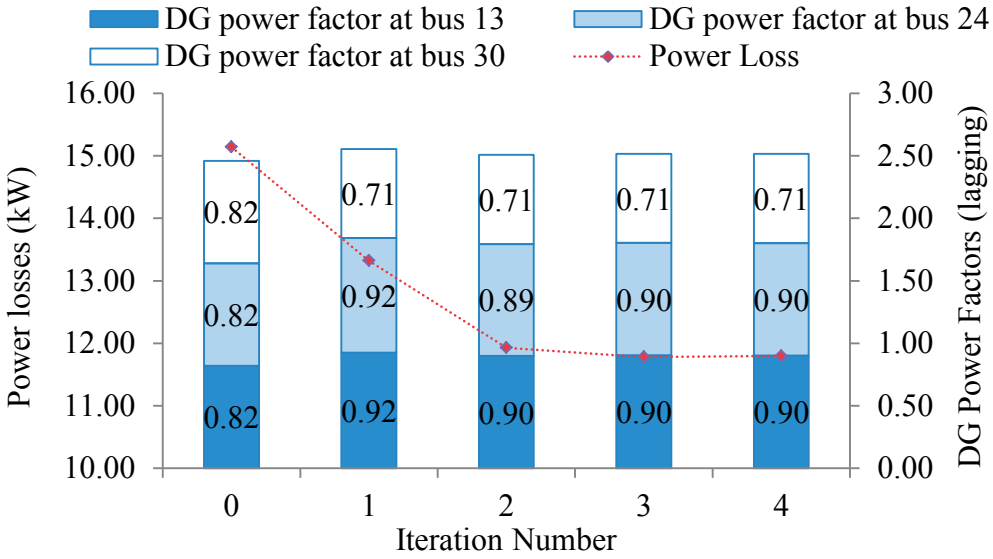

Figure 5.7 Convergence characteristics of the proposed EA method with installation of three DG of Type 3.

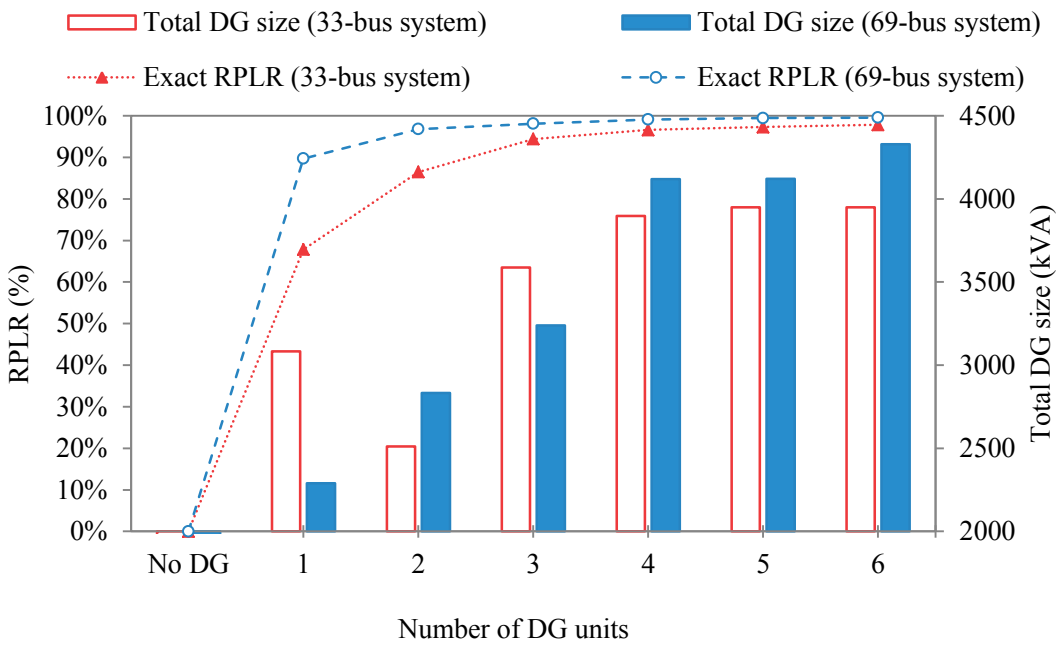

Figure 5.8 Effect of number of DG units on RPLR and their total size.

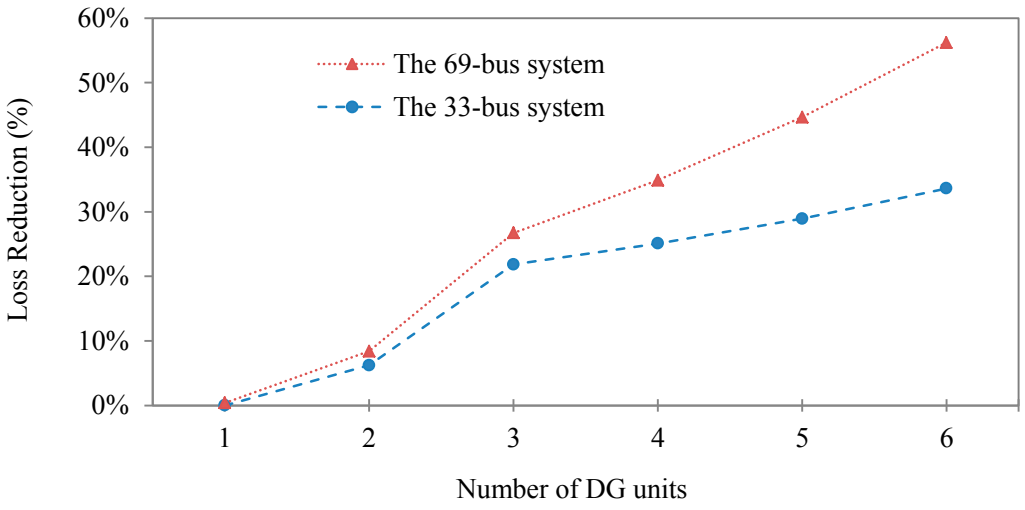

Figure 5.9 Relative loss reduction between the two cases for the test systems.

5.6 Summary

This thesis has proposed Efficient Analytical (EA) and hybrid EA-OPF methods for allocating different DG types in distribution systems in order to minimize the system losses. The effectiveness of the proposed methods has been demonstrated using two distribution systems to determine the optimal DGs sizes and locations. The superiority of the proposed methods in accuracy and computation speed has been confirmed by comparing with existing methods including exact exhaustive OPF solution and traditional analytical method.

Chapter 6

Optimal Mix of Multi-Type DG Units

Chapter 6: Optimal Mix Of Multi-Type DG Units

6.1 Introduction

This chapter proposes an efficient method for allocating multiple distributed generation (DG) technologies in distribution systems. The optimal DG sizes, DG locations, and the best combination between different DG technologies are determined. The objective function is to minimize losses in distribution systems. The proposed method is generic since it can solve the optimization problem with different combinations of DG technologies. A direct and fast solution of the DG allocation problem can be obtained using the proposed method without requiring iterative processes. The IEEE 33-bus and 69-bus distribution systems are employed to test the proposed method. Different combinations of DG units are studied and optimally allocated. The results show that the proposed method can handle the optimal solution accurately. It is also demonstrated that determining the optimal combination of different DG technologies can contribute positively on loss minimization in distribution systems.

6.2 Problem Formulation

DG technologies can be classified based on their output characteristics to three types as illustrated in Table 6.1. The models of the three DG types are generic, as they have the capability of producing both active and reactive powers. For each DG type, the active and reactive powers have different conditions. For instance, the reactive power for DG Type A is supposed to be specified, while the active power is a state variable which requires to be computed. Photovoltaic systems are an example of DG Type A, whereas DG Type B and DG Type C can be synchronous compensators and synchronous machines, respectively. It is worth to note that DG types A and B can be employed to model many DG technologies, according to the values of their specified active and reactive power, respectively. For a DG allocation problem, once the state variables for the DG technologies are optimally computed, the design parameters of these technologies can be computed.

TABLE 6.1 CLASSIFICATIONS OF DG MODELS

DG Model Type	DG Active Power	DG Reactive Power
DG Type A	State Variable	Specified
DG Type B	Specified	State Variable
DG Type C	State Variable	State Variable

Few methods, recently, have been proposed to solve such allocation problem for determining the optimal combination between different DG technologies. In [9], a probabilistic based method has been presented to find the optimal DG mix to minimize the energy losses, where the DG units are assumed to inject only active powers. A mix integer method has been employed in [65] to solve the allocation problem with different DG technologies. In [66], the DG units have been allocated with introducing a new probabilistic index. A genetic algorithm has been employed in [67] to find the optimal sizes and locations of different DG types.

In this paper, an effective method for determining the optimal DG combination in a distribution system to minimizes the real power losses. The method is based on a

generalized analytical method for DG allocation presented in Chapter 5. The proposed method is capable of accurately computing the best combination between different DG technologies and determining their corresponding optimal locations and sizes. Another effective advantage of the proposed method is its high computational speed, as there is no need to perform iterative processes for determining the optimal DG combination. Only power flow results for the base case are required to solve the allocation problem of different DG technologies. Therefore, a direct solution for the optimization problem is applicable.

6.3 Number of Combinations

The optimal allocation of DG units in distribution systems is a complex optimization problem due to system nonlinearity and the huge number of alternative solutions. When allocating (N_{DG}) DG units of the same technology in a distribution system with (N_B) possible locations, the number of possible combinations of DG locations (N_C) is computed by

$$N_C = \frac{N_B!}{N_{DG}! \times (N_B - N_{DG})!} \tag{6.1}$$

In the case of allocating different DG technologies, the number of possible combinations (N_D) can be calculated as follows:

$$N_D = \frac{N_B!}{(N_B - N_{DG})!} \tag{6.2}$$

It is clear that the number of possible combinations is much higher when allocating different DG types compared with allocating only one DG type. For instance, in the case of installing 5 DG units, the number of combinations computed by (6.2) is 120 times greater than that by (6.1). This rise in the number of combinations will not only increase the complexity of the DG allocation problem but also degrade the computational performance (i.e., increase the required CPU time). For instance, Figure 6.1 compares N_C values with employing (6.1) and (6.2) for a distribution system (NB=33) for different numbers of DG to be installed. For instance, in the case of installing 5 DG units, the number of combinations computed by (6.2) is 120 times greater than that by (6.1). Therefore,

determining the optimal combination of different DG technologies is a challenge task and needs to be accurately treated. It is required to accurately assign the best solution form the alternative solutions with fast computational speed.

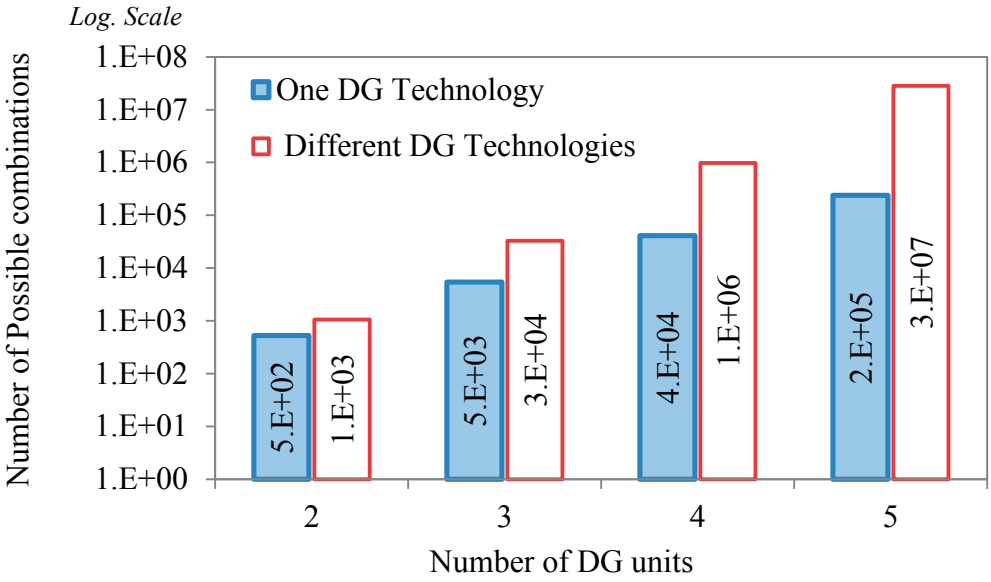

Figure 6.1 Number of possible combinations of DG locations.

6.4 Formulation of Optimal DG Mix Problem

The main objective of DG allocation problem is to determine the optimal DG combination so as to minimize the real power losses. For each possible combination of DG sites, the optimal DG sizes can be computed by (6.3) and (6.4) as follows:

$$\left[P_{DG}^{opt}\right]_{N_{DG}\times 1} = [X]^{-1}_{N_{DG}\times N_{DG}} [Y]_{N_{DG}\times 1} \tag{6.3}$$

$$\left[Q_{DG}^{opt}\right]_{N_{DG}\times 1} = \left[P_{DG}^{opt}\right]_{N_{DG}\times 1} - [U]^{-1}_{N_{DG}\times N_{DG}} [W]_{N_{DG}\times 1} \tag{6.4}$$

where **X**, **Y**, **U**, and **W** matrices can be calculated using distribution system parameters (Chapter 5) and load flow results at the base case (i.e., without DG integration). Equations (6.3) and (6.4) are driven based on generalized formulations for estimating the real power losses with DG units in a distribution system. Therefore, only the power flow results of base case (without DG) and the calculated DG sizes are required to assess all possible DG combinations in terms of loss reduction.

6.5 Solution Process

The proposed method is composed of four steps as follows.

1) ***Data preparation:*** this step starts with reading system data (loads, line parameters, etc.) and DG data (DG number, types, buses that are eligible for installing DG). Then, the power flow solution is computed, where QB method in Chapter 3 is employed. Also, the number of possible DG combinations of sites is computed by (6.1) or (6.2).

2) ***Assessing of combinations:*** For each possible combination of DG locations, the corresponding optimal DG sizes are computed using (6.3) and (6.4), thereby the loss reduction is estimated. Once the losses are estimated for all possible combinations, the optimal combination can be determined.

3) ***Optimal DG Allocation:*** this step involves installing DG technologies with their calculated optimal sizes in their proper locations, computed in step 2. A power flow calculation is required to calculate the steady state conditions with including the DG units. If there are constraints for the distribution systems, such as voltage level, maximum DG sizes, DG penetration level, and maximum line flows, an optimal power flow (OPF) algorithm is performed in this step.

4) ***Print Results:*** The results are finally displayed, including DG benefits (i.e., loss reduction, voltage improvement, etc.) and the calculated optimal DG combination data (DG technologies with their corresponding sizes and locations).

Note that the proposed method can handle the optimal solution for any number of DG technologies to be installed. It is only required the result from the base case for defining the optimal solution, including the optimal combination between available DG technologies. The flow chart that describes the complete solution process is given in Figure 6.2. It is clear that all possible combinations of DG locations are studied to find the optimal combination. This search approach will effectively provide the optimal solution, which is the most important issue in DG allocation problems compared with CPU time.

6.6 Case Studies

6.6.1 Assumptions

- One DG unit is allocated at each bus in the distribution system;
- The maximum DG number to be installed is three units;
- The specified values of DG types A and B, according to Table 6.1, are assumed to be zero. Therefore, their power factors are unity and zero, respectively. The power factor for DG Type C is 0.82 lagging.

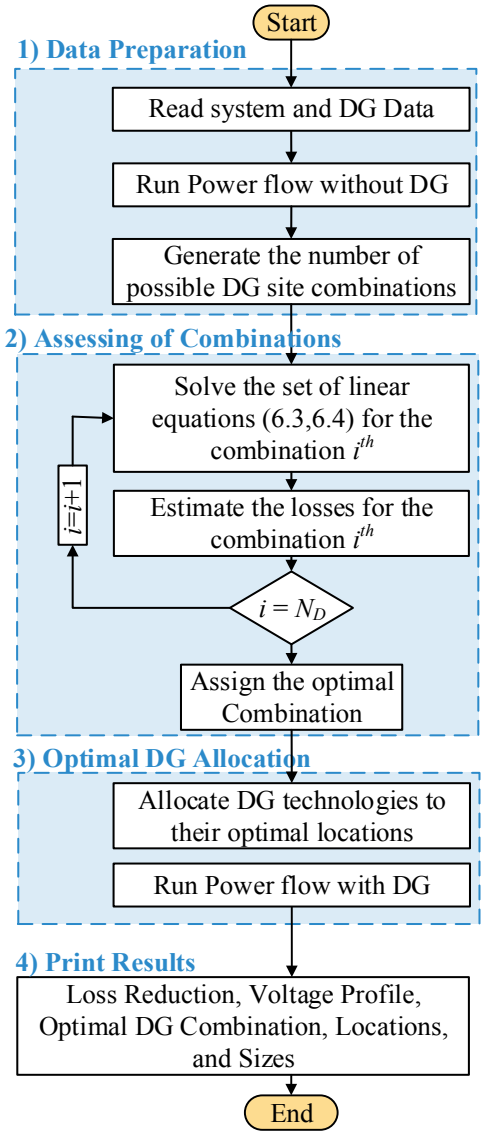

Figure 6.2 Flow chart of the proposed method.

6.6.2 Optimal Mix of different DG Types

This section involves a solution methodology of the optimal mix of different DG types to minimize RPL. Four scenarios are studied as follows:

Scenario 1) DG type 1 and DG type 2.

Scenario 2) DG type 2 and DG type 3.

Scenario 3) DG type 1 and DG type 3.

Scenario 4) Mix of DG type 1, DG type 2 and DG type 3.

Here, the main target is to select the optimal scenario among them. The optimal DG mix is computed by comparing the amount of RPLR for each scenario. The results are illustrated in Tables 6.2 and 6.3 for the two test systems. It is interesting to note that, for all four DG combinations, the RPL is significantly reduced when compared with the base case. The main observations about the differences among the scenarios are summarized as follows:

- The maximum RPLR occurs in scenario 4. Therefore, scenario 4, which involves a mix of the three DG types, is the optimal scenario and highly recommended for attaining effective loss reduction.
- Scenario 1 is not recommended, as the RPLR is the lowest among the scenarios. In addition, the total DG size is the largest, implying that the installation cost is the highest.
- The scenarios that include DG type 3 tend to provide an effective RPLR. Therefore, DG type 3 is superior to the other two DG types in terms of loss reduction.

Because the proposed methods are based on generalized mathematical models, the study can be extended to any DG combination case.

TABLE 6.2 COMPARISON OF THE SCENARIOS FOR THE 33-BUS SYSTEM

Scenario No.	Scenario 1		Scenario 2		Scenario 3		Scenario 4		
DG Types	Type1	Type2	Type2	Type3	Type1	Type3	Type1	Type2	Type3
DG Locations	6	30	30	6	13	30	29	30	13
DG Sizes (kVA)	2528	1245	669	2724	824	1696	1258	1031	806
Total DG Size (kVA)	3773		3392		2521		3095		
RPL (kW)	58.45		55.74		36.36		29.63		
RPLR (%)	72		74		83		86		

TABLE 6.3 COMPARISON OF THE SCENARIOS FOR THE 69-BUS SYSTEM

Scenario No.	Scenario 1		Scenario 2		Scenario 3		Scenario 4		
DG Types	Type1	Type2	Type2	Type3	Type1	Type3	Type1	Type2	Type3
DG Locations	61	62	17	61	17	61	17	18	61
DG Sizes (kVA)	1878	1294	350	2260	531	2225	534	358	2196
Total DG Size (kVA)	3172		2611		2756		3088		
RPL (kW)	23.91		18.27		12.35		7.37		
RPLR (%)	89		92		95		97		

6.6.3 Optimal Mix with different DG zones

The proposed method is tested using the 33-bus distribution system [31], as shown in Figure 6.3. In this paper, to simulate the allocation problem practically, it is assumed that there is a recommended area for each DG type. For this purpose, the test system is divided, as illustrated in the figure, into four zones as follows.

- **Zone A**: this area is eligible for installing DG type A.
- **Zone B**: this area is eligible for installing DG type B.
- **Zone C**: this area is eligible for installing DG type C.
- **Zone D**: this area is not eligible for installing DG.

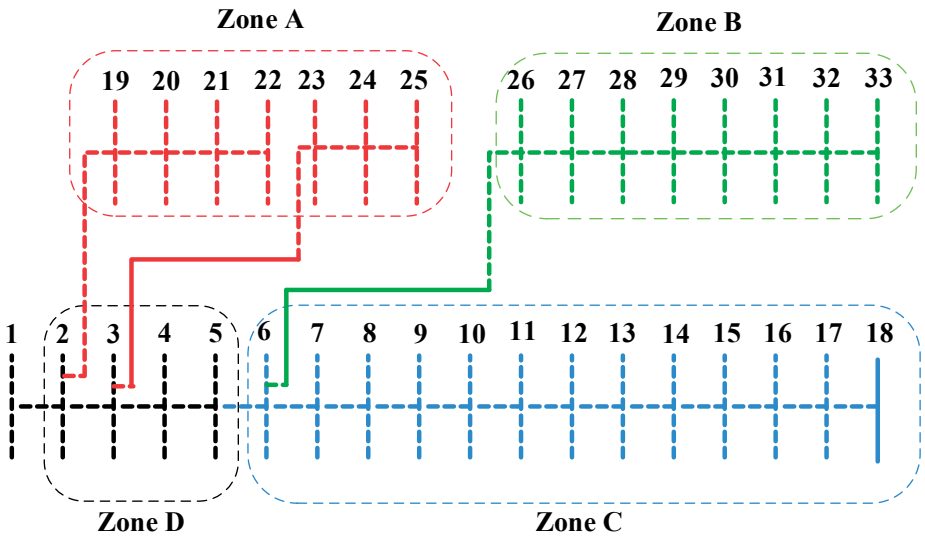

Figure 6.3 The 33-bus distribution system.

TABLE 6.4 DG NUMBERS FOR DIFFERENT CASES

DG Type	C0	C1	C2	C3	C4	C5	C6	C7
DG Type A	-	2	2	1	-	-	1	1
DG Type B	-	1	-	2	2	1	-	1
DG Type C	-	-	1	-	1	2	2	1

Eight different cases (from C0 to C7) are studied, as illustrated in Table 6.4. The first case (C0) is the base case (without DG). The other cases (from C1 to C7) involves installing thee DG units of various types. For each case, the DG units are installed based on their recommended zone.

Table 6.5 shows the calculated DG sizes and their corresponding locations with employing the proposed method. It is clear that, although the DG number is three units of all cases, the calculated DG locations, sizes are almost different for each case. Therefore, the type of the DG units has a great impact on the allocation problem. The differences between the cases can be summarized as follows:

1) ***Losses:*** Figure 6.4 compares the losses for each case after installing the DG units to the 33-bus distribution system. It is worth mentioning that all cases contribute in a

positive way in reducing the losses when compared with base case (C0). However, the amount of loss reduction for each case is different. We noticed that cases that include DG type C; their corresponding losses are relatively small. To demonstrate this notice, the worst case in terms of loss reduction is C3, where the DG type C is not allowed to be installed. Also, the best case is C6, where two DG units of type C are installed. On the other hand, DG type B is not recommended for reducing the real losses, as its contribution in reducing the losses is the lowest compare with DG types A and C.

2) ***Total DG size:*** the total size of the DG units is an important factor in the allocation problem since it can give an image about the cost of installation. With increasing the DG size, it is expected that the installation cost is increased, as the number of DG is the same for each case. The total DG size for each case is given in Figure 6.5. It is obvious from the figure that C1 and C3, which are not included DG type C, have the highest capacity (i.e, the highest installation cost).

3) Voltage Profile: Figure 6.6 shows the voltage profile for different cases. It is clear that the voltage profile is improved for all cases of DG installation compared with the base case.

To sum up, the optimal DG allocation problem is solved, and the losses are reduced for all cases. However, it is demonstrated here that the DG type C can contribute in the best way in reducing the losses. Another benefit, the total DG size tends to be smaller, and the voltage profile is better, compared to those of DG types A and B.

TABLE 6.5 RESULTS FOR THE 33-BUS SYSTEM

DG Type	C1	C2	C3	C4	C5	C6	C7
DG Type A	1.88@6	0.57@8	2.53@6	-	-	0.62@14	0.77@14
	0.65@14	0.51@15					
DG Type B	2.23@23	-	1.15@23	0.27@24	0.47@24	-	0.68@24
			0.30@25	0.20@25			
DG Type C	-	1.58@30	-	2.85@26	1.72@26	1.33@26	1.64@30
					1.13@30	1.13@30	

*DG size (MVA) @ DG bus

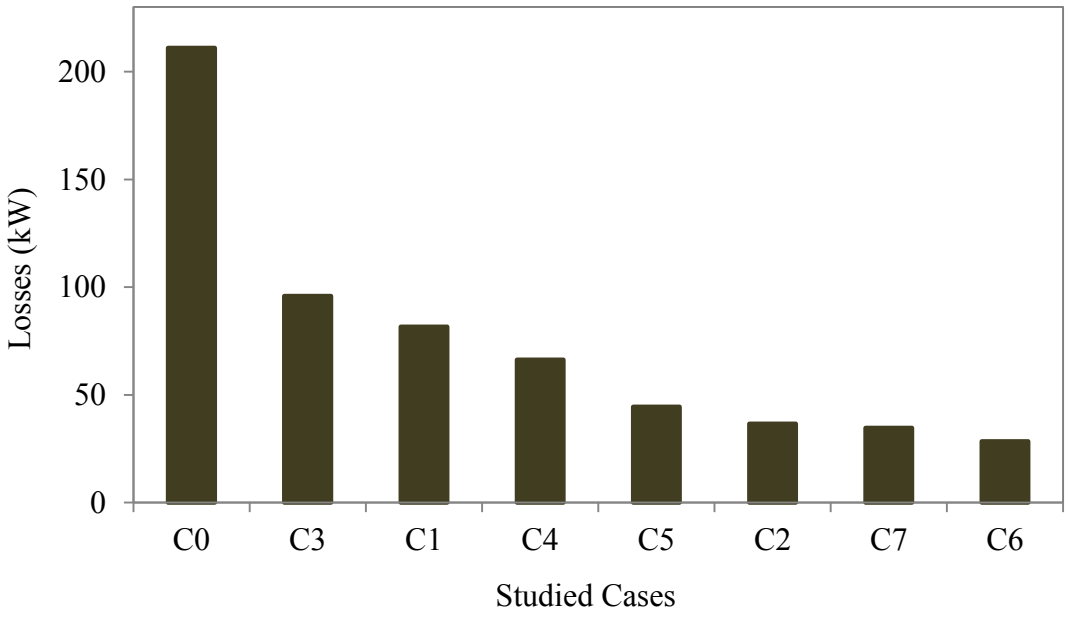

Figure 6.4 The losses after instaling the DG units for each case.

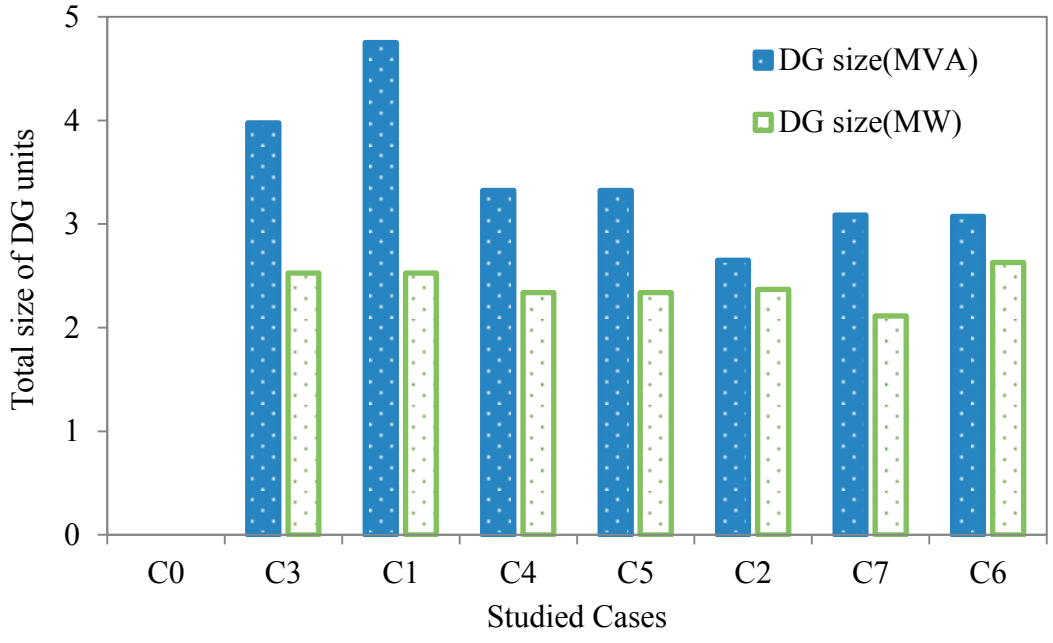

Figure 6.5 The calculated total DG size for each case.

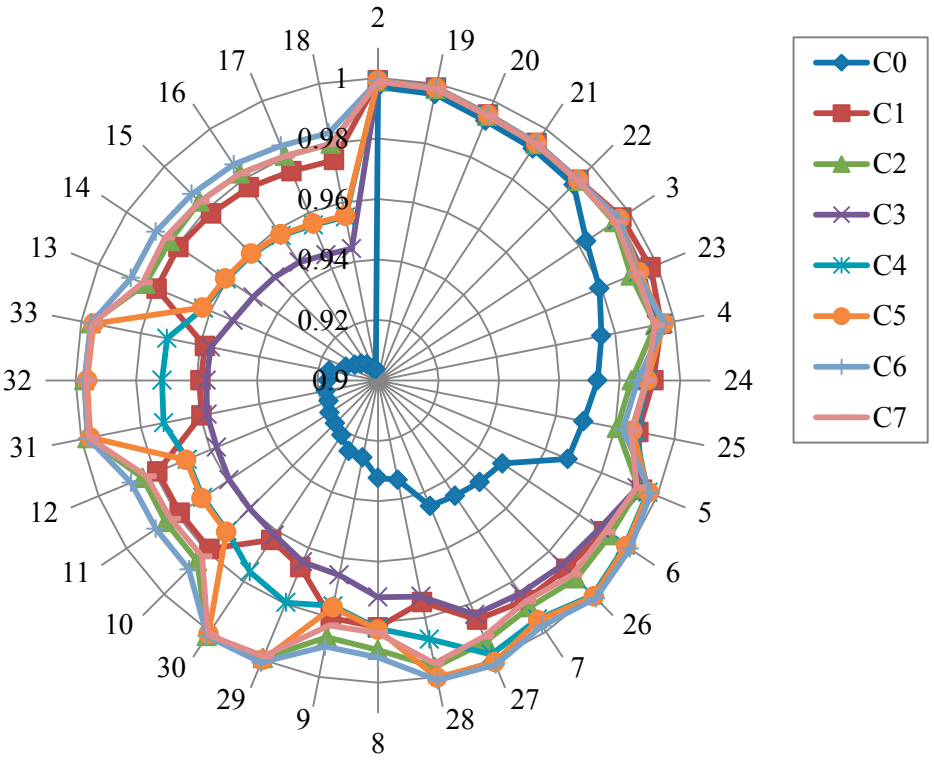

Figure 6.6 Voltage profile for different cases.

6.7 Summary

This chapter has proposed an efficient method for allocating multiple DG technologies in the distribution systems to minimize the losses. Different DG types are considered and the optimal combination between them is accurately obtained. The distribution system constraints are fully considered with employing OPF. The 33-bus and 69-bus distribution systems are used to test out the proposed method. Different case studies are simulated, and the DG units of different technologies are allocated. It has been established from the results that the proposed method can effectively allocate multiple different DG technologies. The results show that the losses can be effectively reduced when optimally allocate different DG types in distribution systems.

Chapter 7

Conclusion and Future Research

Chapter 7: Conclusion and Future Research

7.1 Conclusion

The paper has presented two methods, EA and EA-OPF, for determining the optimal DG locations and sizes in distribution systems to minimize system losses. Two test systems have been used to validate the proposed methods, and a detailed comparison has been conducted with alternative methods in the literature. The proposed methods have been applied to the optimal DG mix problem to allocate different types of DG units in distribution systems. Furthermore, the proposed methods have been applied to determine the optimal number of DG units to minimize the losses. The characteristics of the proposed methods can be summarized as follows:

- The proposed EA and EA-OPF methods can provide a fast and accurate solution compared to existing methods.
- In terms of accuracy, both of the methods can find proper DG locations, but EA-OPF can provide more accurate DG sizes compared to EA.
- In terms of computational speed, the EA method is faster than the EA-OPF method.
- EA-OPF is preferable for highly constrained DG allocation problems.

Finally, the proposed methods are based on generic mathematical models. Therefore, they can be easily extended in several directions, such as for the minimization of reactive power losses. Furthermore, the methods can be applied to more general cases, such as multi-load level and probabilistic load models. Further work will be dedicated to take into consideration the intermittent nature of the renewable energy resources in the optimization problem.

The thesis has also proposed an efficient QBBFS power flow method for analysing distribution systems. QB models of different distribution system components have been introduced. The proposed method is applicable to effectively solve the power flow problem for multi-phase active distribution systems. The OpenDSS software has been employed for validating the proposed formulation. Also, the proposed method has been compared with commonly used BFS methods using several balanced and unbalanced distribution systems. Based on the results, the characteristics of the proposed method can be summarized as follows:

- The proposed method provides accurate power flow solution.
- The proposed method showed robust convergence characteristics, especially at heavy loading and high R/X ratios.
- In the case of high DG penetration, the proposed method showed also robust convergence characteristics.
- As a result of the robustness of the proposed method, the computational burden of the power flow iterative process is significantly reduced.

The proposed method is a helpful tool to study the steady state condition of active distribution systems and assess DG impacts. The future work will be directed to extending

for time-series analysis and voltage regulation in the presence of different DG technologies.

7.2 Future Work

There is further research left for future investigations. Emerging research problems that come from this research include the following:

- Treat the intermit nature of the renewable energy resources in the allocation process.
- Modeling of three-phase center tab transformer in the radial power flow program.
- Modeling and study different types of the DERs such as micro turbine, fuel cell and solar generations system. In addition, including the doubly-fed induction and synchronous machine as a type of WTGSs.
- Extend the work for allocating and sizing of multiple DG for the distribution system.
- Studying the method of reconfiguration of the distribution system to improve system efficiency.
- Extension of the radial power flow for solving meshed distribution systems.
- Studying smart distribution systems and micro-grid systems.

Appendix A: Test Systems Description

A.1 Description of the unbalanced distribution systems

Four different unbalanced distribution systems are employed for evaluating and testing the proposed methods, namely, 4-bus, 10-bus, 25-bus, and 123-bus distribution systems [55], [63]. These systems have different configurations and structures, and the number of different components for each distribution system is given in Table A.1. Figures A.1, A.2, A.3, and A.4 show system diagrams for the three systems.

Table A.1 Descriptions of test systems

Test System	Line	Switch	Spot Load	Distribution Load	Capacitor	Transformer	Regulator
4-Bus	2	0	1	0	0	1	0
10-Bus	9	0	9	0	0	0	0
25-bus	24	0	24	0	0	0	0
123-Bus	117	11	85	0	4	2	4

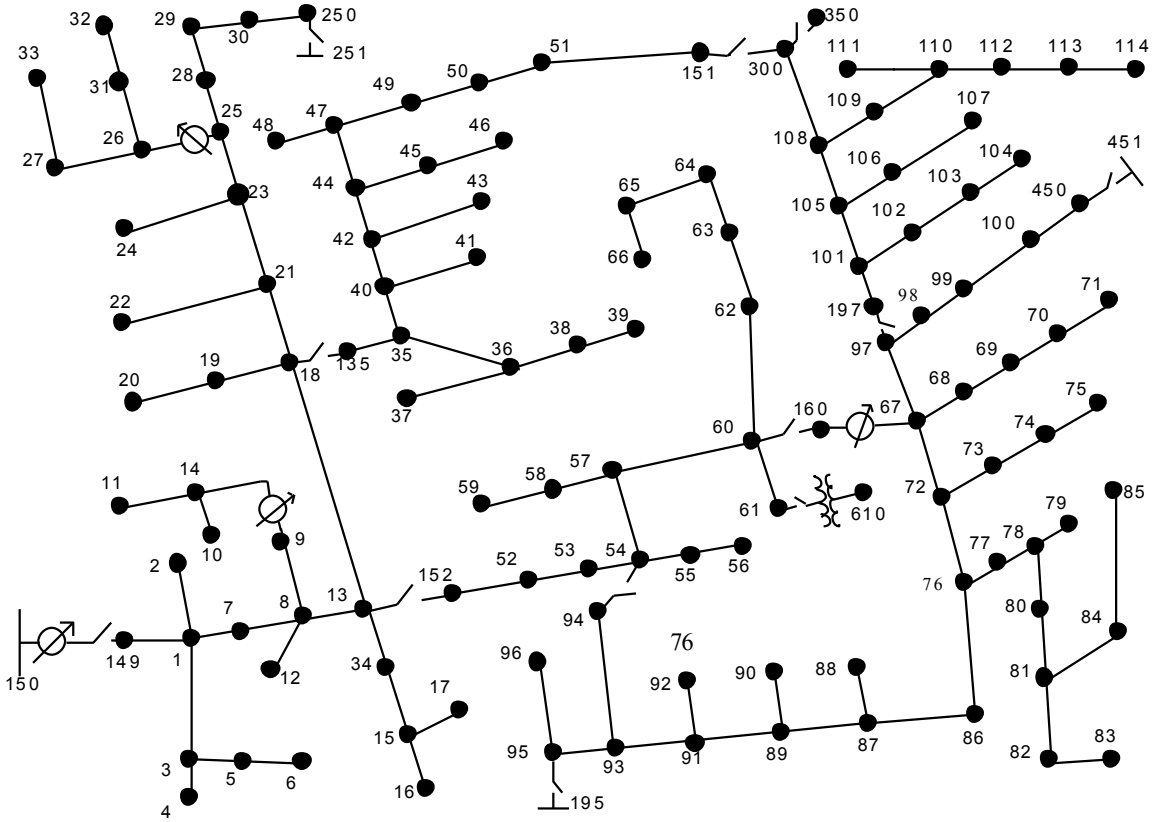

Figure A.1 IEEE 123-busTest Feeder [63].

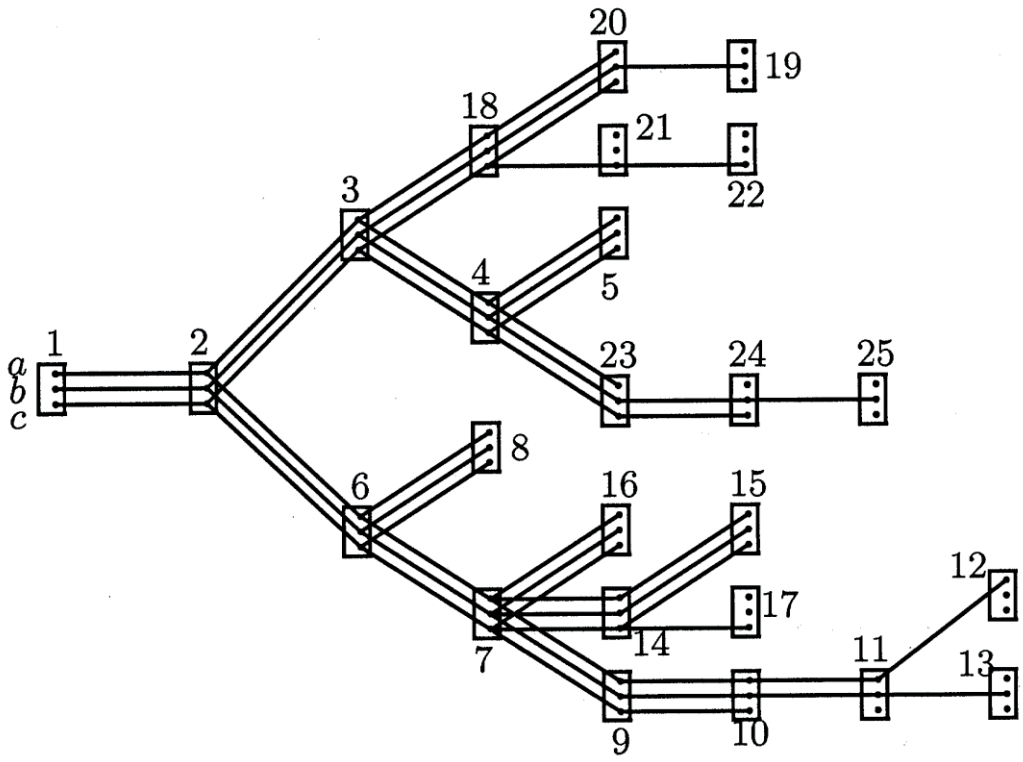

Figure A.2 The 25-busTest Feeder [55].

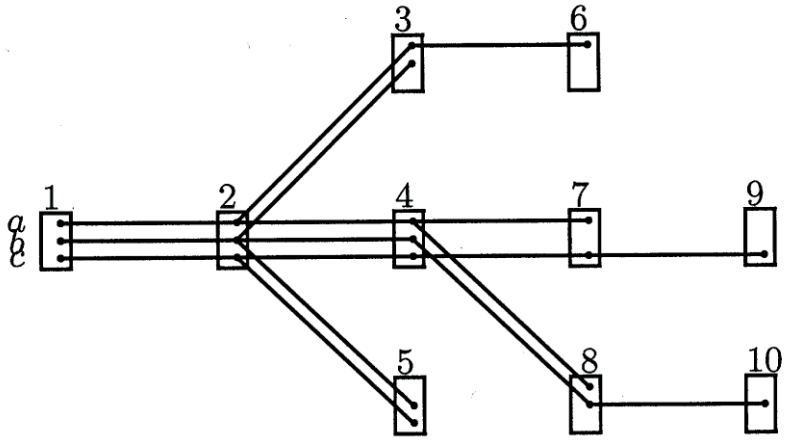

Figure A.3 The 10-busTest Feeder [55].

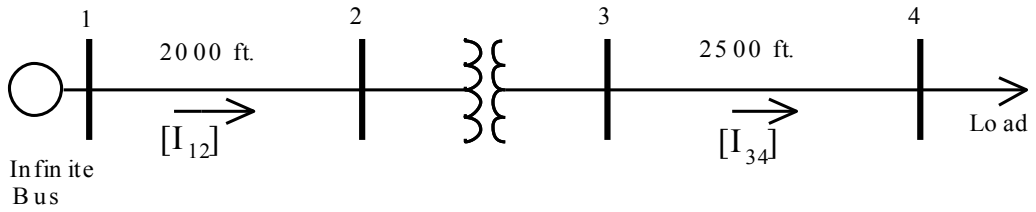

Figure A.4 The IEEE 4-bus Test Feeder [63].

A.2 MV Distribution Systems

Two MV distribution systems are employed for testing the proposed power method and the proposed DG allocation methods. These systems are the 33-bus, 69-bus systems [31], [32]. They are widely used for testing the validity of the allocation methods for DG and capacitors. The total losses of the two test systems are normal loading are 111 kW and 225 kW, respectively. The single line diagrams of the two systems are given in Figures A.5 and A.6.

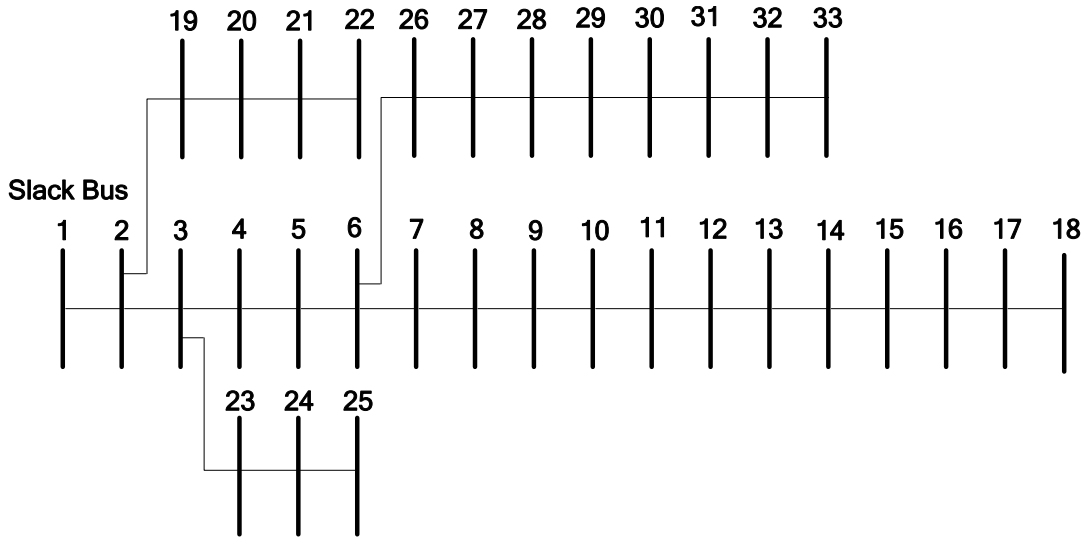

Figure A.5 The 33-bus radial test feeder [31].

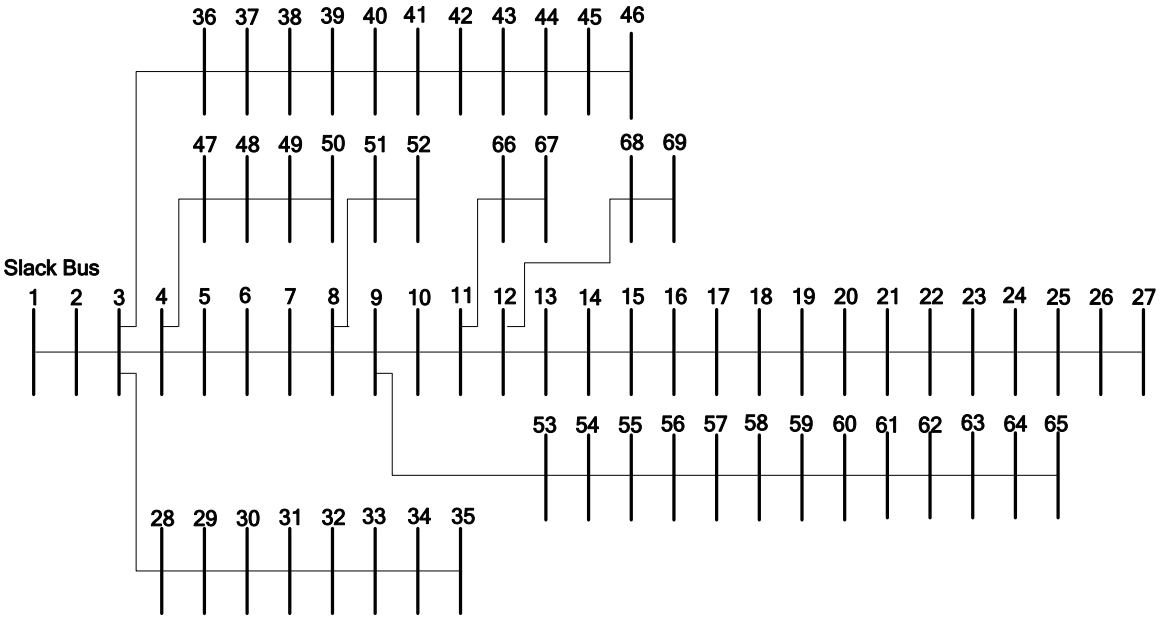

Figure A.6 The 69-bus radial test feeder [32].

Appendix B: QB Formulation

B.1 Proof of the QB formulation

A simple complex power injection equation at bus *j* (Figure 3.1) can be written as follows:

$$S_j = S_{j,injected} + S_{j,laterals} \tag{B.1}$$

where the superscript $S_{j,laterals}$ refers to the power flow through sub laterals after bus *j*, and $S_{j,injected}$ refers to power injections form the load, the DG unit, and line capacitances at bus *j*. The power flow equation that relates the receiving bus variables to the sending bus variables is expressed by

$$V_j - V_i + \left(S_j / V_j\right)^* Z_{ij} = 0 \tag{B.2}$$

where $Z_{ij} = R_{ij} + j\,X_{ij}$ is the line impedance between buses *i* and *j*. Then, transforming (B.2) to its counterparts in rectangular coordinates yields:

$$\left(V_j^{Re} + jV_j^{Im}\right) - \left(V_i^{Re} + jV_i^{Im}\right) + \frac{P_j - jQ_j}{V_j^{Re} - jV_j^{Im}}\left(R_{ij} + jX_{ij}\right) = 0 \tag{B.3}$$

By rearranging (B.3), the real and imaginary parts of this equation can be written as follows:

$$V_j^{Re^2} + V_j^{Im^2} - V_i^{Re}V_j^{Re} - V_i^{Im}V_j^{Im} + P_jR_{ij} + Q_jX_{ij} = 0 \quad \text{(B.4)}$$

$$V_j^{Im}V_i^{Re} - V_i^{Im}V_j^{Re} + P_jX_{ij} - Q_jR_{ij} = 0 \quad \text{(B.5)}$$

Substituting V_j^{Im} from (B.5) in (B.4) and solving the quadratic equation for V_j^{Re}:

$$V_j^{Re} = A_{ij}V_i^{Re} + B_{ij}V_i^{Im} \quad \text{(B.6)}$$

where:

$$A_{ij} = \left[1 \pm \sqrt{1 - 4\left(P_jR_{ij} + Q_jX_{ij}\right) \Big/ \left(V_i^{Re^2} + V_i^{Im^2}\right) - 4B_{ij}^{\ 2}}\right] / 2$$

$$B_{ij} = \left(P_jX_{ij} - Q_jR_{ij}\right) \Big/ \left(\left(V_i^{Re}\right)^2 + \left(V_i^{Im}\right)^2\right)$$

Similarly, substituting V_j^{Im} from (B.5) in (B.4) and solving the quadratic equation for V_j^{Im}:

$$V_j^{Im} = A_{ij}V_i^{Im} - B_{ij}V_i^{Re} \quad \text{(B.7)}$$

Equations (B.6) and (B.7) show that there are two possible power flow solutions under a particular loading condition. The maximum real root of the equations, which can be obtained with considering the positive sign in A_{ij}, is the steady state solution of the receiving end voltage.

Appendix C: Loads and Generations Curves

C.2 Wind Turbine Data

Table C.1

Power and power coefficient of a 330 kW turbine [43]

V (m/s)	P (kW)	C_p
5	13.89	0.25
6	35.12	0.36
7	62.75	0.41
8	96.75	0.42
9	136.15	0.42
10	180.35	0.4
11	227.33	0.38
12	271.61	0.35
13	308.27	0.31
14	335.39	0.27
15	350.86	0.23
16	352.98	0.19
17	342.41	0.15
18	324.20	0.12
19	307.76	0.10
20	295.85	0.08
21	288	0.07
22	282.03	0.05
23	277.2	0.05
24	272.81	0.04
25	271.06	0.03

C.3 PV Module "KC200GT" parameters

Table C.2

Parameters of the KC200GT PV Array [56]

I_{mp}	7.61 A	$I_{0,n}$	825.10e-8 A
V_{mp}	26.3	I_{pv}	8.214 A
P_{max}	200.143 W	a	1.3
I_{sc}	8.21 A	R_p	415.405Ω
V_{oc}	32.9 V	R_s	0.221 Ω

References

[1] H. L. Willis and W. G. Scott. , *Distributed Power Generation: Planning and Evaluation*. New York: Marcel Dekker, 2000.

[2] O. M. Toledo, D. O. Filho, A. S A. C. Diniz, J. H. Martins, and M. H. M. Vale, "Methodology for evaluation of grid-tie connection of distributed energy resources—Case study with photovoltaic and energy storage," *IEEE Trans. Power Syst.*, vol. 28, no. 2, pp. 1132-1139, May 2013.

[3] A. Gomez Exposito, A. J. Conejo, C. Canizares, *Electric Energy Systems: Analysis and Operation*. Boca Raton, FL, USA: CRC/Taylor & Francis, 2008.

[4] X. Zhang, G. G. Karady, and S. T. Ariaratnam, "Optimal allocation of CHP-based distributed generation on urban energy distribution networks," *IEEE Trans. Sustain. Energy*, vol. 5, no. 1, pp. 246 -253, Jan. 2014.

[5] X. Zhang, R. Sharma, and Y. He, "Optimal energy management of a rural microgrid system using multi-objective optimization," *in Proc. IEEE PES Innovative Smart Grid Technol. Conf*., Washington DC, USA, 2012, pp. 1–8.

[6] R. A. Walling, R. Saint, R. C. Dugan, J. Burke, and L. A. Kojovic, "Summary of distributed resources impact on power delivery systems," *IEEE Trans. Power Del.*, vol. 23, no. 3, pp. 1636–1644, Jul. 2008.

[7] T. Ackermann and V. Knyazkin, "Interaction between distributed generation and the distribution network: Operation aspects," *in Proc. 2002 IEEE T&D Conf*., vol. 2, pp. 1357–1362.

[8] D. Singh and K. S. Verma, "Multiobjective optimization for DG planning with load models," *IEEE Trans. Power Syst.*, vol. 24, no. 1, pp. 427–436, Feb. 2009.

[9] Y. M. Atwa, E. F. El-Saadany, M. M. A. Salama, and R. Seethapathy, "Optimal renewable resources mix for distribution system energy loss minimization," *IEEE*

Trans. Power Syst., vol. 25, no. 1, pp. 360–370, Feb. 2010.

[10] P. S. Georgilakis and N. D. Hatziargyriou, "Optimal distributed generation placement in power distribution networks: Models, methods, and future research," *IEEE Trans. Power Syst.*, vol. 28, no. 3, pp. 3420-3428, Aug. 2013.

[11] N. S. Rau and Y.-H. Wan, "Optimum location of resources in distributed planning," *IEEE Trans. Power Syst.*, vol. 9, no. 4, pp. 2014–2020, Nov. 1994.

[12] A. Keane and M. O'Malley, "Optimal allocation of embedded generation on distribution networks," *IEEE Trans. Power Syst.*, vol. 20, no.3, pp. 1640–1646, Aug. 2005.

[13] G.P. Harrison and A.R. Wallace, "Optimal power flow evaluation of distribution network capacity for the connection of distributed generation", *IEE Proc. Gener. Transm. Distrib.*, vol.152, no.1, pp. 115-122, Jan. 2005.

[14] D. Zhu, R. P. Broadwater, K. S. Tam, R. Seguin, and H. Asgeirsson, "Impact of DG placement on reliability and efficiency with time-varying loads," *IEEE Trans. Power Syst.*, vol. 21, no. 1, pp. 419–427, Feb. 2006.

[15] D. Singh, R. K. Mirsa, and D. Singh, "Effect of load models in distributed generation planning," *IEEE Trans. Power Syst.*, vol. 22, no. 4, pp. 2204–2212, Nov. 2007.

[16] K. Vinothkumar and M. P. Selvan, "Fuzzy embedded genetic algorithm method for distributed generation planning," *Elect. Power Compon. Syst.*, vol. 39, no. 4, pp. 346–366, Feb. 2011.

[17] K.-H. Kim, Y.-J. Lee, S.-B. Rhee, S.-K. Lee, and S.-K. You, "Dispersed generator placement using fuzzy-GA in distribution systems," *in Proc. 2002 IEEE Power Eng. Soc. Summer Meeting*, vol. 3, pp. 1148–1153.

[18] W. Prommee and W. Ongsakul, "Optimal multiple distributed generation placement in microgrid system by improved reinitialized social structures particle swarm optimization," *Euro. Trans. Electr. Power*, vol. 21, no. 1, pp. 489–504, Jan. 2011.

[19] M. F. Shaaban, Y. M. Atwa, and E. F. El-Saadany, "DG allocation for benefit maximization in distribution networks," *IEEE Trans. Power Syst.*, vol. 28, no. 2, pp. 639–649, May 2013.

[20] M. E. H. Golshan and S. A. Arefifar, "Optimal allocation of distributed generation and reactive sources considering tap positions of voltage regulators as control variables," *Euro. Trans. Electr. Power*, vol. 17, no. 3, pp. 219–239, May 2007.

[21] H. L. Willis, "Analytical methods and rules of thumb for modeling DG-distribution interaction," *in Proc. 2000 IEEE Power Eng. Soc. Summer Meeting*, vol. 3, Seattle, WA, July 2000, pp. 1643–1644.

[22] C. Wang and M. H. Nehrir, "Analytical approaches for optimal placement of distributed generation sources in power systems," *IEEE Trans. Power Syst.*, vol. 19, no. 4, pp. 2068–2076, Nov. 2004.

[23] S.-H. Lee and J.-W. Park, "Selection of optimal location and size of multiple distributed generations by using Kalman filter algorithm," *IEEE Trans. Power Syst.*, vol. 24, no. 3, pp. 1393–1400, Aug. 2009.

[24] T. Xiao-bo, and W. Xue-hong, "A new method of distributed generation optimal placement based on load centroid," *in Proc. IEEE Power and Energy Engineering Conf. (APPEEC),* 2011*,* pp.1–5.

[25] A. Elmitwally, "A new algorithm for allocating multiple distributed generation units based on load centroid concept," *Alexandria Engineering Journal*, vol. 52, no 4, pp. 655–663, Dec. 2013.

[26] N. Acharya, P. Mahat, and N. Mithulananthan, "An analytical approach for DG allocation in primary distribution network," *Int. J. Elect. Power Energy Syst.*, vol. 28, no. 10, pp. 669–678, Dec. 2006.

[27] D. Q. Hung, N. Mithulananthan, and R. C. Bansal, "Analytical expressions for DG allocation in primary distribution networks," *IEEE Trans. Energy Convers*., vol. 25, no. 3, pp. 814–820, Sep. 2010.

[28] D. Q. Hung and N. Mithulananthan, "Multiple distributed generator placement in

primary distribution networks for loss reduction," *IEEE Trans. Ind. Electron.*, vol. 60, no. 4, pp. 1700–1708, Apr. 2013.

[29] M. J. E. Alam, K. M. Muttaqi, and D. Sutanto "A three-phase power flow approach for integrated 3-wire MV and 4-wire multigrounded LV networks with rooftop solar PV," *IEEE Trans. Power Syst.*, vol. 28, no. 2, pp. 1728-1737, May 2013.

[30] K. Mahmoud, and M. Abdel-Akher, "Analysis of hybrid photovoltaic and wind energies connected to unbalanced distribution systems," *in Proc. IEEE International Conf. on Power and Energy(PEcon)*, 2010*,* Kuala Lumpur, pp. 79 – 84.

[31] M. A. Kashem, V. Ganapathy, G. B. Jasmon, and M. I. Buhari, "A novel method for loss minimization in distribution networks," *in Proc. IEEE Int. Conf. Elect. Utility Deregulation Restruct. Power Technol.,* 2000, pp. 251–256.

[32] M. E. Baran and F. F. Wu, "Optimal sizing of capacitors placed on a radial distribution system," *IEEE Trans. Power Del.*, vol. 4, no. 1, pp. 735–743, Jan. 1989.

[33] A. Soroudi, M. Aien, and M. Ehsan, "A probabilistic modeling of photo voltaic modules and wind power generation impact on distribution networks," *IEEE Syst. Journal*, vol. 6, no. 2, pp. 254–259, June 2012.

[34] K. Mahmoud and M. Abdel-Akher, "Analysis of hybrid photovoltaic and wind energies connected to unbalanced distribution systems," *IEEE International Conference on Power and Energy (PECon2010)*, Kuala Lumpur, Malaysia.

[35] William D. Stevenson, *Elements of power system analysis*, vol. 3, McGraw-Hill, New York, 1975.

[36] K. Mahmoud and M. Abdel-Akher, "Efficient three-phase power-flow method for unbalanced radial distribution systems," Proc 15-th*, the IEEE Mediterranean electro technical conference (MELECON)*, Valletta, pp. 125–130, April 2010.

[37] U. Eminoglu and M. H. Hocaoglu "Distribution Systems Forward/Backward Sweep-based Power Flow Algorithms: A Review and Comparison Study," *Elect.*

Power Compon. Syst., Vol. 37, No. 2, pp. 91–110, Jan. 2009.

[38] G. X. Luo and A. Semlyen, "Efficient load flow for large weakly meshed networks," *IEEE Trans. Power Syst.,* vol. 5, no. 4, pp. 1309–1316, Nov. 1990.

[39] C. S. Cheng and D. Shirmohammadi, "A three-phase power flow method for real-time distribution system analysis," *IEEE Trans. Power Syst.*, vol. 10, no. 2, pp. 671–679, May 1995.

[40] Murat Dilek, and Francisco leon, " A robust multiphase power flow for general distribution networks," *IEEE Trans. on Power Del.*, vol. 25 , no.2, pp. 760–768, May 2010.

[41] L. R. de Araujo, D. R. R. Penido, S. C. Júnior, J. L. R. Pereira, and P. A. N. Garcia, "Comparisons between the three-phase current injection method and the forward/backward sweep method", *Electrical Power and Energy Systems* ,vol. 32, no.7, pp. 825–833, Sep. 2010.

[42] X. Jiang, Y. C. Chen, and A. D. Domínguez-García "A set-theoretic framework to assess the impact of variable generation on the power flow," *IEEE Trans. Power Systems*, vol. 28, no. 2, pp. 855–867, May 2013.

[43] M. Abdel-Akher and K. Mahmoud, "Unbalanced distribution power-flow model and analysis of wind turbine generating systems," *Int. Trans. Electr. Energy Syst.*, Vol. 23, No. 5, pp. 689–700, July 2013.

[44] D. Shirmohammadi , H. W. Hong, A. Semlyen, and G. X. Luo, "A compensation-based power flow method for weakly meshed distribution and transmission networks," *IEEE Trans. Power Syst.*, vol. 3, no. 2, pp. 753–762, May 1988.

[45] S. Ghosh, and D. Das, "Method for load-flow solution of radial distribution networks," *IEE Proc. Generat. Transm. Distrib.*, vol. 146, no. 6, pp. 641–648, Aug. 1996.

[46] S. Mok, S. Elangovan, C. Longjian, and M. Salama, "A new approach for power flow analysis of balanced radial distribution systems," *Elect. Machines Power Syst.*,

vol. 28, no. 4, pp. 325–340, Nov. 2000.

[47] R. Ranjan, B. Venkatesh, A. Chaturvedi, and D. Das, "Power flow solution of three-phase unbalanced radial distribution network," *Elect. Power Compon. Syst.*, vol. 32, no. 4, pp. 421–433, Jan 2004.

[48] Wang Z., Chen F., and Li J., "Implementing transformer nodal admittance matrices into backward/forward sweep-based power flow analysis for unbalanced radial distribution systems", *IEEE Trans. Power Syst.*, vol. 19, no. 4, pp. 1831–1836, Nov. 2004.

[49] U. Eminoglu and M. H. Hocaoglu, "A new power flow method for radial distribution systems including voltage dependent load models," *Electric Power System Research*, vol. 76, no. 1, Sept. 2005, pp.106–114.

[50] M.A. Mates, "A new power flow method for radial networks" *Power Tech Conference Proceedings*, Bologna 2003.

[51] Ranjan, R., and Das, D., "Simple and efficient computer algorithm to solve radial distribution networks," *Elect. Power Compon. Syst*., vol. 31, no. 1, pp. 95–107, 2003.

[52] S. Satyanarayana, T. Ramana, S. Sivanagaraju, and G. K. Rao, "An efficient load flow solution for radial distribution network including voltage dependent load models," *Elect. Power Compon. Syst*., vol. 35, no. 5, pp. 539–551, Feb. 2007.

[53] G. R. Cespedes, "New method for the analysis of distribution networks," *IEEE Trans. Power Delivery*, vol. 5, no. 1, pp. 391–396, 1990.

[54] R. M. Ciric, A. P. Feltrin, and L. F. Ochoa, "Power flow in four-wire distribution networks—general approach," *IEEE Trans. Power Syst.*, vol. 18, no. 4, pp. 1283–1290, Nov. 2003.

[55] E. R. Ramos , A. G. Exposito, and G. A. Cordero, "Quasi-coupled three-phase radial load flow," *IEEE Trans. Power Syst.*, vol.19, no.2, pp. 776–781, May 2004.

[56] KC200GT High Efficiency Multicrystal Photovoltaic Module Datasheet Kyocera.

[Online]. Available: http://www.kyocera.com.sg/products/solar/pdf/kc200gt.pdf

[57] Picciariello, A., Alvehag, K., Soder, L.: 'Impact of network regulation on the incentive for DG integration for the DSO: opportunities for a transition toward a smart grid', *IEEE Trans. Smart Grid*, 2015, **6**, (4), pp.1730–1739

[58] Jennett, K.I., Booth, C.D., Coffele, F., Roscoe, A.J.: 'Investigation of the sympathetic tripping problem in power systems with large penetrations of distributed generation', *IET Gener. Transm. Distrib.,* 2015, **9**, (4), pp.379–385

[59] Fan, J., Borlase, S.: 'The evolution of distribution', *IEEE Power Energy Mag*., 2009, **7**, (2), pp. 63–68

[60] Khushalani, S., Solanki, J. M., Schulz, N. N.: 'Development of three-phase unbalanced power flow using PV and PQ models for distributed generation and study of the impact of DG models', *IEEE Trans. Power Syst*., 2007, **22**, (3), pp. 1019–1025

[61] Moghaddas-Tafreshi, S. M., Mashhour, E.: 'Distributed generation modeling for power flow studies and a three-phase unbalanced power flow solution for radial distribution systems considering distributed generation', *Electric Power Systems Research*, 2009, **79**, (4), pp. 680-686.

[62] Kersting, W. H.: 'Distribution System Modeling and Analysis', Boca Raton, FL: CRC, 2002.

[63] Kersting, W.H.: 'Radial distribution test feeders', *IEEE Trans. Power Syst*., 1991, 6, (3), pp.975–985

[64] OpenDSS. [Online]. Available: http://sourceforge.net/projects/electricdss/

[65] A. Keane and M. O'Malley, " Optimal utilization of distribution networks for energy harvesting," *IEEE Trans. Power Syst*., vol. 22, no. 1, pp. 467–475, Feb. 2007.

[66] S. A. Arefifar, and YA-RI Mohamed, "DG mix, reactive sources and energy storage units for optimizing microgrid reliability and supply security," *IEEE Trans. Smart Grid*, vol. 5, no. 4, pp. 1835–1844, May 2014.

[67] K. Buayai, "Optimal multi-type DGs placement in primary distribution system by NSGA-II," *Res. J. Appl. Sci. Eng. Technol.* vol. 4, no. 19, pp. 3610–3617, Oct. 2012.

List of Publications

I. Transactions/ International Journal Papers

No	Title and Authors of Published Papers
I-(1)	K. Mahmoud, N. Yorino and A. Ahmed, "Optimal distributed generation allocation in distribution systems for loss minimization," *IEEE Trans. Power Syst.*, vol. 31, no. 2, pp. 960-969, 2016.
I-(2)	K. Mahmoud, N. Yorino and A. Ahmed, "Power loss minimization in distribution systems using multiple distributed generations," *IEEJ Trans. Elec. Electron. Eng.*, vol. 10, no. 5, pp. 521–526, 2015.
I-(3)	K. Mahmoud and N. Yorino, "Robust Quadratic-Based BFS Power Flow Method for Multi-Phase Distribution Systems" accepted to *IET Generation, Transmission & Distribution,* March 2016.

II. International Conference Papers Related to This Thesis

No	Title and Authors of Published Papers
II-(1)	K. Mahmoud and N. Yorino, "Optimal Combination of DG Technologies in Distribution Systems" *Power and Energy Engineering Conference (APPEEC), 2015 IEEE PES Asia-Pacific*, Brisbane, QLD, 2015, pp. 1-5.

Contents of the Thesis and Published Papers Relationship

Chapters	Title of Chapters	Published Papers
Chapter 1	Introduction	I-(1), I-(2), I-(3), II-(1)
Chapter 2	Distribution System Analysis	I-(1), I-(2), I-(3)
Chapter 3	An Improved QB Power Flow Method for Distribution Systems	I-(3)
Chapter 4	Direct Assessment and Analysis of DG Impacts	I-(2), I-(3)
Chapter 5	Efficient DG Allocation Methods for Power Loss Minimization	I-(1), I-(2), II-(1)
Chapter 6	Optimal Mix Of Multi-Type DG Units	I-(1), I-(2), I-(3), II-(1)
Chapter 7	Conclusions and Future Work	I-(1), I-(2), I-(3), II-(1)